DC Railway Power Supply System Reliability Evaluation and Optimal Operation Plan

by

Yilin Chen

A thesis submitted to

the University of Birmingham

for the degree of

DOCTOR OF PHILOSOPHY

Department of Electronic, Electrical and Systems Engineering

College of Engineering and Physical Sciences

University of Birmingham, UK

March 2021

Abstract

With the continuous and rapid development of the economy and the acceleration of urbanisation, public transport in cities has entered a period of rapid development. Urban rail transit is characterised by high speed, large traffic volume, safety, reliability and punctuality, which are incomparable with those of other forms of public transport. The traction power supply system (TPSS) is an important part of an electrified railway, and its safety issues are increasingly prominent. Different from the substation in a general power system, the load of a TPSS has a great impact on the traction transformer; moreover, in order to ensure normal operation of the train in case of failure, the traction substation must be able to access a cross-district power supply, as it has a high demand for reliable operation. The safe and reliable operation of DC TPSSs is the basis of the whole urban railway transit system.

Previous studies have investigated the reliability of the TPSS main electrical wiring system. However, the impact of traction load and the actual operation of trains on system reliability has not been considered when designing a DC railway power supply system. The purpose of the research for this thesis is to find an optimal system operation plan for urban railways, considering load characteristics.

This thesis begins with a review of the main arrangements of DC railway power supply systems and the literature on railway reliability studies. A model of single train

simulation and a power supply system is established in MATLAB. The developed simulator is then integrated with a TPSS reliability model to evaluate the energy and reliability performance of DC railway power systems. Based on the train traction load model and train schedule, a comprehensive method for evaluating a DC TPSS considering traction load is proposed. Through simulation of the actual operation of the train group, the system energy consumption and substation life loss generated under different train operation diagrams and schedules are compared to provide a reference for the reasonable design of the timetable. Taking the life loss and energy consumption of the whole TPSS as the objective function, a genetic algorithm is used to optimise the train speed, coasting velocity, station dwell time and headway to find the optimal operation strategy. This is illustrated with a case study of the Singapore East–West metro line.

The study has addressed the following issues: development of a multi-train power simulator, evaluation of reliability performance, and finally the search for an optimal operation plan. The train running diagram and timetable are optimised jointly. This can help railway operators make decisions for an optimal operation plan and reduce the operation risk of the power system.

Acknowledgement

I would like to thank my supervisors, Prof. Clive Roberts and Dr. Stuart Hillmansen, for their encouragement and valuable guidance in my studies and their care in my daily life. They led me into the railway industry and taught me a lot. Their enthusiasm for research and teaching, their care and love for students, and their extensive knowledge has constantly inspired me to engage in research work.

Thanks to all my colleagues and friends in BCRRE; they have always made my study life full of fun. I am especially grateful to Dr. Zhongbei Tian and Dr. Ning Zhao, who have always provided me with valuable knowledge, thoughtful guidance and inspiration for my research.

Finally, I want to thank my family and friends. Thanks to my parents for their understanding and support during my Ph.D. study. Thanks for your encouragement all the time. Without you, I could not have successfully completed my studies.

Table of Contents

List of Figures

List of Tables

List of Acronyms

Term	Explanation / Meaning / Definition
ACO	Ant Colony Optimisation
AGREE	Advisory Group on Reliability of Electronic Equipment
ASME	American Society of Mechanical Engineers
ATO	Automatic Train Operation
BCRRE	Birmingham Centre for Railway Research and Education
BF	Brute Force
CIF	Critical Importance Factor
CPSC	Consumer Product Safety Commission
DAS	Driver Advisory System
DNO	Distribution Network Operator
DP	Dynamical Programming
EBF	Enhanced Brute Force
EMM	Energy Management Model
EMU	Electric Multiple Units
ENS	Electric Network Simulator
FMEA	Failure Mode and Effects Analysis
FTA	Fault Tree Analysis
GA	Genetic Algorithm
GUI	Graphical User Interface
HGA	Hierarchical Genetic Algorithm
HSR	High Speed Rail
HV	High Voltage
ICCG	Incomplete Cholesky Conjugate Gradient
IEEE	Institute of Electronics Engineers
MIF	Marginal Importance Factor

MRT	Mass Rapid Transit
MTBF	Mean Time Between Failures
MTS	Multi-train Simulator
MTTF	Mean Time to Failure
NERC	North American Electric Reliability Corporation
PSO	Particle Swarm Optimization
RAMS	Reliability, Availability, Maintainability and Safety
RR	Revenue Requirement
RRW	Risk Reduction Worth
SCG	Scheduling and Control Group
STS	Single-train Simulator
TPS	Train Performance Simulator
TPSS	Traction Power Supply System

List of Nomenclature

Symbol	Definition	Units
F	Traction force	N
B	Braking force	N
W_0	Basic resistance	N
W_j	Additional resistance	N
N	Supporting force	N
G	Gravity	N
u_f	Train tractive factor	$u_f \in [0,1]$
V	Train speed	m/s
E_t	Traction network voltage	V
u_b	Train braking factor	$u_b \in [0,1]$
W_i	Unit slope resistance	N/kN
W_r	Unit curve resistance	N/kN
W_s	Unit tunnel resistance	N/kN
W_k	Total resistance during train movement	N
m	Total mass of the train	tonnes
v_e	Vehicle speed at the last moment of electric braking	m/s
s	Running distance of the locomotive at the last moment of electric braking	m
l	Distance between stations	m
P_M	Input power of traction motor	kW
η	Working efficiency of the inverter	$\eta < 1$
E_{sub}	Substation energy consumption	kWh
E_{train}	Train energy consumption	kWh
E_{regen}	Train regenerative energy	kWh
E_{loss}	Energy loss	kWh
V_{noload}	Substation no-load voltage	V
V_{rated}	Substation no-load voltage	V
I_{rated}	Substation rated current	A
R_e	Equivalent resistance	Ω
$R(T)$	Reliability	-
$\lambda(t)$	Failure rate	-
$\mu(t)$	Repair rate	-
$Q(t)$	System unavailability,	-
$q_x(t)$	Unavailability for event X	-

T_A	Ambient temperature	℃
ΔT_{TO}	Top-oil temperature rise over the ambient temperature	℃
T_G	Winding hottest-spot temperature rise over top oil temperature	℃
F_{aa}	Acceleration Aging Factor	-
θ_h	Hot-spot temperature	℃
F_{eqa}	Equivalent Ageing Factor	-
V_{train_max}	Train maximum speed	km/h
$V_{coasting}$	Coasting velocity	km/h
T_{dwell}	Station dwell time	s
$T_{headway}$	Train headway	s
$T_{journey}$	Single train journey time	s
P_{sub}	Substation rated power	kW
RUL_{sub}	Substation remaining useful life	year

1 Introduction

1.1 Background

With the continuous and rapid development of the economy and the acceleration of urbanisation, the problems of urban environmental pollution and traffic congestion have become an important problem to be solved in large and medium-sized cities around the world, and the public transport in cities has entered a period of rapid development. Urban rail transit is characterised by high speed, large traffic volume, safety, reliability and punctuality, which are incomparable with those of other forms of public transport.

Most of the cities in the world with a high level of motorisation have a relatively mature and complete rail transit system, and the traffic volume of urban rail transit can account for more than 50% of the urban public transport volume in some cities. According to incomplete statistics, so far, 320 cities in more than 40 countries have built a rail transit system [1]. For example, Paris, with a population of 10 million, has a long rapid rail transit network of 219.9km, and rail transit bears 65% of the public transport volume [2]. The ratio is 54% in Berlin and 68% in New York [3]. In UK, a total of 3758 miles of rail have been electrified by March 2020, which accounts for 38% of the UK railway network [4]. According to the report by Network Rail, over 36% of the electrified railway networks use DC power supply systems [5], and there is a growing demand for

the DC system of urban rail transit. The construction of urban rail transit systems in the world has a history of more than 140 years. At peak hours, the MRT (Mass Rapid Transit) in Hong Kong carries an average of 80,000 passengers per hour, which is four times higher than the volume of buses [6].

The characteristics of urban rail transit are short dwell time and headway, a large number of stations, short distance between stations, and frequent adjustment of the train schedule. Thus, the traction load of an urban rail transit system has the characteristics of high power, high density, non-linearity and randomness, which causes power supply problems such as voltage fluctuation and impulse load for the traction power supply system. With the development of the national economy, the demand for urban rail transit is increasing. In order to meet the demand, train timetables are adjusted continuously considering the newly built railways that are put into operation, which will inevitably have a certain impact on the reliability and service life of the traction power supply system. How to evaluate and predict the influence of current or future traction load on a traction power supply system is a problem worthy of study.

Against this background, this thesis starts by looking at the influence of train traction load characteristics on the system, studies DC traction power supply systems and the reliability and life loss of traction substations, and proposes an optimal operation strategy for the system.

1.2 Aims and objectives

The aims of this research are to study the reliability of TPSS in a DC electrified railway system, and to make decisions for an optimal operation plan.

To evaluate power system reliability and develop an optimal operation plan for an urban rail system, the following objectives need to be addressed:

- State-of-the-art literature on railway power supply systems is required. Through the comparative analysis of previous railway reliability research and energy optimisation research, the advantages and disadvantages of the existing methods can be fully evaluated and the existing research gaps can be found, thus the assumption of this thesis and the research that needs to be improved are put forward.

- Simulation of train movement and the traction power supply network is an important tool for understanding railway power systems and for subsequent analysis. It is necessary to develop power supply system simulation software which can evaluate the energy consumption, life and reliability of a railway system according to specific infrastructure data and operation conditions. In the development of simulation software, the following problems need to be considered: dynamic operation simulation, power flow analysis with regeneration, and efficient computing speed.

- It is necessary to establish a reliability and life evaluation model for each component in the power supply system, which can reflect the influence of traction load on the system.

- Train trajectory and timetable optimisation. Taking energy consumption and system reliability as the objective function, the driving strategy and timetable of railway trains are optimised by using optimisation algorithms such as a genetic algorithm. Finally, an optimal operation strategy can be obtained.

1.3 Thesis structure

This thesis contains seven main sections which address the research aspects shown in Figure 1.1 and are described below:

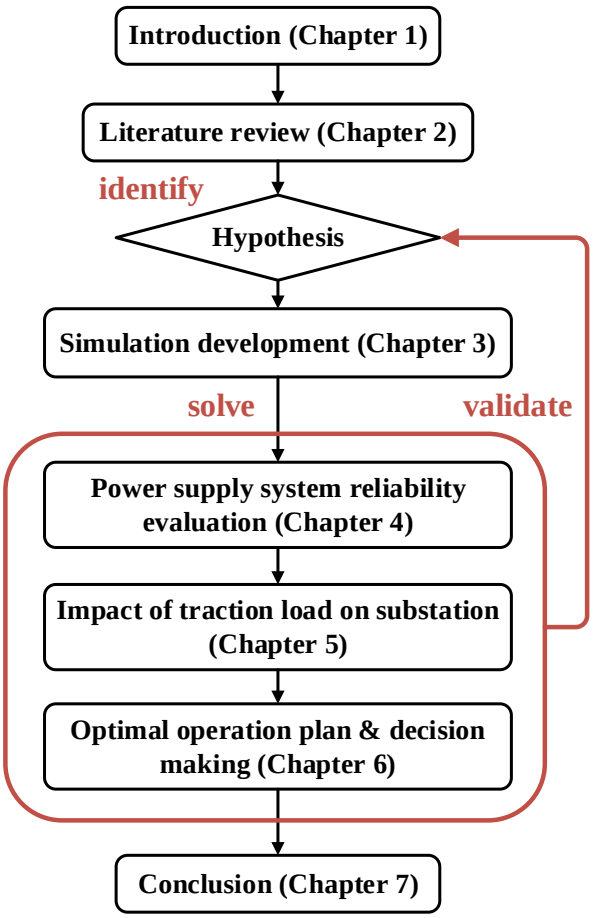

Figure 1. 1 Structure of the thesis

Chapter 1 – Introduction

The background of current railway systems is presented in Chapter 1. This chapter provides a general introduction to the research significance, main purpose and objectives of the study.

Chapter 2 – Literature Review

A literature review was carried out to investigate the existing power supply problems and methods to evaluate system reliability. The research gap of previous literature is identified in this chapter and the research hypothesis of this study is proposed.

Chapter 3 – DC traction power network simulation

Firstly, this chapter studies the dynamic modelling method of traction load. The force condition of a single train movement is analysed in detail and the corresponding motion equation is established, and the single train operation strategy is described.

Secondly, the chain network model of the power supply system is studied. Static mathematical models of the utility system and the traction substation are established, respectively. And based on the dynamic traction load model and the topology of the traction power supply system, the dynamic mathematical model of the traction power supply system is established.

The developed software is used as a tool to evaluate the energy and reliability performance of DC railway systems.

Chapter 4 – Power supply system reliability evaluation

This chapter presents an evaluation and analysis of the reliability of the power supply system. The weakest links of the system, which will influence the system reliability, are determined, and the causes of system failure are summarised. In theory, the research in

this chapter can provide a reference for the operation and maintenance of an electrified railway and for improvement of its safety level.

Chapter 5 – Impact of traction load on traction substations

An innovative method is proposed to investigate the influence of traction load on traction power supply system reliability and life. A comprehensive evaluation and simulation model of a DC traction power supply system is established based on the thermal model of a transformer, and the influence of traction load on system reliability is clarified. The model can be used for system evaluation and decision-making of an optimal operation plan.

Chapter 6 – Optimal operation plan

An optimal operation plan is proposed in this chapter. From the aspects of energy consumption, load impact on the traction power supply system, reliability and operation and maintenance cost, a comprehensive evaluation is carried out to get the optimal system operation scheme. A genetic algorithm is selected to find the optimal operation strategy, because it is simple and flexible to implement, which provides a fast solution for this non-linear and interdependent optimisation problem.

Chapter 7 – Conclusion

A review of the findings on reliability evaluation and the optimal operation plan is given and addresses the research questions set in the hypothesis development section.

Reflection on the inadequacies of this study and recommendations for future work are also concluded.

1.4 Original contributions

This research involves train traction calculation, optimal operation, traction power supply calculation, etc. The original contributions of this thesis can be described as follows:

1.4.1 Description of research background

In this thesis, the background and significance of simulation research on the traction power supply systems of urban rail transit are described in detail. On the basis of reading a lot of relevant literature and papers, the thesis summarises the current situation and development trends of train optimal control, urban rail traction power supply calculation, traction power supply simulation software development and traction power supply system reliability research.

The structure of an urban rail power supply system is described and summarised in detail, and the components of a DC traction power supply system are analysed emphatically, and then the modelling objectives of this thesis are pointed out.

1.4.2 Development of single train simulator and power simulator

In this thesis, the traction load of an urban rail train is modelled and simulated. The characteristics of regenerative braking and the process of train movement are analysed in detail, and a train traction calculation program is developed. Through the calculation of train traction, the position and power consumption of train operation are obtained, which provides the basic data for the DC power flow calculation program.

The power flow calculation method for a DC traction network is studied and the corresponding subprogram is completed. The power flow results obtained by the Newton–Raphson method are used as the basis for the DC traction substation model. After repeated iterative calculations, the power flow distribution of the whole traction power supply system is obtained.

Aiming to solve the problem that the voltage model of a regenerative braking locomotive makes the power flow calculation difficult to converge, this thesis studies the power correction model of a regenerative braking locomotive to ensure the convergence of the iterative algorithm of power flow calculation.

1.4.3 System reliability evaluation and impact of traction load on traction power supply systems

The existing traditional reliability analysis method is not fully applicable to a railway power supply system and cannot accurately reflect the influence of traction load on the reliability and life of the system. In order to solve the shortcomings of previous studies, a new evaluation method based on evaluation of transformer life is proposed.

By using a computer to simulate the dynamic process of urban rail train operation and system power flow with time, and combining it with the thermal model of a transformer, the effect of traction load on traction power supply system in different periods is displayed intuitively.

1.4.4 Train operation optimisation

Based on the train traction load model and train schedule, a comprehensive evaluation method of a DC traction power supply system considering traction load is proposed. Through simulation of the actual operation of the train group, the system energy consumption and substation life loss generated under different train operation diagrams and schedules are compared to provide a reference for the reasonable design of the timetable. Taking the life loss and energy consumption of the whole traction power supply system as the objective function, a genetic algorithm is used to optimise the train speed, coasting velocity and headway to find the optimal operation strategy.

2 Literature review of electrified railway systems and operation

2.1 Introduction

The DC traction power system plays an important role in the reliable operation of urban railways. Outage of the power supply will not only cause transportation paralysis, but also cause serious economic losses. Nowadays, the requirements of electrified railway system power supply are higher and higher. The increasing demand for railway transport services has a significant impact on important railway stakeholders, and the sustainability, reliability and cost of operation need to be fully considered. In order to ensure that the power supply can be provided continuously according to the operation demand and so that the traction power can reach the train continuously, the reliability evaluation of traction power supply systems (TPSSs) must be considered in the process of planning, operation and maintenance. It is of great importance to conduct research on DC TPSS reliability and energy evaluation and to design a reliable and efficient operation plan for existing TPSSs.

This chapter first summarises the composition and characteristics of railway DC TPSSs, as well as two aspects of energy saving and reliability evaluation. Secondly, the chapter summarises the current power supply system design and system operation scheme of an electrified railway, and summarises the problem of insufficient research on the effect

of load on a railway power system. By comparing and summarising the previous research results and the shortcomings of previous studies, the research gap is found and the research hypothesis is proposed. The specific objective of this research is to integrate the load characteristics into system optimisation.

2.2 Electrified railway power systems

The power supply systems of modern electrified railways are divided into two types according to the current type: DC power supply and AC power supply. AC power supply systems are mainly used in high-speed railways and long-distance cross-city railways. DC power supply systems are mainly used in metros, subways, light rails and short-distance intercity railways. This chapter will introduce the most common DC TPSSs in the industry and focus on studies on DC power system problems.

2.2.1 DC railway power systems

Compared with a 25 kV AC power supply system, a DC system has lower power supply voltage, which will lead to higher transmission loss under the same rated power [7, 8]. The reason why urban rail transit uses DC mode to power electric multiple units is that a DC TPSS is more advantageous than an AC TPSS. First of all, a locomotive with an AC power supply must have its own rectifier equipment, and the space on the vehicle is limited; as it is impossible to install such complex and huge equipment, the train can

only be supplied with single-phase rectified power. The single-phase power supply will lead to three-phase asymmetry and affect the power quality. On the contrary, for a DC traction substation, more complete rectifier equipment can be installed on the ground, thus no rectifier equipment on the vehicle is necessary and the total weight of the electric multiple unit is reduced. Secondly, urban rail transit power supply lines are located between buildings or under the ground, with limited line space and small power supply radius of the traction substation, so the power supply voltage does not need to be too high. Moreover, a DC system has no reactance voltage drop, and the voltage loss is relatively small, so it is unnecessary to use AC power supply. Based on the above advantages, almost all urban railways in the world adopt a DC power supply system.

Figure 2.1 shows the power supply and feeding network of a typical DC railway system [7]. According to the scale and demand of the railway system, the high-voltage side of the railway takes power from the power grid, usually 132, 66 or 33 kV AC. A medium voltage distribution network is usually 11 kV and supplied by a step-down transformer. Then the voltage is stepped down and rectified to 600, 750 or 1500 DC by the traction substation to supply power for the locomotives.

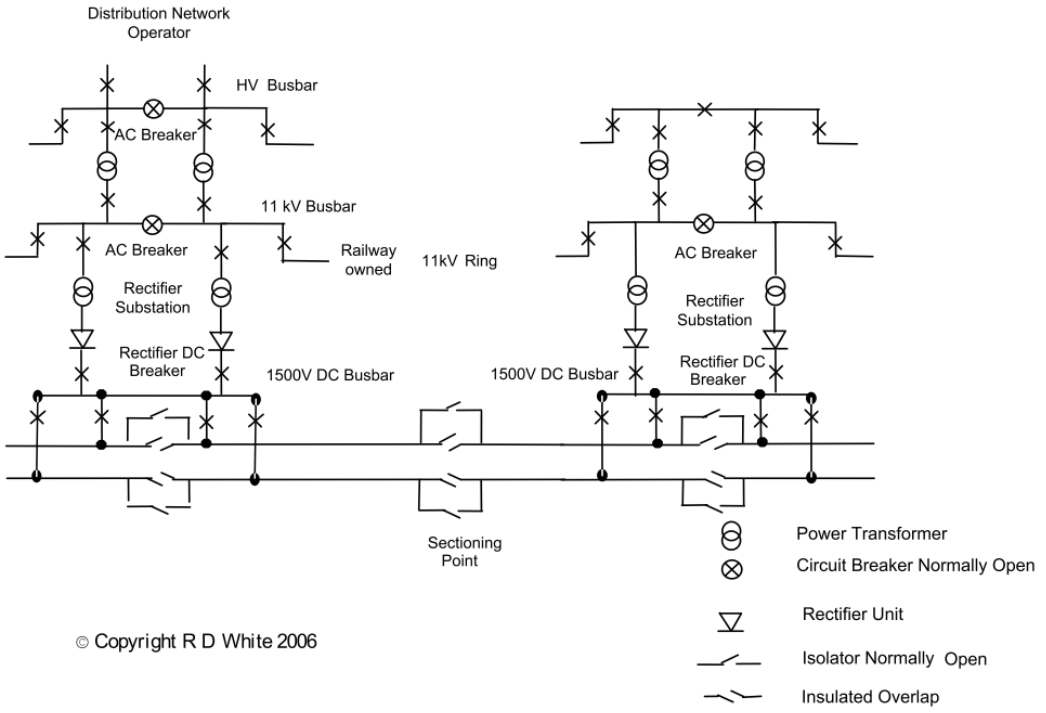

2.1a Typical feeding arrangement of 1500 V DC electrification system (heavy metro)

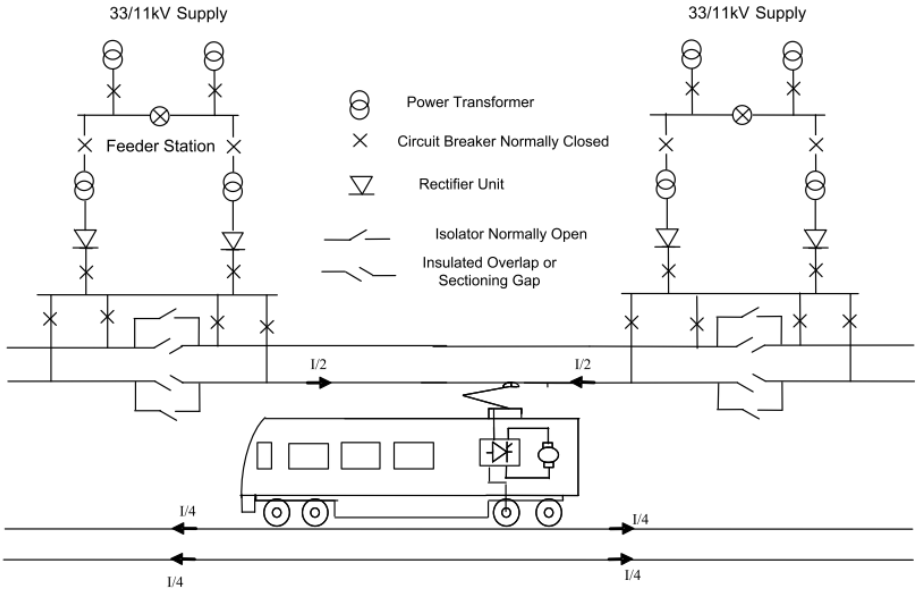

2.1b Typical feeding arrangement of 750 V DC electrification system (tram)

Figure 2. 1 DC electrification system arrangement, produced by Dr. Roger White [7]

A typical 750/1500 V DC traction substation usually adopts 12-pulse rectification, which is composed of two 6-pulse bridge converters in parallel, as shown in Figure 2.2. Fundamentally speaking, the circuit equivalent model and modelling method of AC and DC power supply systems are different. The AC system is more complex and will not be discussed in this thesis. The modelling of DC power supply system will be described in detail in Chapter 3.

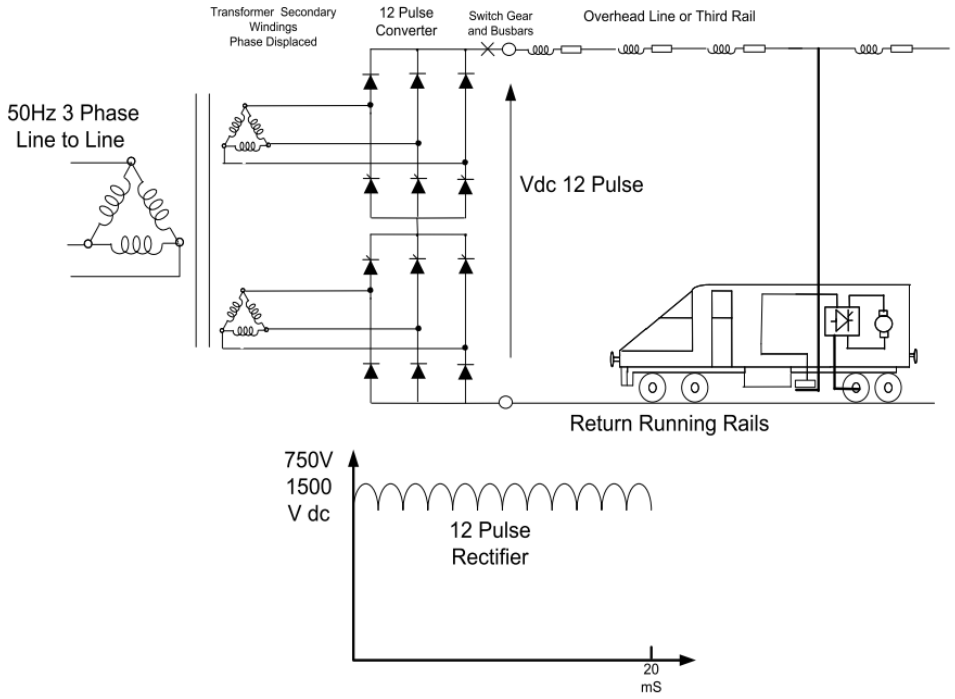

Figure 2. 2 Transformer rectifier unit, produced by Dr. Roger White [7]

2.2.2 Energy-saving techniques

With the increase of the amount of railway services, the total energy consumption and operation costs are getting higher [9]. Energy consumption has occupied a large

proportion of the operation cost in urban mass transit systems; therefore, energy saving has become an important issue. Energy-efficient train operation techniques are paid more attention as one of the best approaches to reduce operation costs. The energy-saving operation must also ensure the safety and punctuality of the train, which is a complicated multi-objective optimisation problem.

A range of studies and research have been carried out to optimise train trajectory and operation in recent years. The Scheduling and Control Group of Howlett, Pudney and Xuan Vu [10-12], at the University of South Australia, did a lot of research on optimal train control and switching strategy during an inter-station run. They built up several mathematical models to modify the running process of the train on a simulated route, and then developed some control algorithms to obtain energy-efficient driving strategies. Train regeneration also has an important effect on traction energy. Adinolfi et al. [13] demonstrated that at least 11.7% of energy can be conserved using regenerative braking in an electrified subway line. Khmelnitsky [14] also studied the effect of regenerative braking. He proved that by designing an optimal switching strategy for train operation, the energy could be fully recovered during the braking phase.

Other studies of energy-efficient train operation focus on the coasting control strategy. The application of evolutionary algorithms was found to be successful in solving this complex and multi-objective problem. Singapore scholars Chang and Sim [15] applied genetic algorithms to train trajectory optimisation. They created a coast control lookup

table by using chromosomes to represent the relative positions between stations, where the coasting is initialised. Wong and Ho [16] developed single and multiple coasting point control with both a simple genetic algorithm (GA) and hierarchical genetic algorithm (HGA). A max-min ant colony optimisation algorithm was also applied to optimise train trajectory curve and to improve the computation efficiency [17].

There has also been some research on railway system energy optimisation. Compared with traction energy optimisation, system energy optimisation is more complex, because it needs to comprehensively consider the energy consumption changes of the power supply system, driving mode, timetable and other factors. Zhao et al. proposed an integrated train trajectory and timetable optimisation method to reduce the whole-day energy consumption of a metro substation [18]. A search algorithm was used to search and optimise train trajectory, inter-station journey times and service intervals. A total energy saving of 25% was reached. Tian et al. proposed a comprehensive energy optimisation method, using a Monte Carlo method to obtain an optimised energy-saving driving mode and timetable results for a DC metro system [19]. The example of the Beijing Yizhuang metro line shows that the energy consumption of the system is 39.3% lower than that for automatic train operation and 13.8% lower than that for traction optimisation.

2.2.3 Reliability evaluation

With the rapid development of electrified railways, the safe, reliable and economical operation of TPSSs is crucial to the railway system. Standard EN 50126, an earlier standard of railway reliability, was first published in 1999 [20]. Standard IEC 62278 [21], a derivative of EN 50126, was issued in 2002. It gives the initial qualitative evaluation standard for railway power supply reliability. It further refines the evaluation of a TPSS into a comprehensive assessment of system reliability, availability, maintainability and safety, that is, RAMS assessment.

Research on the reliability of TPSSs began in 2004. Sagareli published a typical paper at the annual meeting of ASME (American Society of Mechanical Engineers) and IEEE (Institute of Electrical and Electronics Engineers) [22]. The paper first proposed the concept of reliability of TPSSs. The definition of the reliability of a TPSS is clearly stated in this article, but it does not give a method for evaluating the reliability. The paper also proposed the establishment of a power reliability organisation similar to NERC (North American Electric Reliability Corporation) to ensure the development and improvement of North American power system reliability. Since then, there have been more and more studies on the reliability of railway power systems. Research on the reliability of TPSSs is still in the initial stage of exploration. Its analysis method mainly relies on the reliability theory of power systems and is combined with the characteristics of TPSSs.

There are a few reliability-related studies on the electrified railway and its power system. Most of the existing reliability studies focus on AC-electrified railways, but a few focus on DC railway power supply systems. Wang et al. developed an analytical simulation method to evaluate the railway catenary system [23]. Feng et al. applied Failure Mode and Effects Analysis (FMEA) to high-speed railways for reliability evaluation considering relay protection [24], which provides guidance for the maintenance of high-speed railways. Chen et al. used Fault Tree Analysis to evaluate the power supply system in AC railways [25]. Ku and Cha applied Fault Tree Analysis and a Minimal Cut Sets algorithm to assess the reliability of an AC railway substation [26]. There has also been some research [27-31] focusing on power electronics reliability in the railway traction systems.

Much of the current literature on the reliability of traction power systems pays particular attention to the power grid and its components. Hayashiya et al. evaluated the reliability of each component in a DC power supply system based on 10 years of metro operation data in Japan and conducted quantitative analysis on a redundant system configuration [32]. Li et al. used an improved sequential Monte Carlo method to evaluate the system reliability of a metro traction substation, to determine the weakest links of the system [33]. These studies analysed the links and factors that affect the reliability of power supply systems from the perspective of power electronics and systems. The traditional reliability analysis methods are applicable to both AC and DC railway power systems. The main difference lies in different components with different failure rates. A constant

failure rate was adopted when conducting reliability assessment, which is not able to reflect the real-time operating conditions of the system. This is the deficiency of current reliability research on railway power supply systems.

Existing research only considers the reliability of the power grid itself or of its electrical components. However, the impact of traction load and the actual operation of the trains on system reliability is not considered when designing a DC railway power supply system. Previous studies of railway power supply networks usually focused on infrastructure design and capacity, rather than system operation. In many cases, due to the complexity and cost of the power supply system equipment, it is impossible to carry out extensive upgrades. Under the condition that the power supply system has been built and the infrastructures are not changed, optimisation of the traction load and operation schedules can be considered to maximise the reliability of the system.

2.3 Studies on the power supply problem

A power system is a network of electrical and electronic devices used to provide, transmit and use electricity. A typical example of a power system is the power grid that can supply electricity to extended areas. In a general electrical power distribution system, load balancing is a common problem. Load balancing helps optimise the utilisation of transformers and feeders, which can reduce the investment planned for increased capacity [34]. Research [35] shows that an impulsive load will not only affect

the normal operation of the main output substation, but also have a great impact on adjacent power plant units, reducing their service life and level of quality. In order to adapt to the growing demand of the load, it is necessary to optimise the existing power supply system while considering energy and environmental factors, and to ensure a high degree of system operation reliability.

Different to the substation in a general power system, a railway TPSS has a single load, and the impact on the traction transformer is very large, while the load of a general power system is mostly industrial or household load. There is usually no impulsive overload on a general power grid system, so the transformer output is relatively more stable. In addition, the rated capacity of the large distribution substations used in the power grid system (ranging between 10 and 100 MVA) is designed to be relatively large, and usually there will not be very frequent overloads. Thus, the load has a greater influence on the reliability of a traction substation. For DC systems, traction substations have harsher operational and stability constraints than normal power distribution substations. These include frequent short circuits, transient spikes, voltage drops and voltage rises due to load. Considering the unique issues related to railway power systems, the design, construction and operation of traction substations face many technical challenges. It is necessary to carry out related research to eliminate or reduce the impact of overload on traction substations.

2.3.1 Electrified railway system design

The design of a TPSS for an electrified railway is a complex multi-attribute decision-making problem, which needs to consider many quantitative and qualitative factors. R. D. White [7, 36, 37] has summarised the infrastructure design and industry standards of DC- and AC-electrified railway in the current railway industry, including the layout of electrical components, the capacity and location of substations, the selection of transformers, etc.

In the design of a TPSS, the optimal distribution of traction substations and their capacity has also been studied by some scholars. Chang et al. [38] used a tabu search algorithm to determine the optimal locations and fire angles of a set of DC railway rectifier stations. This heuristic optimisation method can get approximate and fast results. A GA is used to find the optimal number and location of substations, as well as the number, type and location of catenaries [39]. However, the power supply system model is simplified and the description is not detailed enough. Chen and Jiang [40] used a particle swarm optimisation (PSO) algorithm to find the optimal location of traction substations. By finding a reasonable length of the power supply arm, the power loss of the traction network is minimised, and the capacity of the traction transformer under each connection mode after optimisation is calculated, which provides the basis for the selection of the traction transformer. However, the established optimisation model is based on the instantaneous current at a certain moment, which cannot reflect the

influence of different train positions and speeds on the results in the process of vehicle movement.

2.3.2 Electrified railway system operation

In recent years, Milroy, Benjamin, Howlett et al. of SCG (Scheduling and Control Group), University of South Australia, have developed the METROMISER system to guide the optimal operation of trains with a computer [10, 41-45]. In the process of train operation, it can calculate and analyse the optimal train operation mode in real time, and provide the optimal energy-saving operation sequence, which can be applied to the DAS (Driver Advisory System) system. The system is suitable for the operation of subways in suburbs and cities with short intervals and can achieve a 15% energy saving.

Chang et al. [46] took the operation scheme of the Taiwan high-speed railway as a specific research object, and built an integer programming model for optimisation of the operation scheme, which comprehensively considers the passenger cost and utility operation cost. In the research, the stop plan of a train on the route is taken as the key content of decision-making. Chuang et al. studied the optimal switching problem of transformer load in an AC/DC MRT system [47]. The study takes into account peak and off-peak traffic conditions. Thus, the loss is reduced and the load factor of the main transformer is increased. In addition, Schobel and Schwarze [48, 49] proposed a model of an operation plan based on game theory. The operation route is considered to be the

role of the game theory, and the operation frequency is its decision-making quantity. The idea is to equalise the use of equipment and distribute the frequency of operating lines on the railway network, to reduce the delay caused by the time interval.

2.3.3 Maintenance plan

The reasonable formulation of a maintenance plan for a traction substation is an important part of ensuring the normal transportation of railway electric power. The maintenance plan should take into account the reliability of the system and cost–benefit analysis and should not affect the normal power supply at ordinary times. For a TPSS, making a maintenance plan is a process to determine the appropriate maintenance intervals of different equipment with the goal of minimising failure risk and maintenance cost [50].

At present, there is relatively little published research on the optimisation of maintenance plans for traction power supply and transformation systems, and no systematic research results have been achieved. Higgins proposed an algorithm based on the tabu search method to solve the problem of railway maintenance plan optimisation [51]. Chen et al. [52] established an optimisation model for a catenary system maintenance schedule based on the minimum maintenance cost, with system reliability as the constraint condition. In contrast, the research on other system maintenance plan optimisation problems is relatively extensive, and the main

achievements include the application by El-Amin et al. and Gopalakrishnan et al. of the tabu search method in the optimisation model of a generator maintenance plan [53, 54]. Moudani and Mora-Camino studied the dynamic planning model of an air transportation maintenance plan based on a heuristic solution [55]. Sriram and Haghani used a heuristic algorithm to solve an aircraft maintenance plan optimisation problem in air transportation [56]. Lapa et al. proposed a maintenance planning solution based on a cost–reliability model, and searched for the optimal solution of the model through a GA [57]. On the basis of condition-based maintenance theory, Faith established a maintenance plan optimisation model based on availability and cost through fault probability prediction, and applied a GA to solve the model [58]. These models basically aim at improving system reliability and reducing maintenance cost.

2.3.4 Effect of traction load

The main difference between a TPSS and a general power system is that the load of a TPSS is constantly moving, so it has outstanding characteristics of time, location, capacity and power factor. The latest research takes into account the effects of traction loads and uses the dynamic failure rates of the components. Feng et al. studied the characteristics of a high-speed rail traction load and pointed out that the non-linearity of traction load cannot be ignored [28]. A moving load of a power system for system dimensioning was studied by Fortouhi et al. [59]. The voltage level should not drop too much, otherwise the traction force will be reduced too much or the protection system

will be triggered. Liu et al. evaluated the effects of the traction load of a high-speed rail on the power quality using related power quality indicators. When there is a heavy traction load demand on an AC power supply system, the current unbalance factor can be up to 90%, which will worsen the power quality and reduce system reliability [60]. In addition, there are some studies on the impact of traction loads on transformers in railway substations [61, 62]. Studies show that overload can greatly affect transformer life expectancy. These papers only analyse the load conditions of a single transformer and do not propose practical methods to eliminate the impact of overload and methods to improve system reliability. In the process of daily operation, the traction load is affected by stations, route, passenger flow and other aspects. Research [35] shows that an impulsive load will not only affect the normal operation of the main output substation, but also have a great impact on adjacent power plant units, reducing their service life and level of quality. However, the current research on railway power system reliability has not taken into consideration the real-time load. There is potential to study the influence of traction load on TPSSs for better system operations.

2.4 System operation optimisation

Under the pressure of environmental concerns and higher power demand while maintaining reasoning cost, the optimal allocation of energy, system optimisation and application of algorithms has become a major research topic. The application of

appropriate algorithms to optimise system operation can improve the computational efficiency in decision-making.

2.4.1 Train operation and timetabling

Train driving strategy and timetabling are the two most important parts of railway system operation. They are two relatively independent research directions, and there are many research and papers in this field. Train operation research mainly focuses on the performance of a single-particle vehicle on the line, which can also be described as the planning of acceleration, cruising, coasting, deceleration and other motion states at every moment [15, 18, 63-66]. The research on timetabling is mainly to summarise and optimise the departure, interval and arrival time of all trains based on train operation and running diagrams [67-69]. The above research focuses on the effective utilisation of traction energy and regenerative braking energy, or the saving of system operation cost. Another focus of timetable research is to reduce the impact of system interruption and interference [70, 71]. The key point is to optimise the departure intervals and turnaround time of trains in a system while keeping the transportation system operating effectively without interference.

The comprehensive optimisation of train operation and the railway timetable is the research trend of current railway academics. Tian et al. [19] combined single train operation with the whole power supply system, proposed an approach for whole system

energy optimisation based on train trajectory and dwell time, and compared the results of system energy optimisation with those of traction energy-efficient operation and automatic train operation. In the research on system operation optimisation, Borndorfer, Grotschel and Pfetsch [72] [73] adopted a multi-commodity network flow model based on the free travel of passengers, and added the objective of minimum operation cost on the basis of the constraint model of the minimum travel time of passengers. Their research uses a column-generation algorithm, which greatly improves the efficiency of the solution.

2.4.2 Optimisation and algorithms

There are some studies on railway timetable optimisation and train trajectory optimisation to save system energy and achieve the optimal energy configuration. Most railway timetabling focuses on the usage of regenerative braking energy and passenger flow prediction. Study has shown that with proper railway timetabling, up to 20% of energy can be saved. Nasri et al. [74] and Yang et al. [67] both applied GAs to provide the maximum usage of electrical regenerative energy of braking in subway systems. Sun et al. [75] took into consideration the passenger flow and applied Lagrangian duality theory to determine the optimal train schedule by optimising the train dwell time and headways. Zhang et al. [76] considered the uncertainty of a maintenance plan on railway timetabling, and proposed a two-stage integrated model to determine a robust train schedule. Train trajectory optimisation is another significant research topic for

energy-efficient driving. Most train trajectory optimisation focuses on the trade-off between single train energy consumption and journey time. Different searching algorithms such as Enhanced Brute Force (EBF), Ant Colony Optimisation (ACO) and GA have been applied in train trajectory optimisations [65, 77]. Lu et al. [64] used Dynamical Programming (DP) and found that it performed better than both GA and ACO in searching for energy-efficient driving strategies.

2.4.3 Discussion

The state-of-the-art literature on railway system operation optimisation and the optimisation algorithms are summarised and compared in Table 2.1. The current research on system operation optimisation mainly focuses on train energy consumption and power supply energy flow, but ignores factors such as system reliability and service life, and the influence of traction load on the system has not been considered. The lack of research in this area should be taken into account.

Table 2. 1 Recent literature on railway system operation optimisation

	Optimisation objective	**Variables to be optimised**	**Publications**	**Methodology and algorithms**
Train operation	Traction energy saving	Coasting point	Chang and Sim [15]	GA
		Coasting point	Acikbas and Soylemez [66]	Artificial neural networks, GA
		Coasting speed	Chuang et al. [63]	Artificial neural network models
		Train driving speed	ShangGuan et al. [78]	Hybrid evolutionary algorithm

		Train trajectory	Lu et al. [64]	ACO, GA, DP
		Train trajectory	Wang et al. [79]	Gauss-pseudospectral method
	Energy saving and punctuality	Train trajectory	Yan et al. [80]	Moving horizon approach
	Energy cost and train delay minimisation	Driving speed curve	Zhao et al. [18, 65, 77]	EBF, ACO, GA
	Regenerative braking energy saving	Train trajectory	Liu et al. [81]	GA
Timetable	Time synchronisation	Departure and arrival time of trains	Ramos et al. [68]	Mathematical programming approach
	Regenerative braking energy utilisation	Headway and reverse time	Nasri et al. [74]	GA
		Train dwell time and headway	Yang et al. [67]	GA
	Operation cost minimisation	Train dwell time and headway	Sun et al. [75]	Lagrangian duality theory
	Maintenance plan	Departure and arrival time	Zhang et al. [76]	Mixed-integer linear programming
	System robustness	Headway and turnaround time	Caprara et al [70] Kroon et al. [70] Goverde and Hansen [71]	Mathematical approach
System operation	Operation cost minimisation	Passenger flow and travel time	Borndorfer et al. [72, 73]	Column-generation algorithm
	System energy optimisation	Train trajectory and dwell time	Tian et al. [19]	Monte Carlo algorithm

Shortcomings of the above research

To sum up, the state-of-the-art research in these areas is relatively weak in the following aspects:

1. Previous studies mostly considered energy consumption or system reliability separately, such as optimising a certain part of the energy. These two parts can be considered simultaneously when optimising the system operation.

2. The research on train trajectory optimisation and timetabling is relatively independent, and there is relatively less research on system operation optimisation, which is not very comprehensive. There is little research on system operation optimisation.

3. In system reliability evaluation, a fixed failure rate is usually used, and load characteristics are not considered. Such a model is not linked with the operation of the system and cannot reflect the impact of traction load.

4. The model of train operation control optimisation has been simplified to some extent, and the complexity of real routes has not been considered generally.

2.5 Hypothesis development

A DC traction power system plays an important role in the reliable operation of urban railways. A power supply outage will not only cause transportation paralysis, but also cause serious economic losses. At present, the research on railway power supply systems focuses more on energy saving. However, from the perspective of long-term management of railway systems, reliability is more important. Improving system reliability is an effective solution to save the total cost of operation, maintenance and

economic loss caused by power supply failure. It is necessary to conduct research on DC TPSS fault analysis and power supply system reliability evaluation.

In the state-of-the-art literature, few studies have taken into consideration both energy and system reliability. The impact of traction load and the actual operation of the trains on system reliability is not considered when designing a DC railway power supply system. Judging from the current actual operating conditions of the United Kingdom's urban rail transit system (such as the London Underground) and the departure arrangements for a considerable period of time in the future, its traffic volume is relatively large as is the departure density. The current load level of a traction substation is close to the maximum value of the designed power supply capacity, and the traction transformer will sometimes experience an impulsive overload. Under the condition that the power supply system has been built and the infrastructures are not changed, it can be considered to optimise the traction load and operation schedules to maximise the reliability of the system, without reducing the number of trains running throughout the day and without increasing energy consumption. This method can be used to minimise the impact of impulsive load during peak hours of railway operation and to develop a cost-effective operation for urban rail transit.

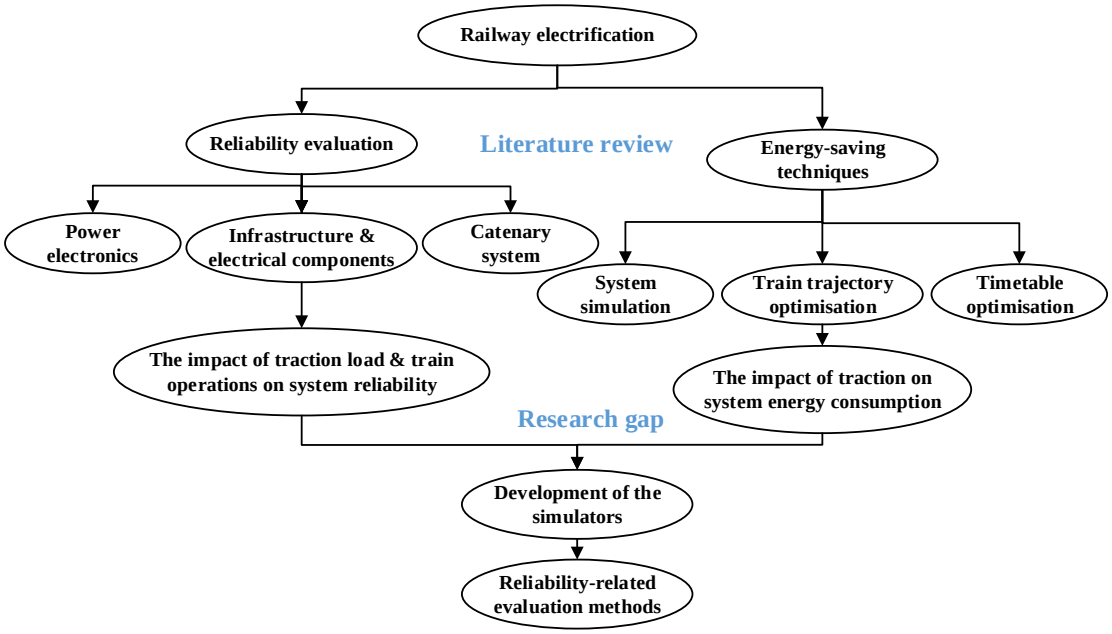

Figure 2. 3 Hypothesis development flow chart

This thesis introduces some reliability-related indices and proposes the Fault Tree Analysis (FTA) method to evaluate the system reliability of a DC-electrified railway. To fill the stated research gaps and help make decisions for an optimal railway operation plan, this research will focus on the effects of overload on the substations of railway traction power systems and determine the factors that can reduce the impact of overload. The purpose of this study is to take into account the substations of the entire line, and optimise the timetable and train running diagram to balance the traction load of the whole line, so that the average reliability of all substations is maximised. At the same time, the total revenue requirement including energy consumption and maintenance cost is considered. The optimisation problem is intuitively unified as the operation cost of railway utilities. This method is proposed for the railway operators to maximise the optimal use of their existing infrastructure, to select the appropriate

transformer size, and to determine the operation strategy. It can help make decisions for an optimal operation plan and reduce the operation risk of the power system as well as saving energy.

The overall objective is to find an appropriate method for system evaluation and to develop an optimal model to operate and design the TPSS. It basically involves developing a DC power simulator and train movement simulator for energy and power evaluation; linking the simulator to the relevant concepts of reliability assessment; investigating the impact of loads on system reliability; and then transforming the research problem into an optimal solution problem.

2.6 Summary

This chapter gives a review of the state-of-the-art literature on electrified railway power supply systems and some existing problems. Through analysis and comparison of the existing literature, it is found that there are some defects in the reliability and energy evaluation of TPSSs, and the optimisation of system operation has not been fully studied. This thesis presents a whole system optimisation method to improve the reliability and life of railway TPSSs, considering traction load characteristics. The next chapter will introduce the development of a multi-train power simulator which is used to solve the system optimisation problem and design an optimal operation scheme.

3 DC traction power network simulation

3.1 Introduction

How to establish the dynamic model of a DC urban rail transit traction power supply system, and then calculate the dynamic power flow, is the precondition for analysing and evaluating reliability-related indices of a traction power supply system and system operation optimisation. The modelling and simulation of a DC traction power supply system can be conducted by computer. By means of simulating the movement of trains and dynamic changes of the system power flow over time, the impact on a traction power supply system caused by traction load for different passenger flows will show up intuitively. The simulation software of the traction power supply system will provide us with reference data to select a power supply scheme and system operation plan, which is an effective power system design tool.

This chapter introduces the structure and operation mode of the urban rail transit power supply system and analyses the train movement rules. The regenerative braking and the arrival process of the train are also elaborated in detail. Through the train traction calculation, time-dependent changes of the position and power requirements of the vehicle are obtained. Then the results of the single-train simulation are used as dynamic load data for a multi-train power flow calculation. Finally, MATLAB language is used

to compile the above calculation program and a GUI (Graphical User Interface) is used to design the software.

3.2 Railway power system simulator

In the simulation calculation of an urban rail transit power supply system, the establishment of an appropriate traction power supply system model is the basis of theoretical analysis. Many scholars have conducted in-depth research on models of DC traction substations and obtained many research results.

The development of power supply system simulation software is relatively mature. For example, the EMM (transportation systems energy management model) software of Carnegie-Mellon University and the SINANET software developed by the company ELBAS are two widely used pieces of simulation and analysis software for DC traction power supply systems. The main body of EMM [82-84] consists of two parts: the TPS (train performance simulator) deduces the operation of a single train from the starting point to the end point (mainly changes in taking current, energy consumption, relative time, position, etc.) under rated voltage. The ENS (electric network simulator) takes the output of TPS as the input, combined with the train operation schedule, and through DC load flow analysis calculates the changes of voltage, current and power at each designated point on the line when *n* groups of trains are running on the line at the same time, as well as the power flow calculation of the AC-side electric network. The power

supply simulation software developed in this chapter refers to the EMM model; its structure is divided into two parts: the train operation simulation program and the electric power flow calculation program.

The traction power supply system simulation software developed by ELBAS mainly includes WEBANET and SINANET [85, 86], among which WEBANET is developed for AC traction power supply systems. SINANET can simulate a DC traction power supply system effectively and has been widely used in urban rail transit projects in many countries such as Germany, the Netherlands and Hungary. The main functions of the software are: dynamic simulation of train operation and traction power supply infrastructure; dynamic demand for traction load power; dynamic distribution of working voltage on the pantograph during train operation; dynamic simulation of electrical parameters in a traction power supply network. The software mainly includes three programs: a database input program, a simulation program and a graphic output program.

A method for simulating a DC traction power supply is studied in this chapter. This simulation method combines the train traction calculation with the traction power flow calculation, which calculates the static DC traction network power flow at the current moment according to the train position and current taken at each time point. An improved power flow calculation method and power correction model are proposed to solve the power balance problem of braking locomotives. Taking the data of the

Singapore East–West metro line as an example, a validation test is carried out to show the performance of the power flow simulator.

3.3 DC power supply system configuration

3.3.1 Supply voltages of traction systems

At present, two kinds of traction network are generally used in underground railways in the world. One is a 750 V DC contact rail or third rail power supply system; the rated voltage is 750 V DC, and the allowable voltage fluctuation range is 500–900 V. The other is a 1500 V DC overhead catenary system, with a rated voltage of 1500 V DC and an allowable voltage fluctuation range of 1000–1800 V. Detailed DC railway system nominal voltages and their permissible limits are listed in the BSI standard BS EN 50163 Railway Applications – Supply voltages of traction systems [87].

Table 3. 1 Nominal voltages and their permissible limits for DC railway systems [87]

DC railway system	**Lowest non-permanent voltage V_{min2} [V]**	**Lowest permanent voltage V_{min1} [V]**	**Nominal voltage V_n [V]**	**Highest permanent voltage V_{max1} [V]**	**Highest non-permanent voltage V_{max2} [V]**
DC 600	400	400	600	720	800
DC 750	500	500	750	900	1000
DC 1500	1000	1000	1500	1800	1950
DC 3000	2000	2000	3000	3600	3900

With an increase of voltage level, the investment cost per kilometre distance between substations will also increase. For a 750 V power supply system, the recommended substation spacing is about 4–6 km; for a 1500 V system, the recommended substation spacing is 8–13 km; for a 3000 V system, the recommended spacing is 20–30 km [88]. The spacing and location of each substation shall be set according to local conditions, combined with the surrounding topography, buildings and civil engineering conditions of each substation site, and determined after comprehensive comparison and selection. The capacity of a substation is usually determined by a traction power calculation based on the density of traffic flow, vehicle formation during peak hours of operation, and after comparison of multiple schemes.

The capacity setting of a traction substation shall be designed according to the following principles:

(1) Convenient operation and reasonable power supply to meet the needs of maximum load during peak operation.

(2) When any traction substation in the system breaks down, the overload capacity of its adjacent traction substation shall still ensure the power supply without affecting the normal operation of the train.

3.3.2 Modelling of DC power system and its components

An urban rail transit power supply system is responsible for providing power for vehicles, lighting and other communication equipment. It can be divided into a traction power supply system and an auxiliary power supply system. The traction power supply system provides electric energy for electric vehicles, and is composed of a traction substation and a catenary system; the auxiliary power supply system provides power for all kinds of power equipment such as lighting, escalators, fans, water pumps and communication, automation and other equipment in the station, and is composed of a step-down substation and an auxiliary power distribution line. Figure 3.1 shows the composition of a railway power supply system and the power flow direction, in which the traction power system is the core of the railway power supply system.

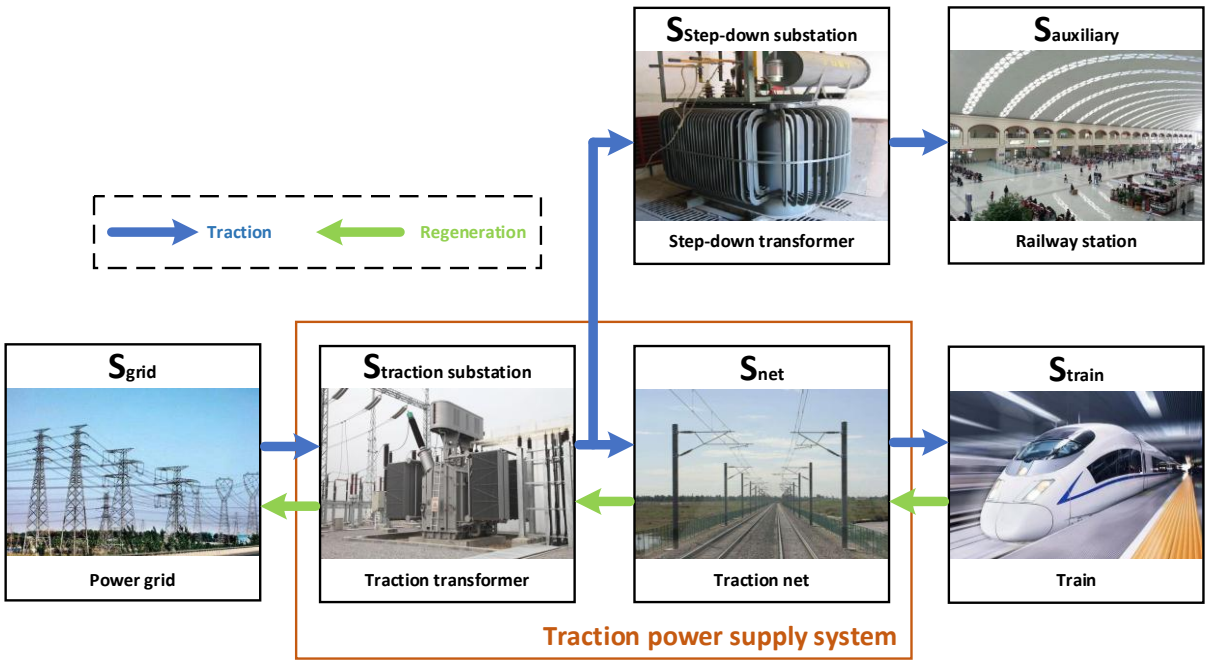

Figure 3. 1 Composition of railway power supply system

In a railway power supply network, the traction rectifier substation is the main power supply providing the required energy for the train. Figure 3.2 [89] shows a typical DC traction grid in which multiple trains are on the up and down tracks at the same time. The rectifier substation receives power from the AC power grid and is connected to the DC busbar after the step-down rectification, which supplies power to the up and down grids.

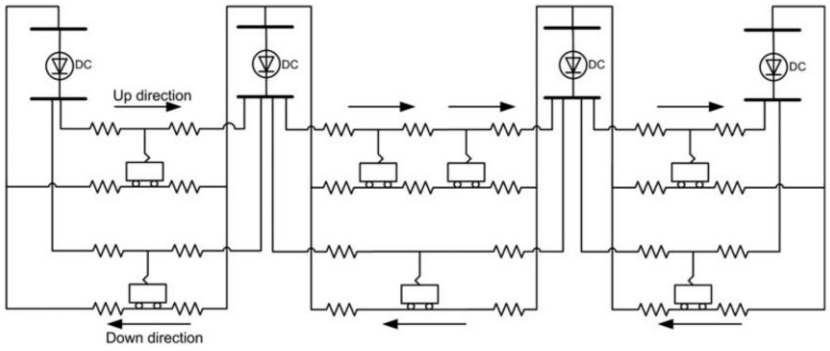

Figure 3. 2 Typical DC traction power supply system [89]

The modelling idea of the simulation model for the traction power supply system is as follows:

According to the electrical characteristics of each component, an accurate mathematical model and calculation equation are determined for each component; combined with the network topology of the traction power supply system, the equivalent mathematical model of the whole power system is established.

3.4 DC railway moving load simulator

The distance between urban rail transit stations is short, the trains start and stop frequently, the daily passenger flow fluctuates greatly, and the number of train departures per hour also changes, which together cause fluctuation of the traction load. Modelling of train load is done to find the mathematical expression that can correctly reflect its motion characteristics. Simulation of the load model is done to simulate changes of train displacement, speed, taking current, power and other changes with time when single or multiple vehicles are running in different periods. After obtaining the dynamic load data, the power flow calculation is carried out and the dynamic simulation of the power supply system is established.

3.4.1 Single-train movement modelling

The train running process is a complex non-linear dynamic process; it is difficult to establish an accurate mathematical model to describe it and solve it. When a train is running, it can be regarded as a particle. In Figure 3.3, F is the traction force acting on the train, B is the braking force, W_0 is the basic resistance, W_j is the additional resistance, and N and G are the supporting force and gravity of the train, respectively. Generally speaking, the study of train operation and simulation mainly considers the external forces on the lateral direction of the train, namely traction force, braking force and resistance, which are the basis of train operation calculations. Traction force and

braking force during train operation can be obtained by checking the tractive effort curve. This section will give a detailed introduction.

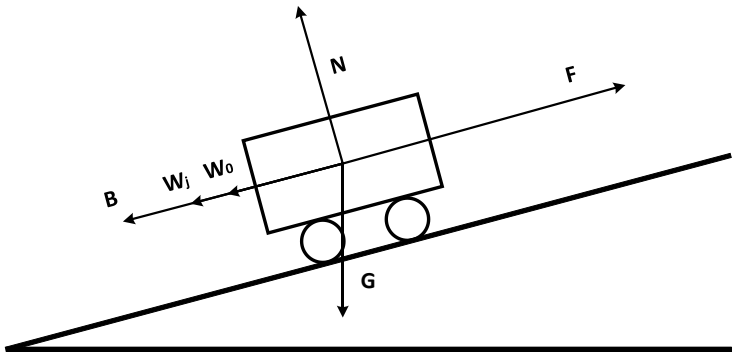

Figure 3. 3 Forces on a moving train

3.4.1.1 Force analysis

The traction force is generated by the power transmission device and can be adjusted in the same direction as the train. The locomotive tractive force *F* can be any value under the traction characteristic curve, as shown in formula (3.1).

$$F = u_f f(V, E_t) \tag{3.1}$$

where u_f is the train tractive factor, $u_f \in [0,1]$, V is the train speed, and E_t is the traction network voltage at the current train location. When simulating a single train running on the line, it is generally considered that the motor works under the rated network voltage.

The braking force is the external resistance to control the train operation. In urban rail transit, resistance braking or regenerative braking is widely used. The braking force *B* is described in formula (3.2).

$$B = u_b f(V, E_t) \tag{3.2}$$

where u_b is the train braking factor, $u_b \in [0,1]$.

In the process of train movement, the inherent resistance caused by mechanical friction, air friction and other factors is called the basic resistance. It is also known as the Davis equation. The calculation of this resistance is complex. In order to simplify the calculation, an empirical formula summarised from experiments is generally used. The basic resistance formula for a train is generally expressed as a quadratic function of the locomotive speed, as shown in (3.3). It is difficult to predict the Davis coefficients a, b and c from the theoretical calculation. Their values are usually determined by empirical experiments [90].

$$W_0 = a + bv + cv^2 \tag{3.3}$$

The additional resistance includes ramp resistance, curve resistance and tunnel resistance, which is also an important parameter for train traction calculation.

$$W_j = W_i + W_r + W_s \tag{3.4}$$

where W_i is the unit slope resistance, W_r is the unit curve resistance, and W_s is the unit tunnel resistance (their units are all N/kN).

3.4.1.2 Train motion equations

There are three working conditions for an urban rail train running on the line: traction, coasting and braking [89]. The traction condition includes motoring and cruising. Figure 3.4 shows an example of a train speed curve in which the four working

conditions occur in sequence. In motoring mode, the power is used to accelerate the train. Cruising means the train is driven at a constant speed, while braking is the phase in which the vehicle decelerates. While coasting, the train is actually moving without being propelled by the engine, so it does not consume energy.

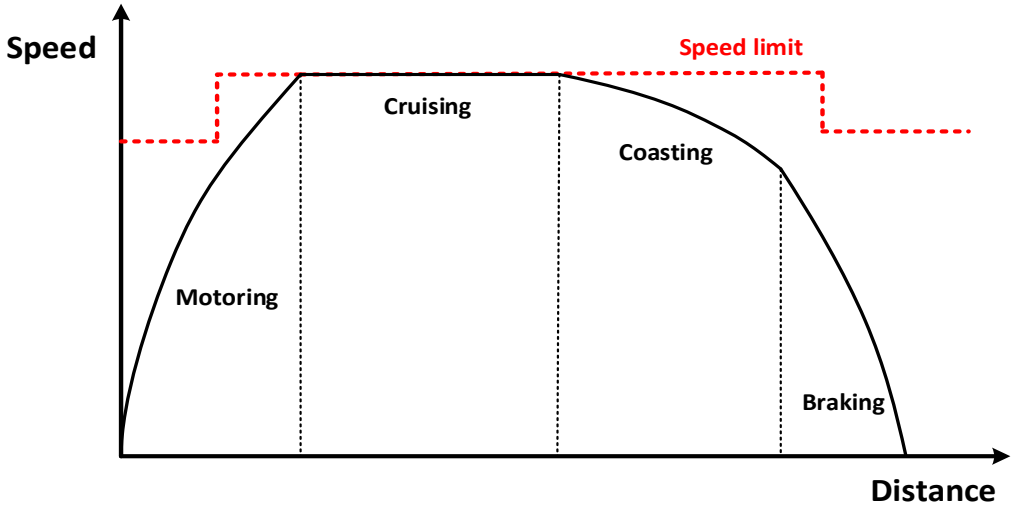

Figure 3. 4 Train speed profile with four working conditions

(1) Traction condition

During traction operation, the resultant force acting on the train is:

$$C = F - W_k \tag{3.5}$$

where F is traction force (N), and W_k is the total resistance during train movement (N).

(2) Coasting condition

When coasting, the traction force is 0, and the resultant force acting on the train is:

$$C = -W_k \tag{3.6}$$

(3) Braking condition

When braking, the resultant force on the train is:

$$C = -(B + W_k) \tag{3.7}$$

where B is braking force (N), and W_k is the total resistance during train movement (N).

According to Newton's law of motion, acceleration can be calculated by knowing the mass of the object and its resultant force, and then the velocity and displacement can be calculated.

The acceleration of the train can be calculated as:

$$a = \frac{dv}{dt} = \frac{C}{m} \tag{3.8}$$

where *m* is the total mass of the train (kg).

The speed of the train is:

$$v = \int_{t_1}^{t_2} a\, dt \tag{3.9}$$

The distance travelled by the train is:

$$s = \int_{t_1}^{t_2} v\, dt \tag{3.10}$$

In a traction simulation calculation, the initial speed at any time is V_1, and the position is S_1. If each time interval Δt of train operation is small enough, it can be considered that in this time period, the force and acceleration are kept unchanged at the initial position of S_1, then the next simulation speed and position of a train are:

$$V_2 = V_1 + a\Delta t$$
$$S_2 = S_1 + \frac{{V_2}^2 - {V_1}^2}{2a} \tag{3.11}$$

3.4.1.3 Tractive effort characteristic curve

The tractive effort curve describes the relationship between traction and train speed. It is produced by a traction motor to overcome resistance and gravity. Different motors will produce different traction curves. However, the tractive effort curve has several common characteristics that can be used to summarise most traction systems. It is generally divided into three sections, as shown in Figure 3.5.

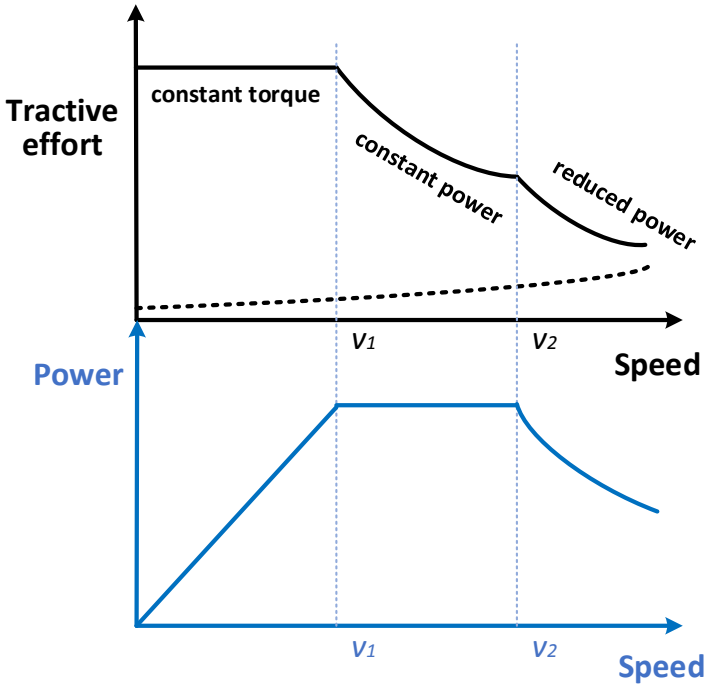

Figure 3. 5 Tractive effort curve

1) Calculation of train traction in constant torque area

In the constant force area, the traction force of the train is constant, and the resistance increases with the increase of speed in the starting process, resulting in a gradual decrease of the resultant force and the acceleration of the train. The analysis shows that the acceleration of the train decreases to a minimum at the end of the constant force area (constant power point). Therefore, the traction force of the train in the constant force area can be calculated according to the constant power point parameters. The calculation process is as follows: according to the requirements of the constant power point speed v_1 and the minimum acceleration of the train, the running resistance $f = f(v_1)$ of the train at the constant power point is calculated, and the minimum acceleration a_{min} in the constant force area is taken as the constant power point

acceleration. Then, the initial acceleration is inverted by time step, and a check of whether the calculation can meet the starting requirements is made. The calculation formula is as follows:

$$F(v) = F_{max} = ma_{min} + f(v_1), \qquad v \in (0, v_1] \tag{3.12}$$

2) Calculation of train traction in constant power area

In the constant power area, the train operates at constant power P_S. The power of the train in the two sections before and after the constant power point is equal, so the power in the constant power area is:

$$P(v) = P_s = F(v_1) \times v_1 = F_{max} \times v_1 \tag{3.13}$$

The relationship between traction force and speed in constant power area is as follows:

$$F(v) = \frac{P_s}{v}, \qquad v \in (v_1, v_2] \tag{3.14}$$

where v_2 is the speed at the power reduction point.

The product of traction force and train speed is a constant.

3) Calculation of train traction in reduced power area

In the reduced power area, the train power decreases gradually, and the traction force is inversely proportional to the square of the velocity, as described in formula (3.15). M is a constant. The product of traction force and the square of train running speed is a constant.

$$F(v) = \frac{P_s}{v} = \frac{M}{v^2} \tag{3.15}$$

However, the power of the train at the power reduction point v_2 is still P_S, according to which the coefficient M can be calculated:

$$F(v_2) \times v_2 = P(v_2) = P_s \quad (v = v_2)$$

$$\Rightarrow F(v_2) = \frac{P_s}{v_2} = \frac{M}{{v_2}^2} \tag{3.16}$$

$$\Rightarrow M = P_s \times v_2$$

The relationship between traction force and speed in the reduced power area is as follows:

$$F(v) = \frac{M}{v^2} = \frac{P_s \times v_2}{v^2}, \qquad v \in (v_2, v_{max}] \tag{3.17}$$

The relationship between power and speed is as follows:

$$P(v) = F(v) \times v = \frac{P_s \times v_2}{v}, \qquad v \in (v_2, v_{max}] \tag{3.18}$$

3.4.1.4 Selection of braking point

The process of the train entering the station is the deceleration process of the train under the braking force, in which the braking force and resistance direction of the train are the same. The arrival process can also be regarded as the reverse process of the train starting from the station and carrying out traction acceleration in the opposite direction. The resultant force of the train is the sum of braking force and resistance.

A computer is used to simulate the train movement process, the time interval is 0.1 s, and the speed and distance of the train shall be calculated at each time step. When the braking distance plus driving distance is greater than or equal to the distance between stations, the braking calculation shall be carried out at the next time step.

The calculation formula of braking acceleration is:

$$a = \frac{0^2 - {v_e}^2}{l - s} \tag{3.19}$$

where v_e is the vehicle speed at the last moment of electric braking (m/s), s is the running distance of the locomotive at the last moment of electric braking (m), and l is the distance between stations (m).

3.4.1.5 Development of STS

Based on vehicle characteristics and route data, a single-train movement simulator (STS) has been developed in MATLAB. Vehicle characteristics include vehicle mass, traction parameters and resistance parameters. The route data include gradient, route speed limit, station locations and dwell time. Different driving strategies are defined by the user as dynamic inputs of the simulator. The output of the simulator is the train speed profile, power requirements, traction energy consumption, journey time, etc. Figure 3.6 describes the main structure of the single-train simulator.

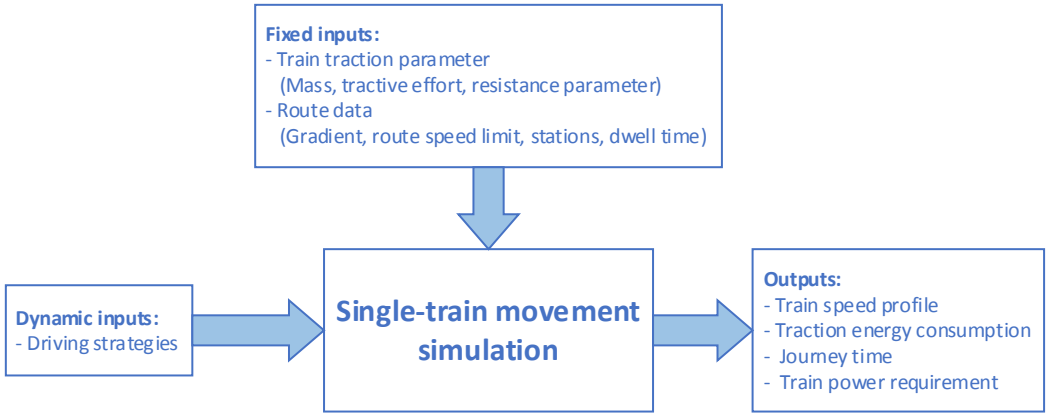

Figure 3. 6 Structure of single-train movement simulator

Based on the above equations and the programming structure, a time-based single-train movement simulator has been developed. The whole journey is discretised in time, and the working condition of the train is the combination of vehicle states in each time step. Figure 3.7 describes the calculation process for a vehicle moving in each time step. It also shows the relationship between distance and time and the relationship between speed and time. Each time interval is represented by Δt. The train driving strategy is represented by the sequence of traction values in each time step. During each time interval, the traction force is set to a constant. According to the driving strategy at each time step, the state of the vehicle, such as acceleration, speed, position and power, is calculated.

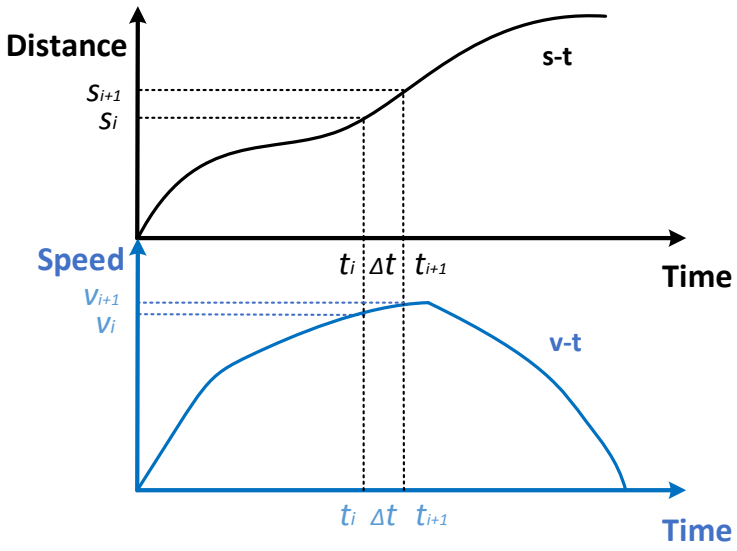

Figure 3. 7 Time-based vehicle movement calculation

The calculation steps of train inter-station operation are as follows:

(1) Program initialisation. The discrete time interval dt = 0.1 s. At the i = 0 time point, the train is at the starting point. The resultant force $F(i)$ = 0, acceleration $a(i)$ = 0, speed $v(i)$ = 0, and displacement $s(i)$ = 0. The working condition flags h1, h2, h3 and h4 represent the motoring, cruising, coasting and braking conditions respectively, and are valid when the flag is equal to 1. The initial state of the flag bit is h1 = 1, h2 = 0, h3 = 0, h4 = 0;

(2) According to the flag bit, judge the working condition of the locomotive at the i = i + 1 time point, find out the resultant force $F(i + 1)$ of the train under the corresponding working condition, and then find out the acceleration, speed and displacement at the i + 1 time point;

(3) If $v(i)$ is less than or equal to 0, the calculation ends; otherwise, continue to the next step;

(4) According to the braking distance s(brake) under speed $v(i)$, it is judged whether $s(i) + s$(brake) is greater than the distance between stations. If it is greater, braking calculation shall be carried out at the next time point. Set h3 to 1 and other flag positions to 0, and return to step (2) for calculation at the next time point; otherwise, continue to the next step;

(5) Judge whether the conditions are met: h1 is equal to 1 and $v(i)$ is greater than or equal to V_{max}. If the conditions are met, it means that the train speed has reached the maximum speed under the traction condition. It should enter the cruise condition at the next time point, modify the corresponding flag bit, set h2 to 1; otherwise, continue to the next step;

(6) Judge whether to choose coasting. Set h3 to 1 if coasting is applied. Return to step (2) and repeat the above steps.

According to the above steps, the flow chart of the STS is designed as shown in Figure 3.8.

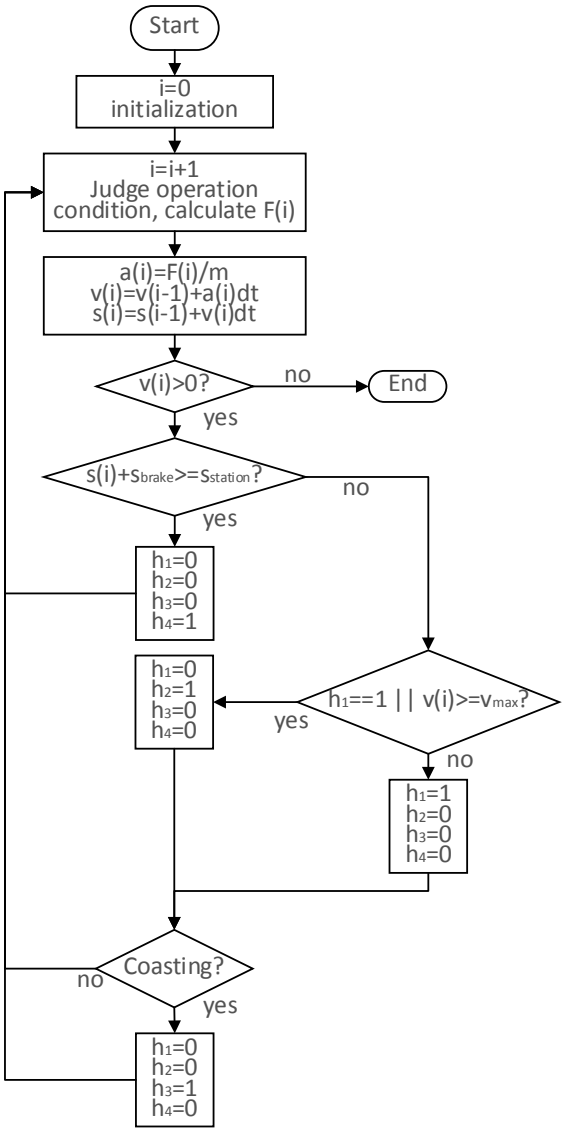

Figure 3. 8 Flow chart of single-train movement simulator

Figure 3.9 shows an example of the curves of train speed and power with time between two stations. In the train traction calculations, the power consumed by the train in the process of moving will be the basic load data of the power flow calculation.

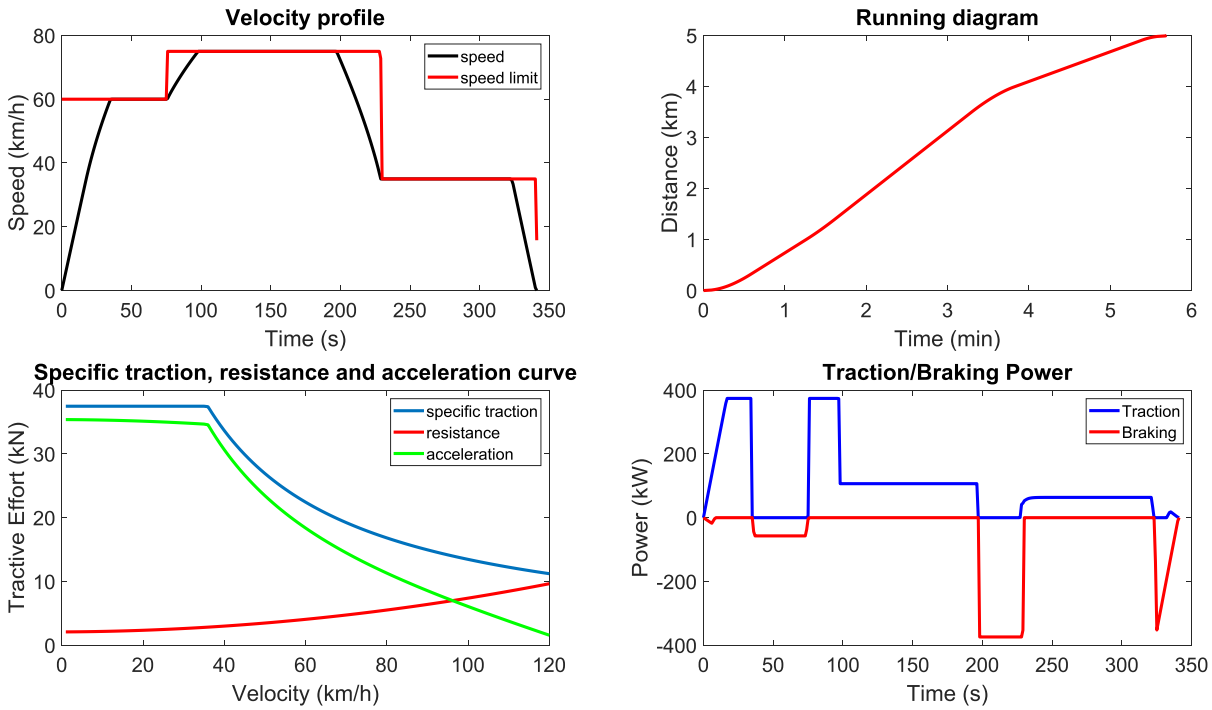

Figure 3. 9 Example train performance curves between two stations

3.4.2 Multi-train power network modelling

There are two models of DC traction network power flow calculation: a linear system model based on node voltage and current [83, 91, 92], and a non-linear system model based on node power [93, 94]. In the linear system model, the train can be represented by the ideal current source or admittance model. The ideal current source model is more recommended in the linear system model because of its shorter operation time and convenient calculation of regenerative braking. In the non-linear system model, the power source is used to model the train, and the power value at a certain time is determined by the traction calculation results and the operation diagram. Because of

convergence, the solution of a non-linear system is more complex than that of a linear system. There are two kinds of mathematical method to solve the linear system model of a DC traction network: direct methods such as the Gauss elimination method, Cholesky decomposition method and Zollenkopf's bifactorisation [95-97]; and iterative methods such as the Newton–Raphson iterative method, Gauss–Seidel algorithm and Incomplete Cholesky Conjugate Gradient (ICCG) algorithm [93, 98, 99]. In order to simplify the calculation, this research uses a linear system model to model the traction power supply system, that is to say, the ideal current source is used to represent the mathematical model of the train.

The idea of modelling and solving the simulation model of a traction power supply system is to branch the DC traction power supply network at a certain time, establish the admittance matrix of the network and then solve the grid model at each time point through iterative calculation.

3.4.2.1 Model of DC traction power supply system

During the operation of the train, the current is taken from all traction substations of the whole line connected by the traction network, and the position of the train is constantly changing, so the traction power supply system is a complex time-varying network. But at a certain time, it can be considered that the position and power consumption of the train are constant, the voltage of the traction substation is constant and the corresponding network is a static network. In this way, the node voltage equations of

the network can be solved by numerical method, and the power flow of the traction power supply system at this time can be obtained. Then, the network parameters of the next time point can be obtained from the train traction calculation, and the calculation can be restarted until the simulation is finished.

The power supply calculation method in this chapter considers the traction of the whole line as a complete network and is based on the following assumptions:

1. The locomotive is equivalent to a constant power source and takes current from the traction network. The power consumption of the locomotive at a certain time and position is given by traction calculation results;
2. The type of locomotive running on the line is the same;
3. Each train adopts the same driving strategy;
4. The rectifier unit of the whole line is regarded as the voltage source branch with internal resistance;
5. The whole DC traction network system has the same resistance per unit length;
6. The locomotives of the whole line run in strict accordance with the specified schedule.

The power supply system model of a DC traction network is shown in Figure 3.10.

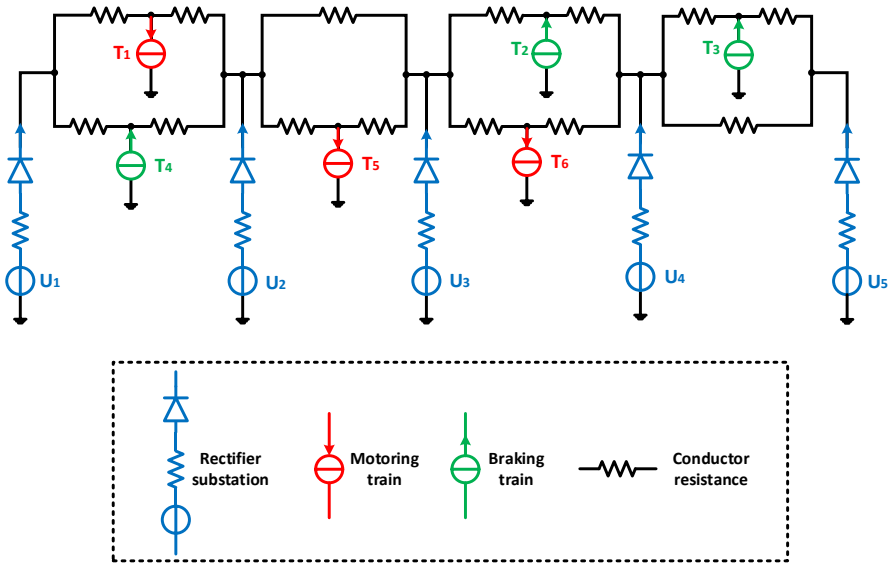

Figure 3. 10 Equivalent circuit diagram of a DC traction power supply system

When modelling the traction network, it is assumed that the impedance per unit length of the whole catenary and return rail is the same. The equivalent circuit of the contact lines is shown in Figure 3.11. The contact rail network is replaced by resistance $R = l \times r$, where l is the length of the contact rail and r is the resistance per unit length of the contact rail.

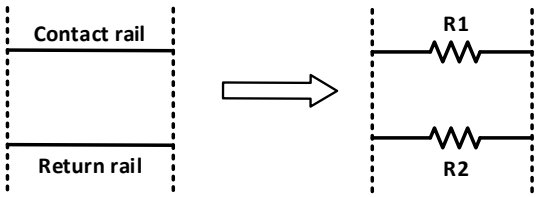

Figure 3. 11 Equivalent circuit of contact lines

In order to form the node voltage equation, the series internal resistance of the voltage source is equivalent to the parallel internal resistance of the current source by using Thevenin's theorem, as shown in Figure 3.12.

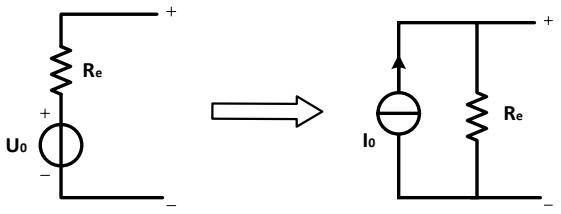

Figure 3. 12 Equivalent circuit of traction substation

The voltage regulation characteristics of traction substation can be simplified as a linear model, as shown in Figure 3.13. Thus, the equivalent resistance R_e is calculated as:

$$R_e = \frac{\Delta V}{\Delta I} = \frac{V_{noload} - V_{rated}}{I_{rated} - 0} \tag{3.20}$$

Where V_{noload} is the substation no-load voltage, V_{rated} is the substation rated voltage, I_{rated} is the substation rated current.

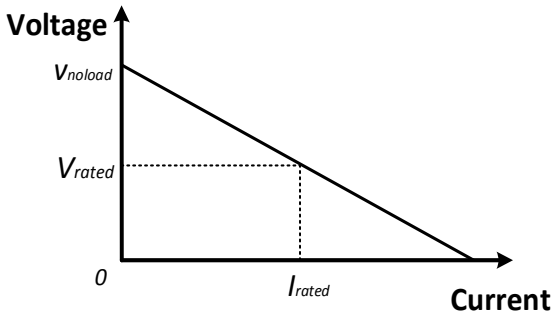

Figure 3. 13 Traction substation voltage regulation characteristics

The traction substation energy loss $E_{sub\ loss}$ is calculated as:

$$E_{sub\ loss} = {I_{sub}}^2 \times R_e \tag{3.21}$$

In the simulation of DC traction power supply, the ideal current source model is used to represent the train [100-103], that is, the train is equivalent to a current source, and

the current value at a certain operation time is determined by the traction calculation results. Figure 3.14 is the circuit diagram of the train equivalent model. The positive and negative directions of the current represent the operation conditions of the train. If the current is positive, it means the train is in a traction condition; if the current is negative, it means the train is in a regenerative braking condition.

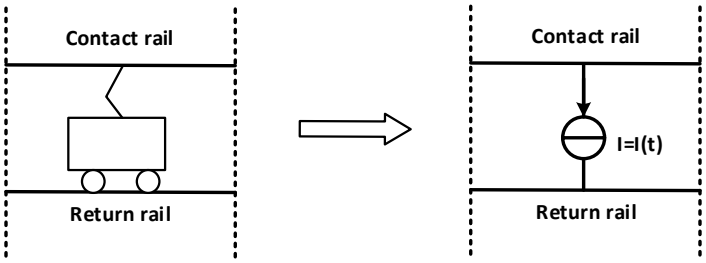

Figure 3. 14 Equivalent circuit of train current source model

When the train is under the traction condition, the traction power is:

$$P_{train} = P_{traction} = UI \tag{3.22}$$

The power consumed by the train is the sum of traction power and auxiliary power:

$$P_{total} = P_{train} + P_{auxiliary} \tag{3.23}$$

Suppose the input power of traction motor is P_M and the working efficiency of the inverter is η ($\eta < 1$), then:

$$P_M = P_{train} \times \eta \tag{3.24}$$

When the train is under regenerative braking, the traction motor operates as a generator and sends back power to the DC power grid. At this time, the pantograph current of the train is:

$$I = -\frac{P_M \eta}{U} \tag{3.25}$$

When the train is in the coasting condition, no electrical power is generated; only the auxiliary system consumes power. At this time, the current taken by the train pantograph is the auxiliary system current.

3.4.2.2 Current vector iterative method

The DC traction power supply system shown in Figure3.10 can be described by the following node voltage equation:

$$[Y][U]^{(n+1)} = [I]^{(n)} \tag{3.26}$$

where *n* is the number of iterations, $[Y]$ is the nodal admittance matrix of $m \times m$, and *m* is the number of nodes. $[I]^{(n)}$ is the current column vector injected by the node in the *n*th iteration, and $[U]^{(n+1)}$ is the object quantity.

In order to form the node voltage equation, the locomotive model is also transformed from a constant power source to an ideal current source, and the current value is calculated by the following formula:

$$I_i^{(n)} = P_i / U_i^{(n)} \tag{3.27}$$

where I is the locomotive number and P_i is the locomotive power of I, which is constant in the iterative calculation process.

$[I]$ is the node current vector corresponding to $[Y]$, which is composed of the current injected by the traction station and the current injected by the locomotive. The initial voltage of the locomotive is the rated voltage of the system. Substitute the initial current of the locomotive calculated from formula (3.22) into formula (3.26) to obtain a new locomotive voltage, then replace the new locomotive voltage into formula (3.27) to update the locomotive current, repeat the loop until the train voltage deviation reaches the allowable value, and the iteration stops.

With a change of time and position, when the train node and the traction substation node overlap or the train runs near the traction substation, the mutual admittance between the two nodes is very large, then the train node should be removed and the traction substation node should be retained.

3.4.3 Energy consumption calculation

The formula for calculating energy consumption is the integration of power and time during operation time, which can be obtained by the integral of the product of instantaneous voltage and instantaneous current. The formula for calculating train energy consumption E_{train} and substation energy consumption E_{sub} is as follows:

$$E_{sub} = \int_0^T \sum_{n=1}^{n_s} (V_{n_s}(t) \times I_{n_s}(t))\, dt \tag{3.28}$$

$$E_{train} = \int_0^T \sum_{n=1}^{n_t} (V_{n_t}(t) \times I_{n_t}(t))\, dt \tag{3.29}$$

where T is the total operation time, n_s is the number of substations, V_{n_s} is the instantaneous voltage of a substation, I_{n_s} is the instantaneous current of a substation, n_t is the number of trains, V_{n_t} is the instantaneous voltage of a train, and I_{n_t} is the instantaneous current of a train.

In the process of power transmission, there will be some energy loss. This energy loss can be classified into substation loss, train loss and transmission line loss.

$$E_{loss} = E_{sub\ loss} + E_{train\ loss} + E_{transmission\ loss} \tag{3.30}$$

The energy balance equation of the whole railway network can be expressed by (3.31):

$$E_{sub} + E_{regen} = E_{train} + E_{loss} \tag{3.31}$$

where E_{regen} is the train regenerative energy. Regenerative braking uses the inertia of the vehicle to drive the motor to produce reverse torque, which converts part of the kinetic energy or potential energy into electric energy and stores or uses it. Therefore, it is a process of energy recovery and can be used for energy saving. Research has shown that the regenerative braking efficiency of metro trains is around 20–30% [104-106].

3.5 Load flow simulation

Power flow calculation is the core of the traction power supply simulation model. Due to the complexity of the topological structure of the traction power supply system, it is difficult for the traditional power flow calculation method to converge in the iterative calculation.

The basic idea of dynamic power flow calculation is that: according to the characteristics of the traction load at any time, establish a real-time mathematical model of a traction power supply system, regard the Electric Multiple Units (EMU) as the power load (its size can be given by STS); according to the voltage between the contact line and the rail, update the real-time equivalent current of the EMU, and then calculate the voltage of each node of the traction power supply system until each node voltage converges. Combined with the real-time model of the traction power supply system, the power flow calculation is carried out to calculate the voltage and current distribution of the traction power supply system at this time.

3.5.1 Power balance in regenerative braking

In the iterative calculation process, the locomotive is represented by the current source. In the node voltage equation of the current vector, the current injected into traction network by the traction locomotive is negative, while the current injected into the traction network by the braking locomotive is positive. If there are fewer traction

locomotives and more braking locomotives in the system at a certain time, the regenerative braking locomotive voltage may exceed the maximum allowable voltage.

In actual operation, the on-board braking resistor should be put into use to absorb the excess braking power and limit the voltage to the maximum allowable voltage U_{max} of the locomotive. In the power flow calculation, the regenerative braking power must be reduced to an appropriate level to bring the locomotive voltage within the limit. The most direct way to solve this problem is to gradually reduce the regenerative braking power until the regenerative braking locomotive voltage drops to U_{max}.

However, this will lead to another problem. Because all locomotive models are represented by ideal current sources, the high voltage will cause all rectifier units in the traction substation to reverse cut-off, and the DC traction network will behave as a high-resistance state. The DC traction loop will become the wrong network, which will cause the power flow calculation to be unable to converge.

In order to solve this problem, a model of internal resistance in a series voltage source is proposed to represent the over-voltage regenerative braking locomotive. The value of the voltage source is set as the maximum allowable voltage U_{max} of the locomotive (such as 1800 V), which is referred to as the voltage model in reference [91]. It is also called the power correction model of the regenerative braking locomotive.

The advantage of the voltage model is that it can ensure that the voltage of the braking locomotive will not exceed the limit. The process of power flow calculation based on

this model is simple. After the solution of the node voltage equation is obtained by the current vector iteration method, the DC bus voltage of the traction substation and the terminal voltage of the regenerative brake are tested. If the voltage of the regenerative braking locomotive is greater than the maximum allowable voltage of the locomotive, the current source will be changed to the voltage model, and the program will automatically reconstruct the network and calculate again. This is repeated until the voltage of any node does not exceed the limit. Then the power of each regenerative braking locomotive is compared with its available power (provided by traction calculation). If the locomotive power is greater than the available power, it means that the voltage of this locomotive cannot reach the maximum allowable voltage when it operates at the available power. At this time, the locomotive will be changed to the ideal current source model, and then the program repeats the above process again.

3.5.2 Timetable formulation

The departure interval (headway) of the trains in a specific period of time is fixed. The displacement curve of a single train running in the whole process is regarded as the running curve of the first train, and the curve is shifted to the right according to the integral times of departure interval, then the running curves of the second, third and subsequent trains with time change can be obtained. When these curves are drawn on a single diagram, the train operation diagram of this period is formed.

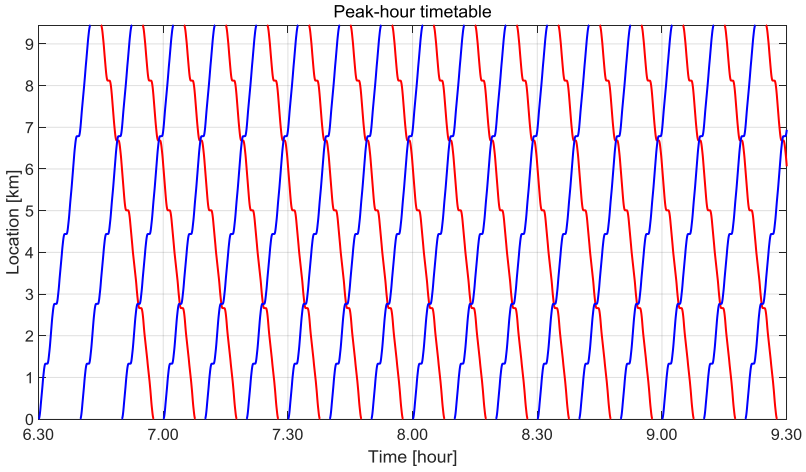

Figure 3. 15 Peak-hour timetable

In Figure 3.15, the horizontal axis is time and the vertical axis is distance. The running track of each train is a continuous curve. The train operation diagram is drawn in strict accordance with the train headways.

3.5.3 Development of MTS

Based on the modelling method of a moving load and power network described in Chapter 3.4, a multi-train simulator (MTS) has been developed to evaluate the power flow and energy consumption in a DC railway system. The structure of MTS is shown in Figure 3.16. The power output of STS is taken as the input parameter of the power network simulation, and the parameter requirement of the train timetable is the dynamic input of MTS. Through MTS simulation, the output is substation power, energy consumption, power loss, etc. Its dynamic input (driving strategy and timetable) can be modified according to different needs to optimise energy consumption and reduce

power loss. The simulator will also be used as the main software to evaluate the impact of load on the traction power supply system.

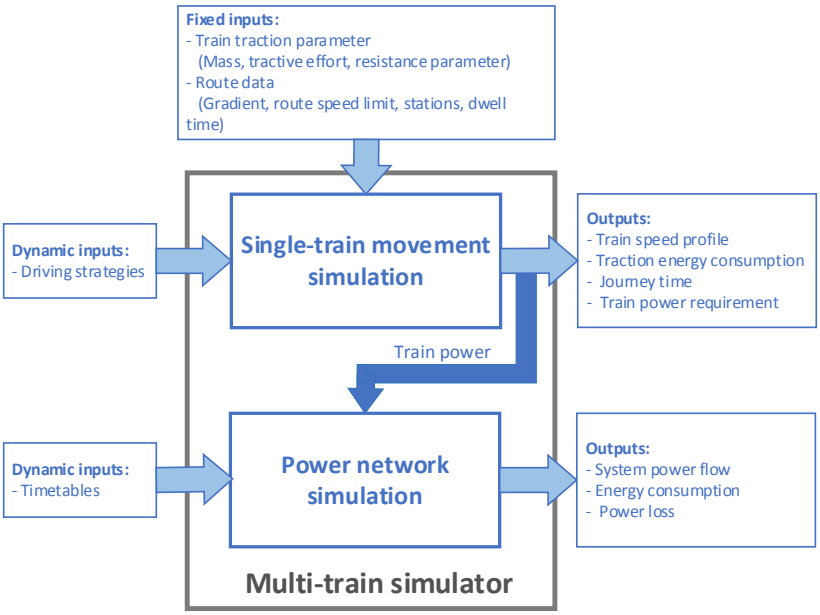

Figure 3. 16 Structure of multi-train power simulator

The specific implementation steps of MTS are as follows:

(1) Input no-load DC voltage, locomotive power requirements from STS;

(2) According to the node voltage and locomotive power, the locomotive current train vector is obtained; according to Thevenin's equivalent theorem, the current vector of the traction substation is formed; finally, the current vector corresponding to the node admittance the matrix is formed, and the node voltage equation is established;

(3) Solve the node voltage equation;

(4) Judge whether the voltage of the braking locomotive is greater than U_{max}. If it is greater than U_{max}, change it to the modified power model and return to step (2) for recalculation, otherwise continue to the next step;

(5) Judge whether the calculation results converge;

(6) Output the power flow calculation results of the DC traction network.

According to the above steps, the flow chart of MTS is designed as shown in Figure 3.17.

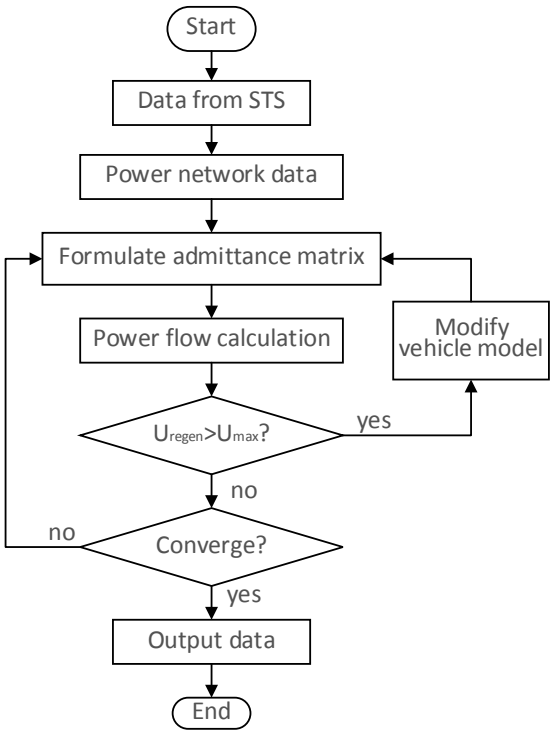

Figure 3. 17 Flow chart of multi-train power simulator

3.6 Case study

3.6.1 Singapore line

In this study, the Singapore East–West line is used as a simulation example. It is a high-capacity metro line operated by SMRT, which is 49.46 km in length with 27 substations, 8 tie stations and 2 stations without a DC-link connection. Figure 3.18 shows the Singapore line's altitude and traction power supply system locations.

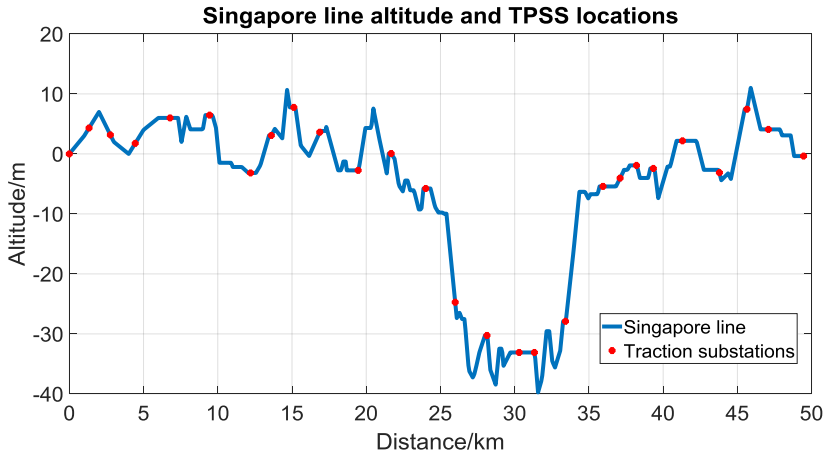

Figure 3. 18 Altitude and station locations of the Singapore line

Table 3.2 lists the vehicle traction parameters. The train uses a 750 V DC third rail power supply and is equipped with a regenerative braking system. The total mass is 300 tonnes with passenger load at AW4. In this research and simulation, the influence of different passenger flow on the train mass and energy consumption is not considered. In fact, in real train operation, the uncertainty caused by passenger flow should be taken into consideration.

Table 3. 2 Train traction characteristics

Parameter	Value/equation
Overall train mass [tonnes]	222.8
Train formation	6 cars, [DT–M1–M2] + [M2–M1–DT]
Train length [m]	140.9
Rotary allowance	0.14 (MT), 0.05 (DT)
Train resistance [N/tonne]	$2.3+(0.6v^2 \times 10^{-3})$ (V: km/h)
Maximum acceleration rate [m/s]	1.2
Maximum braking rate [m/s]	1.2
Maximum traction power [kW]	2414
Maximum braking power [kW]	2414
Maximum operation speed [km/h]	80
Maximum tractive effort [kN]	349
Dwell time [s]	45
Safety margin [m]	100
Train mass (with passenger load AW4) [tonnes]	300
Auxiliary power [kW]	480

There are 27 substations on the East–West line as shown in Table 3.3. Table 3.4 shows the data of the other eight tie stations along the route.

Table 3. 3 Substation data of East–West line

	Platform	Abbreviation	Location [m]	Traction power	Rectifier rating
1	Tuas Link	TLK	0	TPSS	2 MW × 2
2	Tuas West Road	TWR	1330	TPSS	2 MW × 2
3	Tuas Crescent	TCR	2765	TPSS	2 MW × 2
4	Gul Circle	GCL	4440	TPSS	2 MW × 2
5	Joo Koon Station	JKN	6787	TPSS	2 MW × 2
6	Pioneer Station	PNR	9449	TPSS	3 MW × 2
7	Lakeside	LKS	12210	TPSS	2 MW × 2
8	Chinese Garden	CNG	13606	TPSS	2 MW × 2
9	Jurong East	JUR	15125	TPSS	2 MW × 2

10	Sungei Uiu Pandan Online	SUO	16869	TPSS	2 MW ×2
11	Commonwealth Online	CWO	19456	TPSS	2 MW ×2
12	Buona Vista	BNV	21678	TPSS	2 MW ×2
13	Queenstown	QUE	24011	TPSS	2 MW ×2
14	Delta Online	DLO	25992	TPSS	2 MW ×2
15	Outram Park	OTP	28133	TPSS	2 MW ×2
16	Raffles Place	RFP	30299	TPSS	2 MW ×2
17	City Hall	CTH	31325	TPSS	2 MW ×2
18	Lavender	LVR	33421	TPSS	2 MW ×2
19	Aljunied	ALJ	35947	TPSS	2 MW ×2
20	Paya Lebar	PYL	37099	TPSS	2 MW ×2
21	Eunos	EUN	38201	TPSS	2 MW ×2
22	Kembangan	KEM	39337	TPSS	2 MW ×2
23	Bedok	BDK	41301	TPSS	2 MW ×2
24	Sungei Bedok Online	SBO	43787	TPSS	2 MW ×2
25	Simei	SIM	45641	TPSS	2 MW ×2
26	Tampines	TAM	47087	TPSS	2 MW ×2
27	Pasir Ris	PSR	49458	TPSS	2 MW ×2

Table 3. 4 Tie station data of East–West line

	Platform	**Abbreviation**	**Location [m]**	**Traction power**	**Rectifier rating**
1	Boon Lay Station	BNL	10441	Tie	-
2	Clementi	CLE	18613	Tie	-
3	Commonwealth	COM	22782	Tie	-
4	Redhill	RDH	25384	Tie	-
5	Tanjong Pagar	TPG	29119	Tie	-
6	Bugis	BGS	32309	Tie	-
7	Kallang	KAL	34515	Tie	-
8	Tanah Merah	TNM	43165	Tie	-

The power network parameters of the East–West line are shown as follows:

Table 3. 5 Power network characteristics

Parameter	Data
Rectifier no-load voltage [V]	780
Rectifier normal voltage [V]	717
Rectifier rating [MW]	2 MW × 2 or 3 MW × 2
Feeder cable resistance [mΩ]	For 2 MW stations, the resistance per feeder is 3.6 mΩ For 3 MW stations, the resistance per feeder is 2.4 mΩ
Rail resistance [Ω/km]	0.028
Rail resistance per track [Ω/km]	0.007
Track to earth resistance [Ω/km]	10
Third rail resistance [Ω/km]	0.007

The British Standard for Railway Applications – Supply voltages of traction systems [107] is taken as the reference for the voltage limit simulation; the voltage characteristics including under-voltage and over-voltage levels for DC railways are specified in Table 3.6.

Table 3. 6 Voltage permissible limits for DC railways [107]

DC railway system	**Lowest non-permanent voltage V_{min2} [V]**	**Lowest permanent voltage V_{min1} [V]**	**Nominal voltage V_n [V]**	**Highest permanent voltage V_{max1} [V]**	**Highest non-permanent voltage V_{max2} [V]**
DC 750	500	645.3	717	900	1000

3.6.2 Simulation results

3.6.2.1 Train operation simulation

In this case study, the route speed limit is 80 km/h, the vehicle maximum speed is 75 km/h, the speed restriction through stations is 60 km/h and the station dwell time is 45 s. Based on the train traction characteristics and line data shown above, the train operation simulation results are presented in Figure 3.19 and Figure 3.20. The single journey time for eastbound and westbound operation is 4513 s and 4525 s respectively (with station speed limits at 60 km/h).

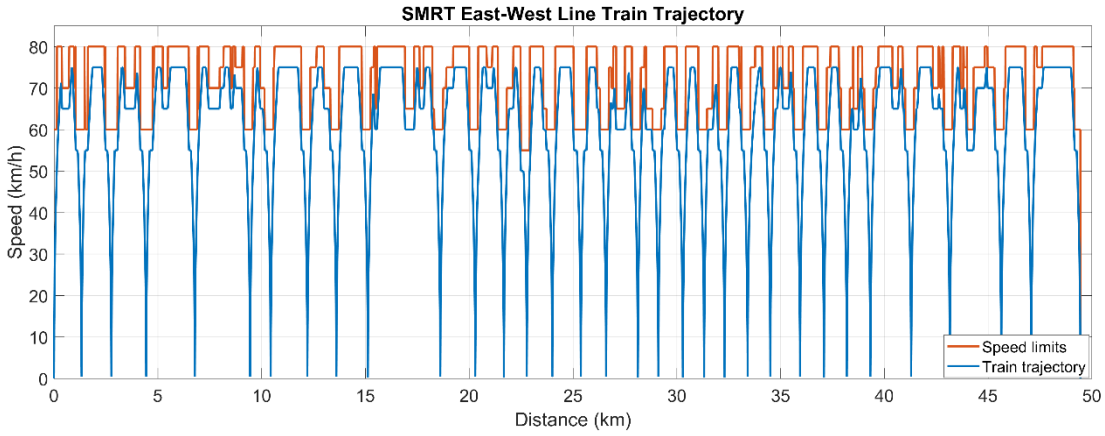

Figure 3. 19 SMRT East–West line eastbound train operation

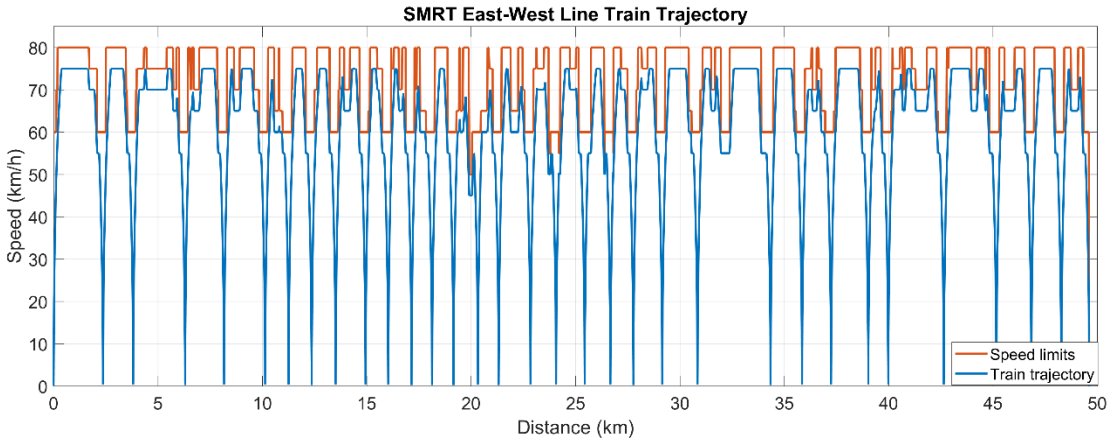

Figure 3. 20 SMRT East–West line west bound train operation

3.6.2.2 Power flow simulation

Figure 3.21 shows a screenshot of the multi-train power simulator. The simulation time for a whole day's train operation on an 8 GB memory, 2.3 GHz Dual-Core Intel Core i5 computer is approximately 10 hours.

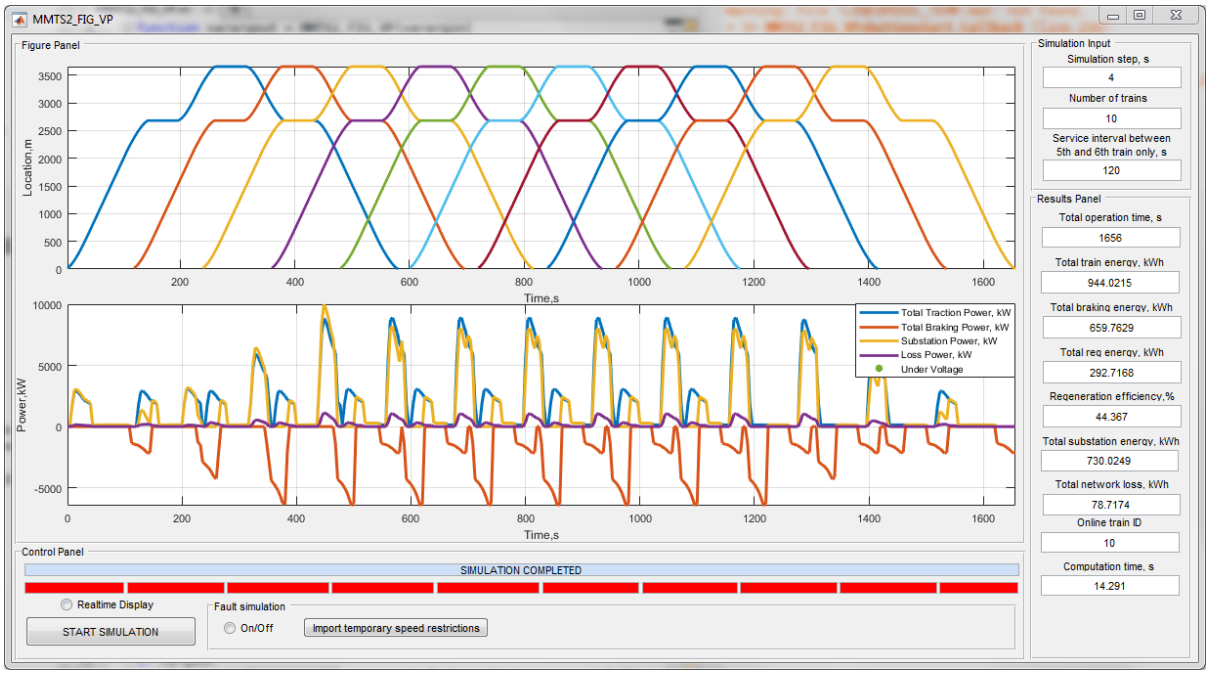

Figure 3. 21 Screenshot of the multi-train power simulator

The simulation results for power flow and energy consumption are analysed in this section. In this case study, the timetable headway is set as 120 s. The multi-train operation repeats every headway period. The operation time of the Singapore East–West line is from 5 a.m. to 11 p.m. The whole day's schedule of the Singapore metro line is simulated in MTS, and the results for energy consumption, system energy loss, average power, current and voltage of each substation are obtained. The total system energy loss is the sum of substation, feeder and transmission loss. The loss accounts for around 10% of the total substation energy consumption. The specific values are listed in Table 3.7.

Table 3. 7 MTS results for each TPSS during 18-hour operation

		Energy consumption [MWh]	System energy loss [MWh]	Maximum traction power [MW]	Average traction power [MW]	Average current [A]	Average voltage [V]
1	**TLK**	26.87	0.05	0.85	0.73	1079	762
2	**TWR**	37.45	0.08	1.50	1.29	1925	748
3	**TCR**	54.68	0.14	2.57	2.21	3353	724
4	**GCL**	73.63	0.25	4.53	3.90	6190	677
5	**JKN**	59.20	0.20	3.64	3.13	4874	699
6	**PNR**	112.85	0.38	6.94	5.97	9509	674
7	**LKS**	70.90	0.24	4.36	3.75	5937	681
8	**CNG**	63.38	0.17	3.10	2.67	4099	712
9	**JUR**	56.97	0.15	2.71	2.33	3547	721
10	**SUO**	59.67	0.20	3.67	3.16	4916	698
11	**CWO**	58.68	0.20	3.61	3.11	4829	699
12	**BNV**	88.10	0.29	5.42	4.66	7573	654
13	**QUE**	85.04	0.28	5.23	4.50	7275	659
14	**DLO**	80.62	0.27	4.96	4.27	6850	666
15	**OTP**	70.28	0.23	4.32	3.72	5879	682
16	**RFP**	57.48	0.19	3.54	3.04	4721	701
17	**CTH**	43.03	0.14	2.65	2.28	3467	722

18	**LVR**	34.81	0.12	2.14	1.84	2775	734
19	**ALJ**	39.06	0.09	1.60	1.38	2056	746
20	**PYL**	43.28	0.08	1.46	1.26	1871	749
21	**EUN**	52.37	0.09	1.62	1.40	2081	745
22	**KEM**	48.66	0.12	2.19	1.89	2846	732
23	**BDK**	50.67	0.17	3.12	2.68	4124	711
24	**SBO**	47.33	0.11	2.11	1.82	2736	734
25	**SIM**	42.11	0.10	1.79	1.54	2304	742
26	**TAM**	42.11	0.10	1.79	1.54	2304	742
27	**PSR**	28.11	0.05	0.93	0.80	1177	760
	Total	1527.34	4.46	-	-	-	-

Figure 3.22 shows the maximum traction power and the average traction power of each substation during operation. The substation index refers to Table 3.3. It can be seen that No. 6 (PNR), No. 12 (BNV), No. 13 (QUE) and No. 14 (DLO) output the highest peak power and average power. PNR is a substation with upgraded rectifiers; its rated power is 2 × 3 MW. The maximum traction power of these substations is around 1.5 times their rated traction power. Based on the simulation results from MTS, it can be seen that the 'hotspot' stations are PNR, BNV, QUE and DLO. When running this timetable, these substations have the highest output power and average current, so they are labelled as hotspots. Based on SMRT operation data, the hotspot stations are JKN (No. 5) and PNR (No. 6) where there was a lot of tripping in the past due to overload. JKN is a 2 × 2 MW rectifier substation, and PNR is a 2 × 3 MW rectifier substation. The simulation results are consistent with the practical operation data.

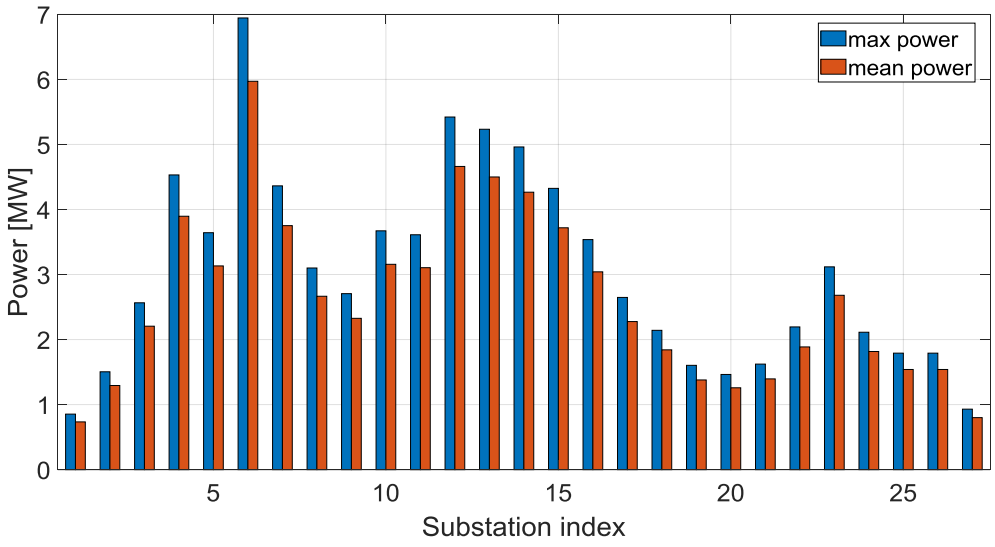

Figure 3. 22 Traction power of East–West line substations

The current and voltage of each substation are compared in Figure 3.23 and Figure 3.24. The current of hotspot stations is usually high and the voltage of hotspot stations is relatively low. The reason for the hotspots is mainly because of the design and location of substations. In addition, train operation has impact on the hotspot stations.

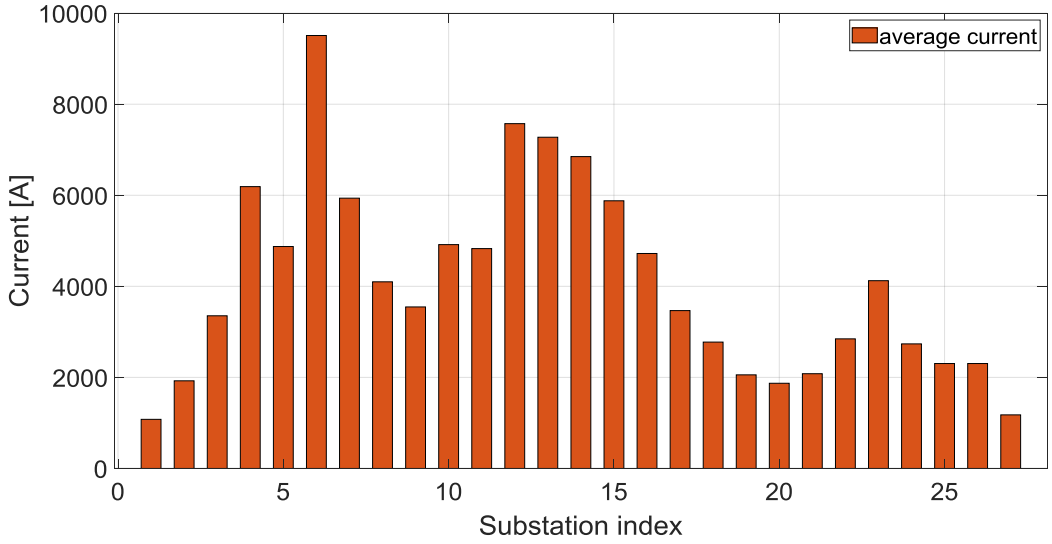

Figure 3. 23 Average current of East–West line substations

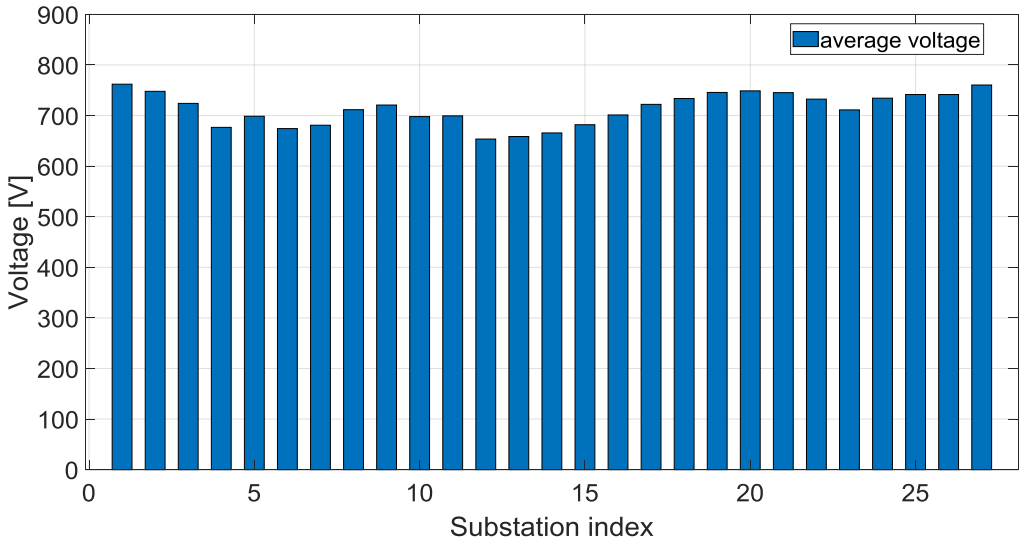

Figure 3. 24 Average voltage of East–West line substations

3.7 Summary

This chapter demonstrates the modelling process of DC power supply system simulation software. The software framework can be divided into two parts: train traction simulation and power network simulation. The train traction simulator simulates the operation of a single vehicle on a given route, while the power network simulator simulates the electrical network with the operation of several vehicles on the entire system.

Train traction simulation is the basis of urban rail traction power flow calculation. Traction calculation gives the functional relationship between the position, current, power and running time of the train on the route. Generally, the same type of train runs on an urban rail route. According to the traction calculation results and operation

timetable, the location and power distribution of multiple trains on the line can be determined at any operation time. The traction network voltage, substation voltage, current, power loss and load change process can be obtained from the traction power supply calculation. The developed software is used as a tool to evaluate the energy consumption and reliability performance of a railway system.

To sum up, power supply network modelling is a key capability in understanding railway system operation. This capability would allow current and future operations to be understood, managed and optimised. The research on power flow calculation and dynamic modelling of a DC traction power supply system provides a basis for reliability analysis of the traction power supply system, optimisation of train operation, etc., and provides a reference for optimisation of train schedules and future expansion of traction substations. It is of great significance to ensure the stable and reliable operation of traction power supply systems.

4 Power supply system reliability evaluation

4.1 Introduction

The traction power supply system is an important part of the electrified railway, and its safety issues are increasingly prominent. Different from the substation in a general power system, the load of a TPSS has a great impact on the traction transformer; moreover, in order to ensure normal operation of the train in case of failure, the traction substation must be able to access a cross-district power supply, as it has a high demand for reliable operation. The safe and reliable operation of DC TPSSs is the basis of the whole urban railway transit system. Due to the irreplaceable important position of TPSSs, it is very important to do research on DC TPSS fault analysis and power system reliability evaluation and to find out the weak links. There is much research on power supply systems, but it is necessary to find a more systematic and scientific research method.

At present, analysis of traction substation reliability mainly focuses on evaluation of the reliability of the main electrical wiring system. This chapter proposes an innovative approach to systematically evaluate the reliability of DC TPSSs. The weakest links of a railway power supply system are determined through reliability evaluation. The reliability analysis method mentioned in this chapter is also suitable for AC power

supply systems. But the components of an AC system are different from a DC system, and the FTA model is also different.

The research in this chapter is an extended version of the conference paper 'DC Traction Power Supply System Reliability Evaluation and Robust Design', which was published in the *2019 IEEE 3rd International Electrical and Energy Conference (CIEEC)*. The author of this paper is the first author and made important contributions to the paper.

4.2 Reliability concept

The issue of reliability engineering dates back to around 1920. During this period, the concepts of reliability were first proposed [108]. After 10 years of research, people gradually learned about reliability issues. Then, around 1940, reliability issues were included in engineering disciplines, and they were developed from the losses caused by the unreliability of products [109]. In 1957, the US Advisory Group on Reliability of Electronic Equipment (AGREE) issued a report in which they clearly pointed out the standard specifications and measurement methods for reliability [110]. From then on, reliability science gradually entered research fields. After nearly six decades of development, reliability science has been well developed, and it has gradually become a comprehensive discipline with a wide range of topics and applications [111], such as

infrastructure designs [112], computer and communication systems, and rail transportation systems [113, 114].

Research on the reliability of TPSS began in 2004. Sagareli [22] published a typical paper at the annual meeting of ASME (American Society of Mechanical Engineers) and IEEE (Institute of Electronics Engineers), in which the concept of the reliability of TPSSs was proposed and the definition of reliability was stated. Generally speaking, the research on reliability evaluation of TPSSs is still insufficient, there are few related papers and there is no systematic evaluation index or method. At present, the method of assessing the reliability of TPSSs in academia is not perfect. TPSSs are a special form of power system. Research on their reliability is bound to be completed on the basis of general power systems, and combined with the characteristics of the structure and parameters of the TPSS itself, a research method suitable for the system is proposed. In order to adapt to the development of railway power supply systems, new quantitative evaluation methods and evaluation models are explored in this chapter.

To study the reliability of TPSSs, a reliability-related method is introduced and applied to the railway system in this research. The purpose is to fully improve the utilisation of various equipment in the system by means of reliability-related theories and methods, so that the railway TPSS can operate more stably. Fault tree analysis can be used to identify the factors affecting the reliability of the substation power supply system for fault diagnosis and maintenance. Based on the existing literature using the more mature fault tree analysis as the theoretical basis, this study analyses the reliability of the UK's

electrified railway TPSS and the causes of system failure, and proposes innovative measures to improve system reliability.

4.2.1 Definition of reliability, a key index

The probability that a single component or system will perform a particular function without failure under specified conditions and time is its reliability. Reliability analysis refers to the use of probabilistic methods to quantitatively analyse the ability of a system to perform certain functions.

Reliability analysis can be divided into the analysis of non-repairable systems and analysis of repairable systems. A non-repairable system is one in which a component of the system cannot be restored to its pre-failure function by repair after a failure and must be improved by replacing the component. A repairable system is one in which a component is restored to its pre-failure function by repairing it after a fault. Most electrical equipment for the main wiring of a traction substation can be considered as repairable components, so this chapter focuses on reliability analysis of the main wiring of a traction substation in a repairable situation.

The reliability index is an important part of reliability theory and generally includes the following indicators:

1. Reliability $R(T)$

The probability that a product will perform the specified function under the specified conditions and within the specified time t is called the reliability of the product, and is defined as R(t) = P (T > t), where t ≥ 0. The reliability of a system at t is the probability that it experiences no failure during time interval [0,t]. Reliability is normally a function of time and can be calculated by equation (4.1).

$$\begin{aligned} R(T) &= \mathrm{P}(\mathrm{T} > \mathrm{t}) \\ &= exp\left[-\int_0^T \lambda(t)dt\right] \end{aligned} \tag{4.1}$$

where $\lambda(t)$ is the system failure rate.

2. Failure rate / occurrence $\lambda(t)$

The ratio of the number of components that fail per unit time to the total number of components is called the failure rate, which is also a function of time. The relationship between failure rate and reliability is as follows:

$$\lambda(t) = -\frac{d}{dt}\ln R(t) \tag{4.2}$$

If the component failure rate obeys an exponential distribution, the reliability R(t) is:

$$R(t) = e^{-\lambda t} \tag{4.3}$$

3. Repair rate $\mu(t)$

Repair rate is the probability that a component will be repaired in the next unit time after it has been in operation for a period of time. It is defined as $\mu(t)$.

4. Average lifespan

For non-repairable products, the average life expectancy is the Mean Time to Failure (MTTF). For repairable products, the average life expectancy refers to the Mean Time Between Failures (MTBF). Both are collectively referred to as average lifespan. Mathematically, it is the mathematical expectation E(T) of life T. MTTF and MTBF can be calculated by equations (4.4) and (4.5).

$$MTTF = \int_0^\infty e^{-\mu t}\, dt = \frac{1}{\mu} \tag{4.4}$$

$$MTBF = \int_0^\infty R(t)\, dt = \frac{1}{\lambda} \tag{4.5}$$

where λ is the failure rate and μ is the repair rate.

5. System availability

The availability of S at time t is the probability that S is working at t, as defined in equation (4.6).

$$A = \frac{MTBF}{MTBF + MTTR} = \frac{\mu}{\mu + \lambda} \tag{4.6}$$

6. System unavailability

The unavailability of S at t is the probability that S is not working at t, as defined in equation (4.7).

$$Q = \frac{MTTR}{MTBF + MTTR} = \frac{\lambda}{\mu + \lambda} \tag{4.7}$$

The average unavailability can be calculated by equation (4.8).

$$Q_{Avg}(T) = \frac{1}{T}\int_0^T Q(t)dt \tag{4.8}$$

The sum of availability and unavailability is 1, and the relationship is shown in equation (4.9).

$$A + Q = 1 \tag{4.9}$$

4.2.2 Reliability analysis of series and parallel systems

1. Series system

In a series system, all series components are in good condition and the system can operate normally; once there is a series component failure, the system will not work normally. Supposing a series system is composed of n components which form the 'AND' logic relationship, the reliability $R_s(t)$, failure rate λ_s, repair rate μ_s, unavailability Q_s and availability A_s of the series system composed of n components are, respectively, expressed as:

$$R_s(t) = R_1(t)R_2(t)R_3(t)\cdots R_n(t) = \prod_{i=1}^{n} R_i(t) \tag{4.10}$$

$$\lambda_s = \sum_{i=0}^{n} \lambda_i \tag{4.11}$$

$$\mu_s = \frac{\lambda_s}{\sum_{i=0}^{n} \lambda_i/\mu_i} \tag{4.12}$$

$$Q_s = \frac{\lambda_s}{\mu_s} = \sum_{i=0}^{n} \frac{\lambda_i}{\mu_i} \tag{4.13}$$

$$A_s = 1 - Q_s \tag{4.14}$$

where $R_i(t)$, λ_i and μ_i are the reliability, failure rate and repair rate of the ith component, respectively.

2. Parallel system

A parallel system is one in which if any parallel element in the system is in good condition, the system can work normally; only if all elements fail will the system stop operating. Supposing that a parallel system consists of n components which form the 'OR' logic relationship, the reliability $R_p(t)$ of the parallel system composed of these n components is:

$$R_p(t) = 1 - \{[1 - R_1(t)][1 - R_2(t)][1 - R_3(t)] \cdots [1 - R_n(t)]\} \tag{4.15}$$

When the failure rate of a parallel system is far less than the repair rate, the failure rate λ_p, repair rate μ_p, unavailability Q_p and availability A_P are, respectively, expressed as:

$$\lambda_p = \prod_{i=1}^{n} \lambda_i \frac{\sum_{i=0}^{n} \mu_i}{\prod_{i=1}^{n} \mu_i} \tag{4.16}$$

$$\mu_p = \sum_{i=1}^{n} \mu_i \tag{4.17}$$

$$Q_p = \lambda_p \mu_p = \prod_{i=1}^{n} A_i \tag{4.18}$$

$$A_P = 1 - Q_P \tag{4.19}$$

where λ_i, μ_i and A_i are the failure rate, repair rate and availability of the ith component, respectively.

4.2.3 Importance factors

Importance analysis is conducted to determine the weakest links / parts of a system from a quantitative point of view. The fault tree formula is used to calculate the probability importance of the bottom event for the top event. By comparing the magnitude of the probability importance, the weakest links can be obtained. Enhancing these weak links can improve system reliability. There are a few importance factors which help evaluate the system:

1. Marginal Importance Factor (MIF)

The MIF, often called the Birnbaum Importance Factor, represents the difference between the unavailability when event X occurs and the unavailability when event X does not occur. The MIF gives the increase in risk associated with the occurrence of event X. The MIF is defined as in equation (4.20).

$$MIF(t) = \frac{\partial Q(t)}{\partial q_x(t)} = Q(t)|q_{x=1} - Q(t)|q_{x=0} \tag{4.20}$$

where $Q(t)$ is system unavailability, $q_x(t)$ is the unavailability for event X, $Q(t)|q_{x=1}$ is the unavailability with $q_x = 1$ and $Q(t)|q_{x=0}$ is the unavailability with $q_x = 0$.

2. Critical Importance Factor (CIF)

The CIF, often called Fussell–Vesely Importance, indicates the risk associated with a given event, that is, how much occurrence of the event contributes to system failure. The CIF can be calculated using the MIF and system unavailability $Q(t)$, as shown in equation (4.21).

$$CIF(t) = \frac{q_x(t)MIF(t)}{Q(t)} = \frac{Q(t) - Q(t)|q_{x=0}}{Q(t)} \tag{4.21}$$

3. Risk Reduction Worth (RRW)

RRW represents the risk that would be reduced by reducing the unavailability of event X to zero. The RRW is defined in equation (4.22).

$$RRW(t) = \frac{Q(t)}{Q(t)|q_{x=0}} \tag{4.22}$$

4.3 Reliability evaluation method

A reliability evaluation method generally refers to a method of analysing the reliability of a product by mathematical statistics or probability theory [22]. It usually includes qualitative analysis and quantitative analysis. There are many methods of system reliability analysis, which can be roughly divided into analytical methods and simulation methods. At present, the method of assessing the reliability of traction power supply systems in academia is not perfect. In order to adapt to the development of railway power supply systems, new quantitative evaluation methods and evaluation

models should be explored. This section introduces three commonly used reliability analysis methods.

4.3.1 Fault tree analysis

The FTA method analyses the hardware, software, environment, human factors and other factors that cause product failure, and draws a fault tree diagram to determine the various combinations of product failure causes and the probability of their occurrence. In 1962, H. A. Watson at Bell Laboratories first developed the concept of FTA to evaluate a control system [115]. FTA has since become a comprehensive evaluation method with a wide range of topics and applications [116-118]. A fault tree diagram is drawn to determine the various combinations of product failure causes and the probability of their occurrence. The purpose of FTA is to fully improve the utilisation of various pieces of equipment in the system by means of reliability-related theories and indices.

The purposes of FTA are to:

1. Calculate the probability of a fault occurring.
2. Help determine the failure modes and causes that may occur.
3. Systematically and comprehensively analyse the cause of a major fault or accident, after it occurs.
4. Find links with weaker security or reliability and take corresponding improvement measures.
5. Develop guidelines for the diagnosis, improvement and maintenance of the fault.

The features of FTA are as follows:

1. Through the fault tree diagram, the various causes and logical relationships leading to an accident can be described comprehensively and visually, so that the relevant personnel can understand and master the key points and measures of safety control.
2. According to the frequency data of each basic event failure, the degree of influence of each basic event on the accident may be determined.
3. FTA can be used to perform qualitative analysis as well as quantitative analysis and systematic evaluation.
4. When performing quantitative analysis on a system, the probability of occurrence of all basic events must be determined in advance, otherwise quantitative analysis cannot be performed.
5. FTA is used to analyse a specific accident rather than a process or equipment system, so it has certain limitations.
6. For complex systems, because there are many steps to compile the fault tree, the fault tree is large and the calculation will be complicated, so it will bring difficulties to the qualitative and quantitative analysis.

4.3.2 Failure mode and effect analysis

FMEA can be defined as the ‘potential failure mode and consequence analysis’. In the product design and process design stages, FMEA analyses the various processes that constitute the product, parts and process of the composition, finds out all the potential failure modes and analyses the possible consequences, so as to take the necessary prerequisites to improve the quality and reliability of the product.

FMEA uses tables to simply enumerate all failure modes of the components of the system, and assumes that failures occur, to determine the possible faults of the system. The disadvantage is that it only sets a single failure mode for hardware, so it is isolated analysis.

4.3.3 GO theory

The GO method is a success-oriented analysis technique for system reliability evaluation and risk assessment. It can estimate the mean value of system reliability parameters, including system failure rate and system maintenance rate, and has guiding significance for the operation and maintenance time of complex systems. The basic idea of the GO method is to translate the system diagram into a GO diagram and analyse the system probability.

The characteristic of the GO method is that it can solve the reliability problems of some complex systems which cannot be done by the fault tree method for systems with multiple states and time series. The disadvantage is that it is complicated to establish a perfect GO diagram.

4.3.4 Discussion

Compared with FMEA and GO, FTA can not only analyse failures caused by component errors, control errors and environmental stresses, but also logically analyse the occurrence process of faults and quantitatively calculate the probability of top events.

By analysing the above-mentioned methods of reliability analysis, it can be seen that FTA can be successfully applied to reliability theory research of electrified railway TPSSs and is the most suitable method for reliability analysis. Therefore, based on the

existing literature using the more mature FTA as the theoretical basis, this thesis analyses the reliability of the UK's electrified railway TPSSs and the causes of system failure and proposes innovative measures to improve system reliability. FTA is used in this research to identify the factors affecting the reliability of substation power supply systems for fault diagnosis and maintenance. The weakest links of the power system will be determined.

4.4 Reliability model of TPSS

4.4.1 Fault tree construction

In FTA, the basic event is connected to one or more top events by logical symbols such as AND gates and OR gates [119]. Top events generally refer to undesired system failures or events that endanger the system. Bottom events usually refer to a component failure or faulty human operation. Figure 4.1 shows the basic event symbols and logic gate symbols used in a fault tree, and an example of a fault tree. X is the top event and A, B and C are bottom events.

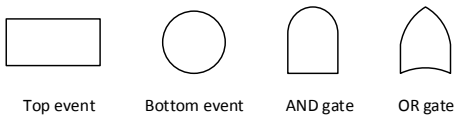

a. Event symbols in the fault tree

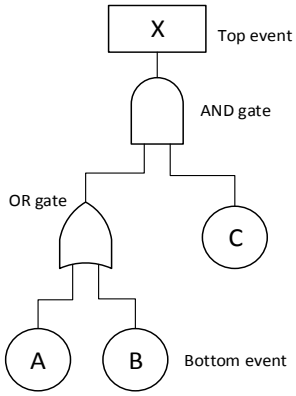

b. Example of a fault tree

Figure 4. 1 Event symbols and example of a fault tree

The basic steps of the FTA method are as follows:

1. Define the system and system failures and determine the bottom events;
2. Build the fault tree model;
3. Conduct qualitative and quantitative analysis.

4.4.2 Schematic layout of a 750 V DC substation

In the UK's DC electrified railway system [88], the National Grid or Distribution Network Operator (DNO) first supplies AC at high voltage (HV), typically 132, 66 or 33 kV to the main substation, then the voltage is stepped down to a medium voltage of 33, 22 or 11 kV. After that, the alternating current is stepped down and rectified to 1500 or 750 V DC through the traction substation to supply power to the train. The train takes power via the pantograph or the third rail, and finally the current is fed back to the

traction substation by the return line. The 750 V level is most widely used for metro and urban rail transport. Figure 4.2 shows the feeding arrangements and basic components of a typical 750 V DC TPSS.

The power supply system shown in Figure 4.2 uses a dual redundant design for the traction power system. All of the electronics are doubled, and if one of the branches is disconnected from the fault and the other is turned on, the entire system can still be powered. Most of the current industrial designs use redundant system design. However, there is a problem with redundant systems. Compared with simple systems, the number of devices in a redundant system increases, and the installation and maintenance costs of the devices also increase.

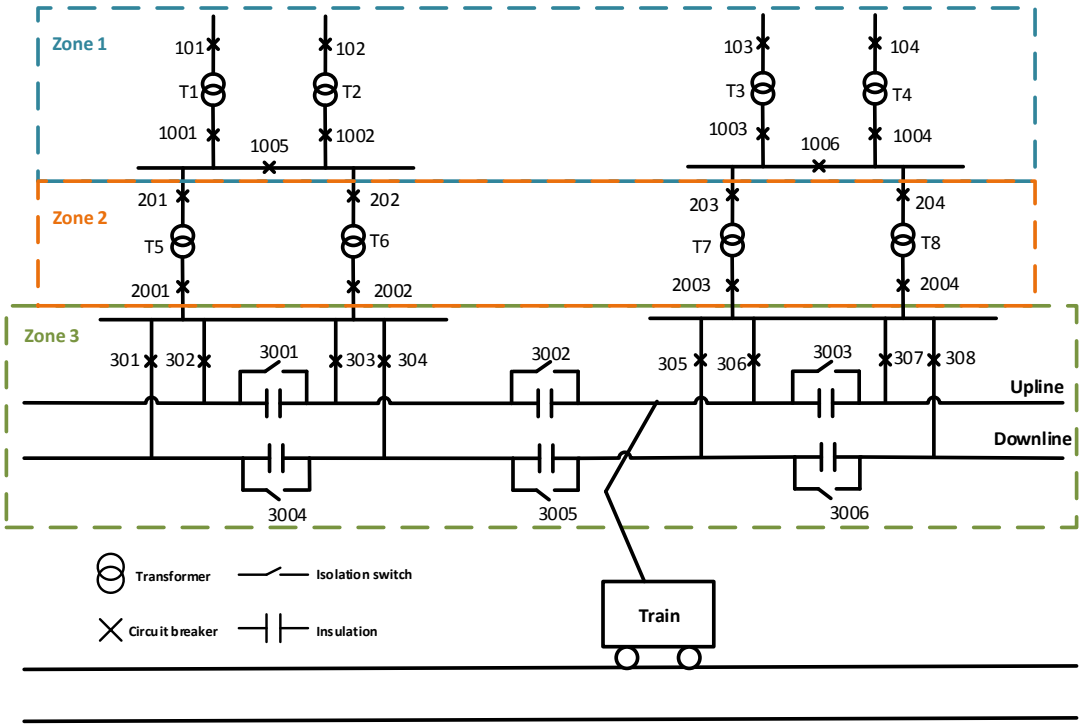

Figure 4. 2 Main electric wiring diagram of a DC traction power supply system

There are three main types of component in the whole power system: rectifier transformers, circuit breakers and isolators. To simplify the evaluation model, the rectifier and transformer are considered as a whole, because rectifier transformers have been widely used in the modern railway industry. Each component is defined and labelled as the bottom event in the FTA, and its corresponding event code is shown in the following Table 4.1. T1–T8 represent the rectifier transformers in the power supply system, 3001–3006 are the isolation switches and the rest represent the circuit breakers.

Table 4. 1 Bottom events and corresponding event codes

Bottom event	Event code	Bottom event	Event code	Bottom event	Event code	Bottom event	Event code
T1	X1	103	X11	305	X21	2001	X31
T2	X2	104	X12	306	X22	2002	X32
T3	X3	201	X13	307	X23	2003	X33
T4	X4	202	X14	308	X24	2004	X34
T5	X5	203	X15	1001	X25	3001	X35
T6	X6	204	X16	1002	X26	3002	X36
T7	X7	301	X17	1003	X27	3003	X37
T8	X8	302	X18	1004	X28	3004	X38
101	X9	303	X19	1005	X29	3005	X39
102	X10	304	X20	1006	X30	3006	X40

4.4.3 Fault tree models

Before building up the fault tree model of the system, two preconditions for the hypothesis are proposed based on the basic characteristics of the TPSS:

- All the pieces of electric equipment involved in the power system can be statistically considered to be independent of each other during reliability analysis. The failure of one device has limited impact on other devices. To simplify the

simulation analysis, the influence of devices on each other is not considered in this study.

- All the pieces of electrical equipment are considered as repairable components in the FTA.

After understanding the structure and basic components of the traction substation, the failure events of the system are determined according to the operation mode of the traction substation. Figure 4.3 shows the fault tree model of the system.

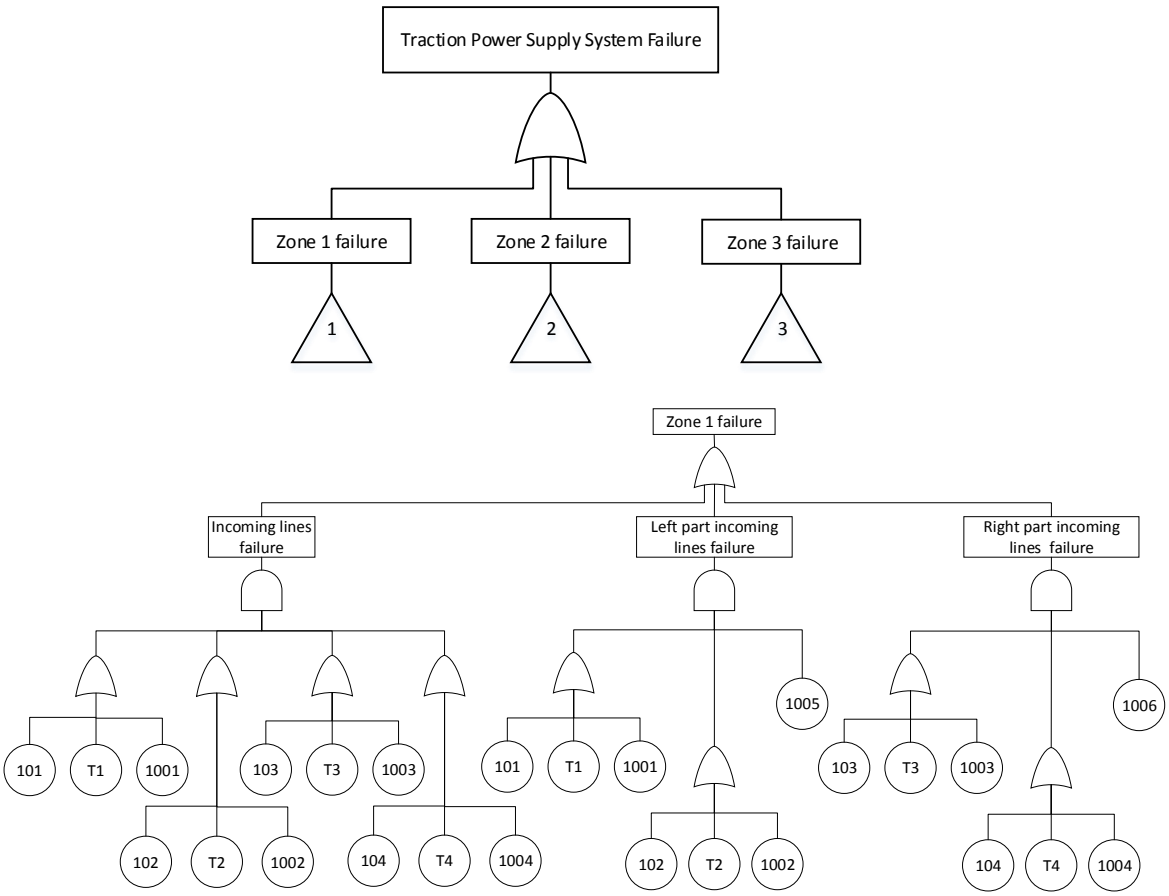

a) Zone 1 fault free model

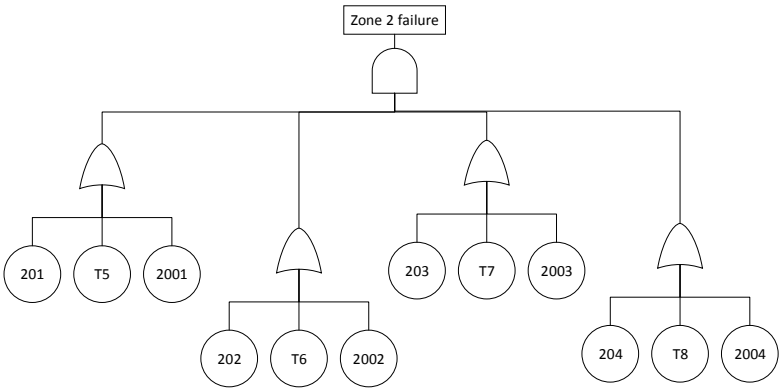

b) Zone 2 fault tree model

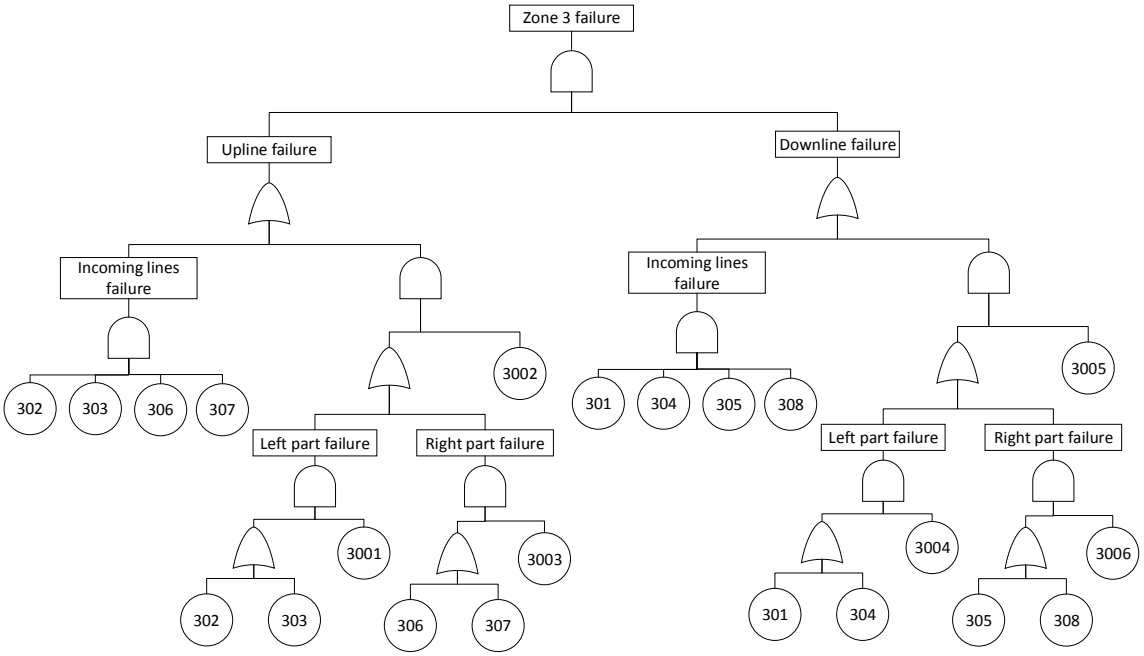

c) Zone 3 fault tree model

Figure 4. 3 Fault tree models of a DC traction power supply system

4.5 Reliability evaluation for a DC TPSS

The FTA method is used to qualitatively and quantitatively analyse the reliability of the traction substation and the traction network, to identify the main cause of the failure and the weak links of the traction power supply network.

4.5.1 Qualitative analysis

Using FTA software and computational algorithms, the fault tree model of the traction substation is qualitatively analysed to obtain the minimum cut sets. The minimal cut set number is 199, in which there are 12 second-order cut sets, 162 fourth-order cut sets, 16 sixth-order cut sets, 8 seventh-order cut sets and 1 eighth-order cut set.

The second-order cut sets are {X2,X29}, {X3,X30}, {X4,X30}, {X9,X29}, {X10,X29}, {X11,X30}, {X12,X30}, {X1,X29}, {X25,X29}, {X26,X29}, {X27,X30}, {X28,X30}.

The fourth-order cut sets are {X9,X10,X11,X12}, {X13,X14,X15,X16}, {X2,X9,X11,X12}, {X1,X10,X11,X12}, {X6,X13,X15,X16}, {X5,X14,X15,X16}, {X4,X9,X10,X11}, {X3,X9,X10,X12}, {X8,X12,X14,X15}, {X7,X13,X14,X16}, {X9,X10,X11,X28}, {X9,X10,X12,X27}, … , etc.

The sixth-order cut sets are {X17,X18,X35,X36,X38,X39}, {X18,X20,X35,X36,X38,X39}, {X18,X21,X35,X36,X39,X40}, {X18,X24,X35,X36,X39,X40}, {X17,X19,X35,X36,X38,X39},

{X19,X20,X35,X36,X38,X39}, {X19,X21,X35,X36,X39,X40}, {X19,X24,X35,X36,X39,X40}, … , etc.

The seventh-order cut sets are {X17,X18,X20,X21,X24,X35,X36}, {X17,X19,X20,X21,X24,X35,X36}, {X17,X20,X21,X22,X24,X36,X37}, {X17,X20,X21,X23,X24,X36,X37}, {X17,X18,X19,X22,X23,X38,X39}, {X18,X19,X20,X22,X23,X38,X39}, {X18,X19,X21,X22,X23,X39,X40}, {X18,X19,X22,X23,X24,X39,X40}.

And the eight-order cut set is {X17,X18,X19,X20,X21,X22,X23,X24}.

The probability of a system failure in a cut set event is inversely proportional to its order. That is, the lower the order of the minimum cut set, the easier it is for the corresponding event to fail the system, so the more important the cut set is. It can be summarised from the minimum cut set result obtained that the second-order minimum cut sets {X1,X29}, {X2,X29}, {X3,X30}, {X4,X30}, {X9,X29}, {X10,X29}, {X11,X30} and {X12,X30}, that is, the transformers T1, T2, T3 and T4, circuit breakers 101, 102, 103 and 104, and isolation switches 1005 and 1006, have the greatest influence on the reliability of the system. From a system perspective, it is necessary to avoid problems with the equipment included in the low-order minimum cut set to ensure that the system can function properly. In the actual system design, highly reliable isolating switches should be used at 1005 and 1006 to minimise the occurrence of

minimum cut set events. Transformers T1, T2, T3 and T4 are also the weakest links of the power system, so should be enhanced.

4.5.2 Quantitative analysis

The devices reliability parameters were tested on a traction substation of Beijing-Shanghai HSR in China using FTA and FMEA method [24, 25]. This study employs the empirical reliability parameters of the electrical components from the field tests in [24, 25] as listed in Table 4.2. The failure rate of each component is a time-related function. These data are used for fault tree simulation and reliability evaluation. Due to the lack of statistical data, the failure rate and repair rate are empirical values, which can not fully reflect the real state of a DC system.

Table 4. 2 Reliability parameters of relevant equipment as repairable components

Equipment	Failure rate	Repair rate
Transformer	$\lambda(t) = (\frac{16.6}{167.25^{16.6}}) \cdot t^{15.6}$	$\mu(t) = 5.15 \times 10^{-2}$
Circuit breaker	$\lambda(t) = (\frac{7.75}{178.67^{7.75}}) \cdot t^{6.75}$	$\mu(t) = 0.10$
Isolator	$\lambda(t) = (\frac{10.88}{175.98^{10.88}}) \cdot t^{9.88}$	$\mu(t) = 0.25$

In the FTA simulation, an assessment of the reliability and unavailability of the substation over 10 years was carried out. As the failure rates of electrical components increase with time, the reliability of the whole system decreases year by year. Figure 4.4 depicts the probability of the top events over time, which are the system unavailability

and reliability over time. After 10 years of operation of the power supply system, its system reliability is 0.962115 and its unavailability is 0.000981057.

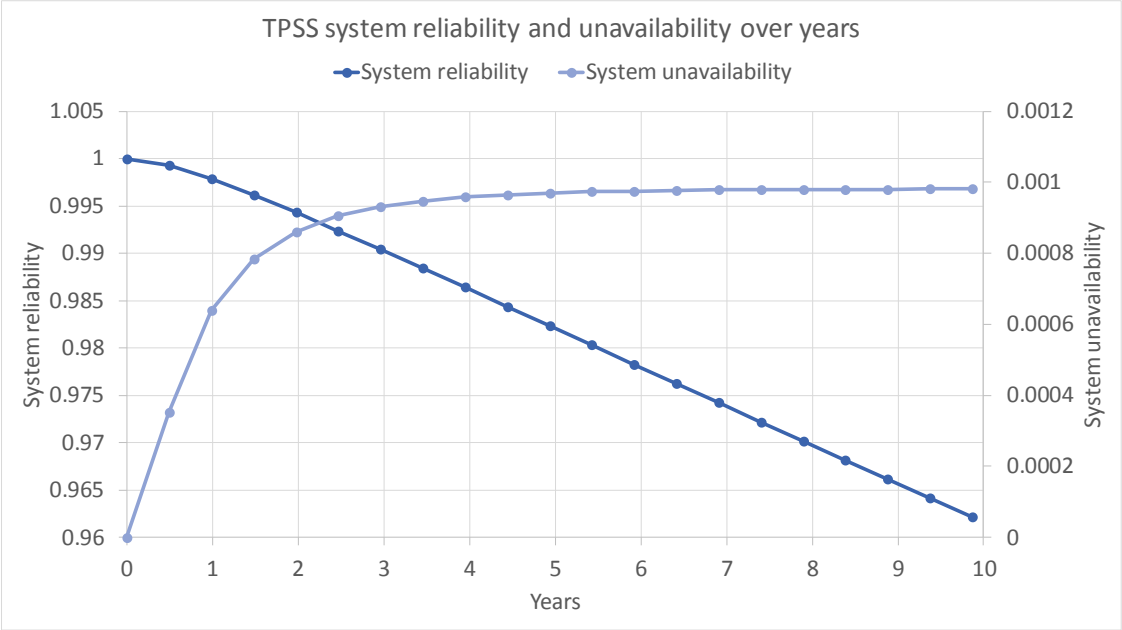

Figure 4. 4 TPSS system reliability and unavailability over time

4.5.3 Importance factors

From the fault tree software and the calculation formulas listed in Section II, the importance indicators of each component to system failure are calculated, as shown in Table 4.3.

Table 4. 3 Importance factor results of relevant components

Bottom events	**Unavailability**	**Marginal Importance**	**Critical Importance**	**Risk Reduction Worth**
X29, X30	0.0056	0.0869	0.4959	1.9837
X1, X2, X3, X4	0.0287	0.0534	0.1563	1.3852

X9, X10, X11, X12	0.0107	0.0053	0.0573	1.0025
X25, X27, X28, X26	0.0056	0.0052	0.0298	1.0608
X13, X14, X15, X16	0.0287	8.65E-05	0.0025	1.0307
X18, X19, X22, X23, X17, X20, X21, X24	0.0287	2.28E-10	6.66E-09	1.0000
X5, X6, X7, X8	0.0107	8.49E-05	9.27E-04	1.0009
X31, X32, X33, X34	0.0056	8.45E-05	4.81E-04	1.0005
X36, X39	0.0056	2.67E-09	1.52E-08	1.0000
X35, X37, X38, X40	0.0056	1.33E-09	7.91E-09	1.0000

It can be seen from the simulation results that bottom events X29, X30, X1, X2, X3 and X4 are of most importance to the system. They have the greatest impact on the reliability of the TPSS. Figure 4.5 lists the MIF and CIF of major components, sorted by the degree of importance. Figure 4.6 shows the RRW rating of major components. X29 and X30 have the largest RRW numerical value, 1.9837. If the probability of failure of the bottom events X29 and X30 is reduced, the probability of the top event occurring can be quickly reduced, that is, the probability of failure of the TPSS, which is more effective than reducing the probability of occurrence of any other bottom events by the same value.

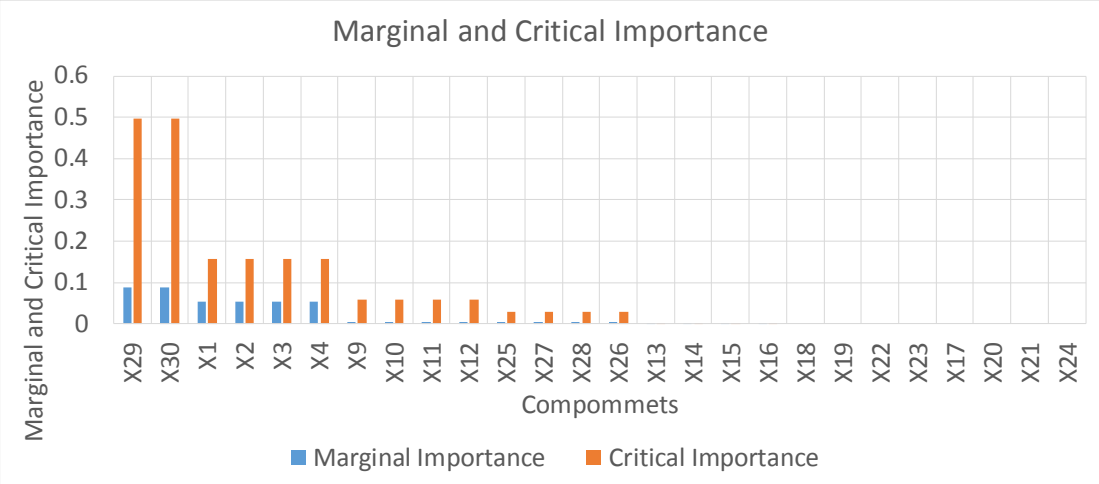

Figure 4. 5 Order of Marginal and Critical Importance of major components in the DC traction power supply system

Figure 4. 6 Order of Risk Reduction Worth of major components

The results of quantitative analysis of the TPSS are consistent with those of qualitative analysis of the minimum cut set. To ensure a highly reliable system, the key components should be monitored and should be repaired and replaced in time.

4.6 Approaches to improve system reliability

This study also explores the most significant parameters which affect outputs like system unavailability and reliability. Three methods can be proposed to maximise the reliability of the DC TPSS for robust design.

4.6.1 Redundant system design

In order to improve the reliability of a system, the method mostly used in industry is system redundancy design. All of the electronics in incoming lines are doubled, and if one of the branches is disconnected from the fault and the other is turned on, the entire system can still be powered. Most current industrial designs use redundant system design.

However, there is a problem with redundant systems. Compared with simple systems, the number of devices in a redundant system increases, and the installation and maintenance costs of the devices also increase. In future research, the cost of equipment should be taken into account.

4.6.2 Important components

The transformer is one of the most important components in a TPSS. The failure rate of transformers can be reduced to improve the reliability of the entire power supply system. High-quality transformers and electronics can greatly improve the system. Improving the quality of other electrical components, such as circuit breakers and

switches, will also have a good impact on system reliability. In addition, new products with high performance and reliability should be introduced to improve the reliability of the whole system.

4.6.3 Train service optimisation

Different from a substation in a general power system, a TPSS has a single load, and the impact on the traction transformer is very large, while the load of a general power system is mostly industrial or household load, and the transformer is relatively more stable. The life expectancy and reliability of a traction transformer is dependent on its temperature and insulation condition. Overloading will cause an unwanted internal rise of the traction transformer's temperature, thus affecting its reliability [120].

Take the railway operation schedule for one day as an example. The power supply system runs for 24 hours a day, and the average load per hour of the substation is used as a variable. Different traction loads can affect the temperature of the transformer and change its life expectancy. From the thermodynamic model of a transformer [121], it is known that optimising the timetable and load of the train operation will have an impact on its life, thereby improving the reliability of the whole system.

4.7 Summary

This chapter focuses on the reliability model of electrified railway TPSSs. The FTA method is used to qualitatively and quantitatively analyse the reliability of the traction

substation included in an electrified railway TPSS and to calculate the failure probability of the top event and various factors leading to system failure. Therefore, the weak links of the TPSS are found, and the cause of system failure is summarised. Comparative analysis of different schemes is also beneficial to the reliability design of a new power supply system. The FTA method will play an active role in improving the reliability design level of traction substation power supply systems.

Theoretically, it provides a reference for the operation, inspection and maintenance of the DC electrified railway, enhances the safety level of electrified railway operation and further improves the reliability of electrified railway TPSSs.

However, there are still some shortcomings in this chapter. It may not be comprehensive and perfect in modelling the traction substation fault tree. It is necessary to continue to refine the construction of the fault tree by summarising other bottom events that may cause system failures (top events) based on actual work experience in the future. At the same time, when quantitative analysis of the fault trees of the traction substation and traction network is carried out, the failure rate of the bottom event is based on the given empirical failure probability. In the next chapter of study, based on the data obtained from the actual work statistics of important components, a more accurate failure probability for the bottom event is calculated by an innovative modelling method and then quantitative analysis of the fault tree is performed.

5 Impact of traction load on traction substations

5.1 Introduction

The impact of traction load and the actual operation of trains on system reliability is not considered when designing a DC railway power supply system. Previous studies of railway power supply networks usually focused on infrastructure design and capacity rather than system operation. Therefore, it is very important to study the influence of traction load on traction substations, because through the analysis of simulation data, a series of indicators such as loss of life, reliability and failure rate can be obtained, which can provide guidance for making a maintenance plan and better system operation plan.

Compared with the general power load, the traction load has its unique characteristics. The position of the train on the route changes in real time, and different operation conditions will cause the load to increase or decrease sharply during the operation process. Traction load is a kind of random load, which has the characteristics of uncertainty and mobility. Therefore, compared with the ordinary power load, the traction load may have strong pulse characteristics. Using the traditional method of evaluating power system reliability, it is difficult to accurately describe the operational state of a TPSS.

This chapter studies the structure of a DC substation and its main components, as well as the failure mechanism of the substation. A method of transformer risk assessment based on the characteristics of traction load is proposed. Using the data of traction load and ambient temperature, the hot-spot temperature of transformer winding is calculated by its thermal model, and a series of indices such as loss of life are used to evaluate the traction transformer quantitatively. On this basis, the impact of load characteristics on the reliability of the substation system is studied.

The research in this chapter is an extended version of the journal paper 'Reliability and life evaluation of a DC traction power supply system considering load characteristics', which was published in *IEEE Transactions on Transportation Electrification*. The author of this paper is the first author and made important contributions to the paper.

5.2 Fault mechanism of a typical 750 V DC substation

5.2.1 Schematic layout of a typical 750 V DC substation

The components and equivalent circuit diagram of a railway TPSS have been introduced in detail in Chapter 3. The structure and equipment of a traction substation are different for different specifications of traction power supply. The structure shown in Figure 4.1 in Chapter 4 is the most typical and commonly used system of DC power supply railway at present. This chapter takes Figure 4.1 in Chapter 4 as a typical example to analyse the impact of load on a substation.

In Figure 4.1, Zone 1 is the high-voltage section which gets AC voltage from the National Grid. Zone 2 is called a traction substation, which is used to convert electrical power as supplied by the National Grid to a certain level for providing power to a rail system. Zone 3 connects to the catenary system. There are four core components in the traction substation system: transformers, rectifiers, circuit breakers and isolators. All the components are in series and function together to enable the system to provide 750 V DC power to the train, as shown in Figure 5.1. It is important to note and understand the major components shown in the diagram and to get an overview of how they work together for the entire system. Although the study focuses on a 750 V DC traction system, it can be applied to various different installations where the same principles will be used.

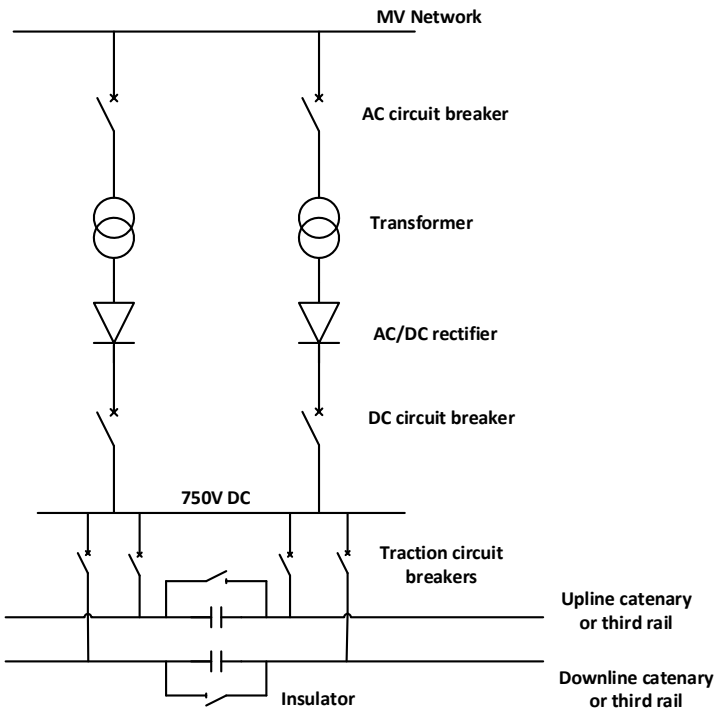

Figure 5. 1 Schematic layout of a typical DC traction substation

5.2.2 Fault mechanism of electronic components

In the product design and process design stages, FMEA analyses the various processes that constitute the product, parts and process of the composition, finds out all the potential failure modes and analyses the possible consequences, to determine the prerequisites to improve the quality and reliability of the product. It is important to understand the function of the major components of a traction substation and their fault mechanisms. Table 5.1 shows FMEA summarised from IEEE standards and some papers [122-124].

Table 5. 1 Failure modes and effects of major components

Equipment	Function	Failure mode	Cause	Effects of failure
Transformer	Step down the supply voltage to 750 V	Over temperature	Overload or over-current due to fault in the system	Protection will cause supply to be switched off; if not, there will be major damage to the transformer
		Short circuit	Isolation materials damaged	High current densities and a rapid increase in winding temperature
		Open circuit	Loose connection, burnt windings	The fault will cause gas and heat to build up in the transformer; protection circuit will switch off the supply

		Low oil level	Leakage at gaskets	If protection circuit operates, the supply will be switched off, otherwise the transformer will blow up
Rectifier	AC input to DC output	Over temperature	Arcing inside rectifier, loose connection between diode and heat sink, cooling fans not working	Over-temperature protection should switch off the supply; if not, the rectifier may be damaged
		Short circuit	Faulty diodes, circuit fault	Protection circuit should isolate the rectifier
		Open circuit	One or more diodes not working, loose connections, circuit fault	No output from the rectifier
Circuit breaker	Protection switch	Not opening	Faulty opening relay, protection circuits not working properly	Substation may be damaged because circuit breaker does not open
		Not closing	Faulty closing relay, protection circuits not working properly	No power supply
		Current leakage to earth	Dirty porcelain or breakdown of isolating materials	Damage to the circuit breaker and possible trip of substation if leakage is detected by AC earth leakage
		External damage	Vandalism, lightning, water	Current leakage and possible disintegration

Isolator	Isolate the substation from supply	Broken insulators	Vandalism, lightning, water in the base plates causing cracking	Isolator short-circuited
		Opening mechanism failure	Rust, broken operating handle	No operation will be possible

To summarise, most transformer failures are related to the deterioration of insulation. Most rectifier failures are caused by faulty diodes or faulty circuits. Human error and the external environment such as weather are a big factor in causing failures, which is sometimes inevitable. Note that it is not always possible to completely prevent damage, but the ultimate goal is to have as much control as possible and minimise the risk of failure with existing conditions. In the following paragraphs, the failure mechanisms of important components in the substation will be analysed based on the existing IEEE standards, and the main factors affecting the fault will be obtained.

5.3 Life of components

There are four major components in a TPSS: transformers, rectifiers, circuit breakers and isolators. In this section, the failure mechanisms of these major components will be described separately and the reliability model of the traction substation will be derived.

5.3.1 Transformers (IEEE Std C57.91-2011 [123])

The transformer is one of the key pieces of equipment for the normal operation of traction power systems. It takes 22 or 11 kV AC from the suppler as primary voltage;

the voltage is then stepped down and fed to a rectifier for running DC motors. Due to the long-term high-efficiency operation of transformers, faults are always inevitable. However, they have no substitute, especially as large transformer equipment is quite expensive so it is impossible to replace it frequently; thus the transformer loss-of-life characteristic is a good research topic.

There are currently two types of distribution transformer: liquid-immersed transformers and dry-type transformers. Oil-immersed distribution transformers are adopted more in the railway industry because they are relatively cheaper. The oil-immersed distribution transformer is one of the core pieces of equipment in the power system. Most transformer failures are related to the deterioration of insulation. A sudden increase in load is identified as the main cause of insulation deterioration.

The load capacity of an oil-immersed transformer is closely related to its top oil temperature and hot-spot temperature. There are several factors affecting the transformer's overall life expectancy and overload capabilities; however, the hottest-spot temperature is the most critical parameter for determining the transformer's life expectancy. A higher winding hot-spot temperature will cause degradation of the winding insulation and increase the potential for transformer failure. The inordinate temperature rise in an oil-immersed transformer is featured by the hot-spot temperature. It is an important parameter to determine the optimum load ability of transformers.

5.3.1.1 IEEE 'Classical Thermal Model' (Clause 7)

IEEE C57.91-2011 [123] presents a commonly used thermal model for calculating the transformer hot-spot temperature and top oil temperature. The specific formulas are not detailed in this chapter; for details, please refer to the IEEE standard and other related papers [120, 121, 125]. The theoretical basis of the model is that an increase in the transformer's loading current will result in transformer losses and then cause an overall temperature rise. The mechanism of hot-spot temperature change can be explained by equation (5.1), which has been verified by IEEE standard C57.91-2011 [123].

$$T_{HS} = T_A + \Delta T_{TO} + T_G \tag{5.1}$$

where T_A is the ambient temperature, ΔT_{TO} is the top-oil temperature rise over the ambient temperature and T_G is the winding hottest-spot temperature rise over top oil temperature.

The temperature rise logic of changing transformer hot-spot temperature with ambient temperature and load is shown in Figure 5.2.

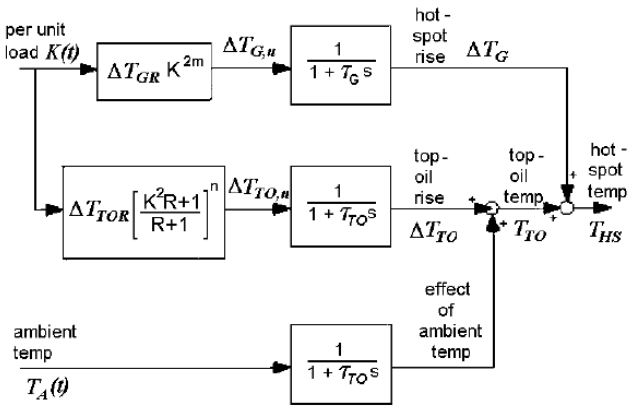

Figure 5. 2 Block diagram of modified transient heating equations

The transformer thermal model is built using Simulink. Figure 5.3 shows the transformer hot-spot temperature changes with different per-unit loads. Take the railway operation schedule for one day as an example. The power supply system runs for 24 hours a day, and the average load per hour of the substation is used as a variable. Different loads can affect the temperature of the transformer and change its reliability. According to the results, the influence of load characteristics on the reliability of a traction transformer cannot be ignored. From the thermodynamic model of a transformer, it is known that optimising the timetable and load of the train operation will reduce the operation risk of the transformer, thereby improving the reliability of the system.

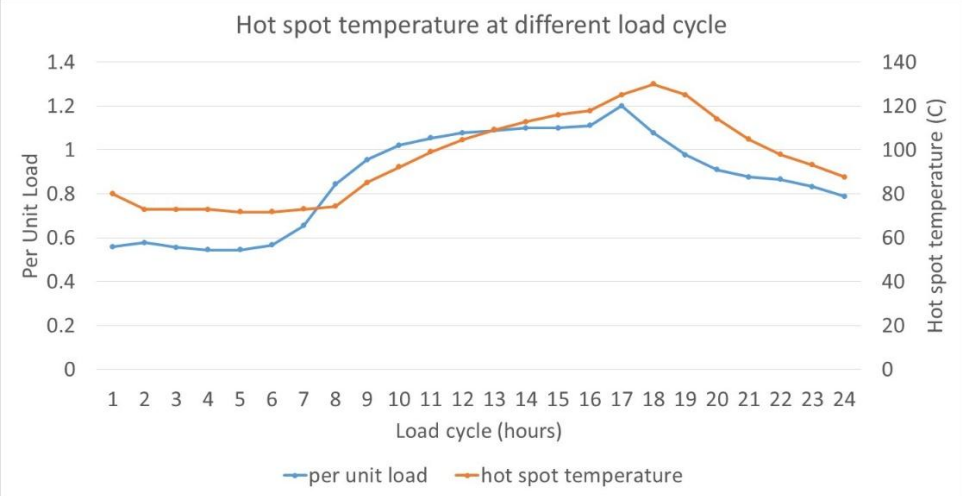

Figure 5. 3 Relationship between overall temperature rise and load (per unit)

5.3.2 Diode rectifiers (IEEE P1653.2-2009 [122])

A traction rectifier is used to convert AC power to DC power. A controlled rectifier means that the DC output voltage can be controlled or adjusted in value based on demand, whereas an uncontrolled rectifier will produce a fixed DC output. Traction rectifiers are either 6-, 12- or 24-pulse. A six-phase full-wave uncontrolled diode rectifier is the basic design in most 750 V DC traction substations.

The standard rating of a rectifier unit for heavy traction service is as follows [122]:

100% rated load amperes continuously until constant temperatures have been reached by all parts of the rectifier unit, followed by either 1) 150% current for 2 h or 2) 300% current for 1 min. Most modern rectifiers have been designed with proper circuits to indicate the condition of the diodes, protect the rectifier against over-temperature and monitor the cooling fan. The standard rating and operation logic of a rectifier for heavy traction service is shown in Figure 5.4.

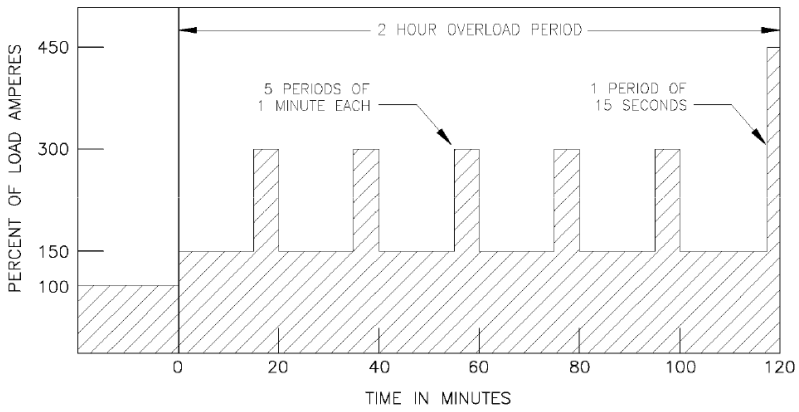

Figure 5. 4 Standard rating of a rectifier for heavy traction service [122]

The failure mechanism of a diode can be static high-voltage breakdown or excessive leakage current. The leakage current of power diodes is usually very low and increases with voltage and temperature. The diode can withstand short periods of overload. After returning to the normal load after overloading, the temperature and leakage current of the diode will return to normal values, so it will not have a great impact on its life. Studying the effect of dynamic load–time characteristics on diode life does not make much sense, as it has little influence on diode failure.

5.3.3 Circuit breakers (IEEE Std C37.14 [124])

The circuit breakers form a very important part of the protection circuits in the substation. They will switch off the supply when a fault occurs inside the substation. The circuit breaker tripping mechanism is operated by protection relays which protect the substation from overloading and high fault currents.

According to the Consumer Product Safety Commission (CPSC) estimation, the life expectancy of a circuit breaker is about 30 to 40 years. Short circuits, power surges and spikes are the main cause of circuit breaker failure. Circuit breakers are not used frequently under the normal operating conditions of a substation. Therefore, under normal operating conditions, the reliability and life of the circuit breaker have little to do with the load. Therefore, in this study, the impact of dynamic load on the circuit breaker is ignored.

5.3.4 Isolators

Isolator switches, also called disconnectors, are used in power grids and substations particularly. The function of isolator switches is to isolate transformers and circuit breakers when they are due for maintenance or when there is a fault. When a fault occurs, the isolator will cut out a portion of the substation. The probability of isolator failure is very low.

5.4 Remaining useful life calculation

The reliability of a power system depends on the condition of its critical components. Therefore, estimating the remaining life of traction transformers, rectifiers and major components is essential for this study. In a typical traction substation system, all the components are in series with each other. But it is difficult to monitor the condition of existing equipment and predict their remaining useful life. In reliability-related analysis of substation systems, since all components are connected in series, the structure of the series system will be used for calculation.

According to their fault mechanisms, only transient high currents can damage the life of rectifiers and isolators. In general, during normal operation, the current does not exceed the maximum allowable threshold of the rectifier and isolator. The load current–time characteristics have a greater impact on the life of a transformer than the other components. The influence of instant load on the rectifiers and isolators can be ignored.

Therefore, this research focuses on the impact of load characteristics on traction transformers. In this study, the single train traction calculation and power supply simulation are considered comprehensively and the dynamic simulation model of a DC TPSS is used to analyse and evaluate its load characteristics, to study the operation risk of a traction transformer under the influence of load characteristics.

5.4.1 Probabilistic assessment of transformer loss of life

The Acceleration Aging Factor F_{aa} (also called the Accelerated Aging Rate or Acceleration Factor) is defined as the ratio of the real-world lifetime to the test duration. The higher the F_{aa}, the less reliable the test is. In the IEEE C57.91-2011 guide, the relationship between the Acceleration Aging Factor F_{aa} and the hot-spot temperature θ_h is presented as:

$$F_{aa} = e^{\frac{15000}{110+273} - \frac{15000}{\theta_h+273}} \tag{5.2}$$

This equation is an adaption of the Arrhenius reaction rate theory. It indicates that the ageing of the transformer is a function of hot-spot temperature because of the load current. F_{aa} is a per-unit quantity for a reference temperature of 110 ℃.

Figure 5.5 describes the characteristics of transformer per-unit life (L) varying with hot-spot temperature. The per-unit life is defined as:

$$\mathrm{L} = 9.8 \times 10^{-18} \times \mathrm{e}^{\frac{15000}{\theta_\mathrm{h}+273}} \tag{5.3}$$

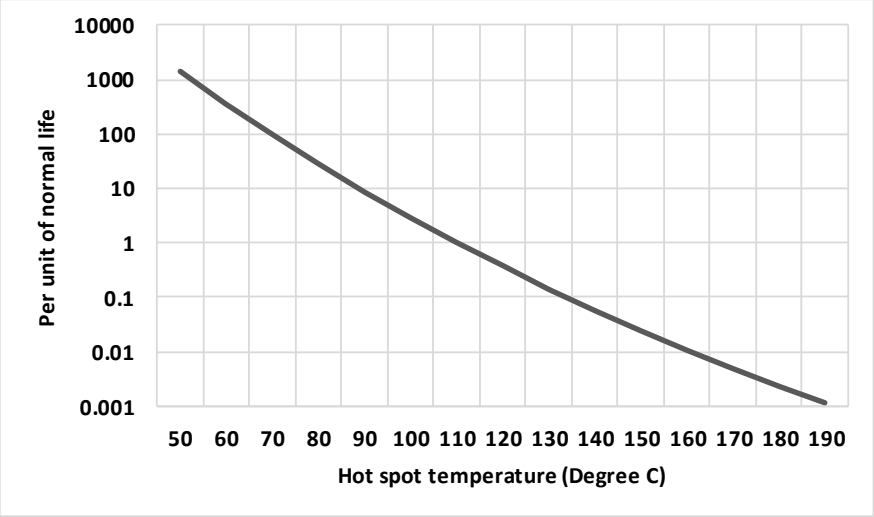

Figure 5. 5 Transformer loss-of-life characteristics

The Equivalent Ageing Factor (F_{eqa}) of the transformer with respect to the reference temperature 110 ℃ over a given period of time (T) is calculated as:

$$F_{eqa} = \frac{\int_{t=0}^{t=T} F_{aa} dt}{T} \tag{5.4}$$

The loss-of-life percentage is the ratio of the loss of life over a period of time T and its normal insulation life, as shown in equation (5.5). Normal insulation life is generally an empirical fixed value, which can be found in the device user manual.

$$Loss\ of\ Life\ \% = \frac{F_{eqa} \times T}{Normal\ Insulation\ Life} \times 100 \tag{5.5}$$

The Remaining Useful Life (RUL) is an estimate of the number of years remaining for a component or system to operate without failure before replacement. In this study, the system's RUL can be calculated as:

$$RUL = Normal\ Insulation\ Life - (F_{eqa} \times T) \tag{5.6}$$

5.4.2 Failure rate

Failure rate is the frequency with which an engineered system or component fails, expressed as failures per unit of time. According to the definition of conditional probability, the probability of failure during time interval Δt after T equivalent operation time can be calculated as:

$$\begin{aligned}\lambda(t) &= P(T \le t \le T + \Delta t \mid t > T, \theta_0) \\ &= \frac{F_{eqa}(T + \Delta t|\theta_0) - F_{eqa}(T|\theta_0)}{1 - F_{eqa}(T|\theta_0)}\end{aligned} \tag{5.7}$$

where θ_0 is the hot-spot temperature at time t. Here, the failure rate is a function related to time and temperature, rather than an empirical fixed value.

By correlating the failure rate with the transformer hot-spot temperature and time, the load-time characteristics of the traction substation is clearly shown. This time-related failure rate is used to replace the empirical failure rate, which can better reflect the condition of the system.

5.5 Impact of traction load on substation systems

Different to the substation in a general power system, a TPSS has a single load, and the impact on the traction transformer is very large, while the load of a general power system is mostly industrial or household load, and the transformer is relatively more stable. After understanding the operating modes and failure modes of the main

components, the load–time characteristics of a DC traction substation can be determined by Matlab simulation. According to their fault mechanisms, only transient high currents can damage the life of rectifiers and isolators. In general, during normal operation, the current does not exceed the maximum allowable thresholds of rectifiers and isolators. The load current–time characteristics have a greater impact on the life of a transformer than the other components. The influence of instant load on the rectifiers and isolators can be ignored. Therefore, this research focuses on the impact of load characteristics on the traction transformer.

A model of single train simulation and a power supply system was established in Matlab to study the influence of traction load. Figure 5.6 describes the inputs and outputs of this system simulation model. In the simulation, the inputs are traction loads and the ambient temperature, and the outputs are substation energy consumption, power and system life, some reliability indicators, etc. The purpose is to explore the impact of load on the system, and whether there is a way to maximise the reliability of the power supply system without affecting its normal operation.

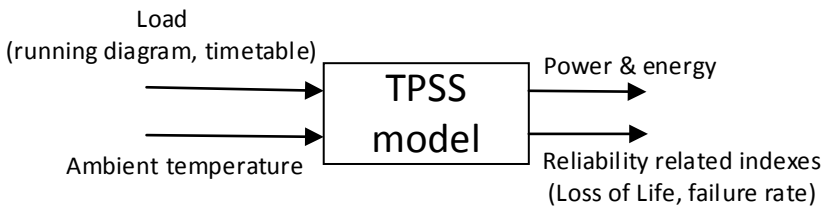

Figure 5. 6 Block diagram of system overload monitoring

In this study, the Singapore East West Line is used as a simulation example. It is a high-capacity metro line operated by SMRT, which is 49.46 km in length with 27 substations, 8 tie stations and 2 stations without a DC-link connection. SMRT parameters, such as route information, vehicle tractive effort and substation rating, have been introduced in detail in Chapter 3.6.1. Figure 5.7 shows the Singapore line's altitude and TPSS locations.

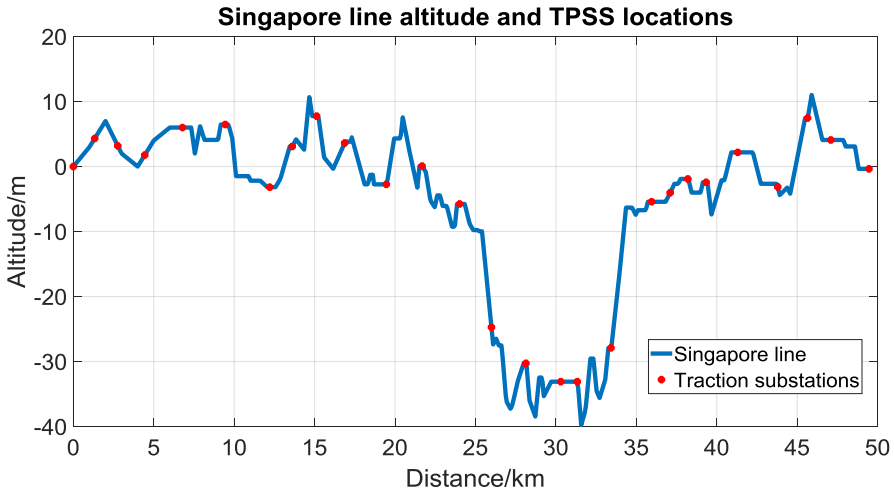

Figure 5. 7 Line altitude and station locations of the Singapore line

5.5.1 Matlab simulation results – scenario 1 (No. 1 TPSS)

The normal lifespan of a distribution transformer is 20.55 years, which is 180,000 h. Suppose the power system is at its first day of operation. The rated power of the TPSS is 4 MW. The ambient temperature is held constant at 25 °C. A full day's timetable is adopted in this simulation. For more accurate results, the simulation runs every 120 s and repeats to reach a full day's timetable.

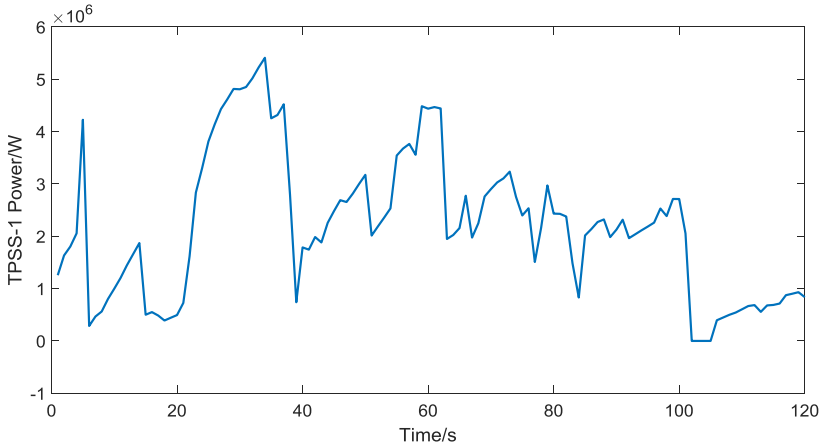

Figure 5. 8 No. 1 TPSS power vs time

A distribution of power usage for Tuas Link traction substation (No. 1 TPSS) is shown in Figure 5.8. These data are for a single train journey of 120 s and show the amount of power that is drawn from the substation. There is a peak between 20 s and 40 s where the load is higher. The power system experiences an overload for a short period of time. The hot-spot temperature of the traction transformer changes with time, as shown in Figure 5.9.

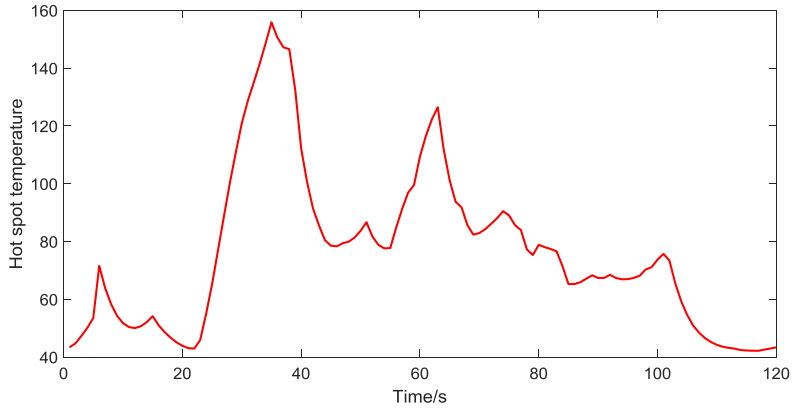

Figure 5. 9 No. 1 TPSS hot-spot temperature vs time

At the maximum load of the substation, between 30 s and 40 s, the Ageing Acceleration Factor of the transformer is highest, meaning that the system is most likely to fail at this point in time.

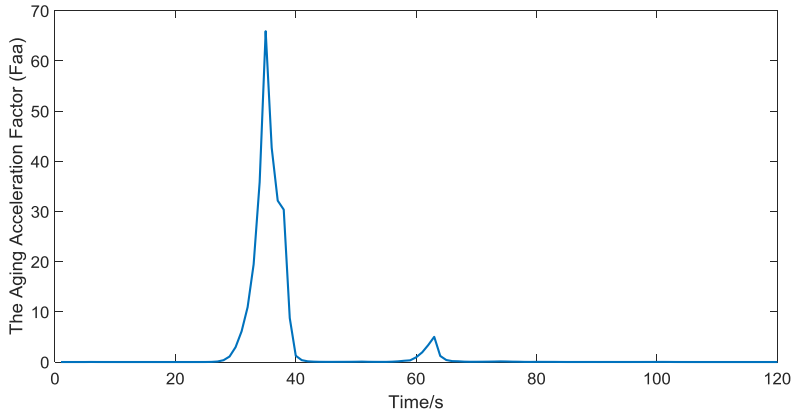

Figure 5. 10 No. 1 TPSS Ageing Acceleration Factor vs time

Figure 5.11 shows the percentage loss of life over given periods of time compared to the system's normal life. From the simulation results, it can be seen that the total loss of life over a single run of 120 s (2 min) is 5.2156 $\times 10^{-6}$ years, which is equivalent to 0.0457 h (2.74 min).

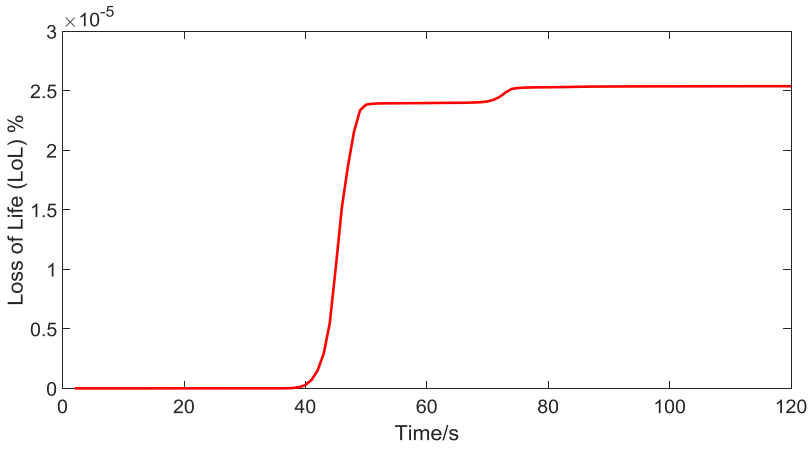

Figure 5. 11 No. 1 TPSS loss of life vs time

5.5.2 Scenario 2 (No. 7 TPSS)

Under the premise that the entire metro line runs on the same schedule, the reliability and loss of life for different substations are different due to the different output power and load cycle of each substation. Scenario 2 gives the simulation results from Lakeside traction substation (No. 7 TPSS), in which the system is under normal operation and experiences no overload.

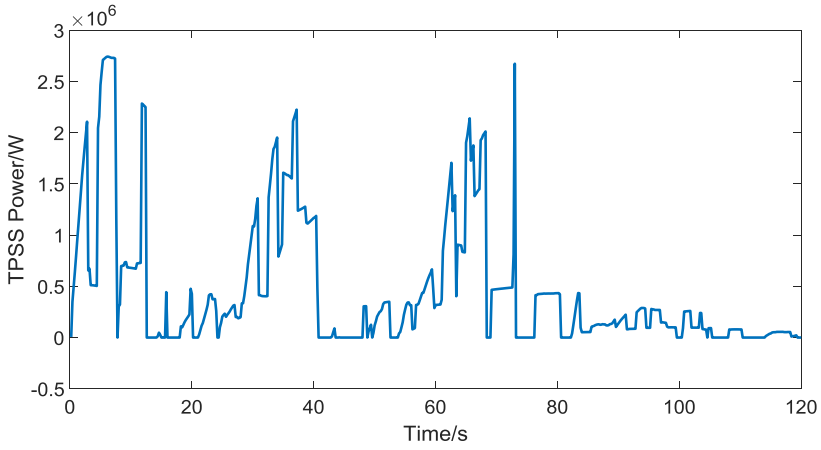

Figure 5. 12 No. 7 TPSS power vs time

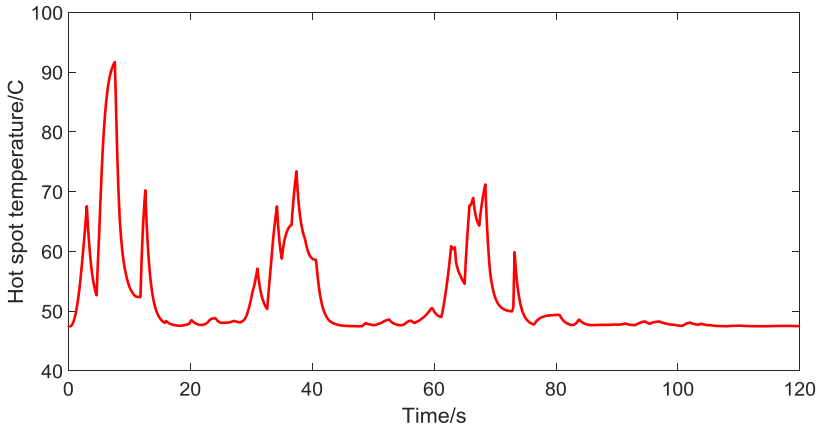

Figure 5. 13 No. 7 TPSS hot-spot temperature vs time

The Ageing Acceleration Factor, as shown in Figure 5.14, is less than 1 when the hot-spot temperature is lower than 110 ℃, meaning there is little loss of life.

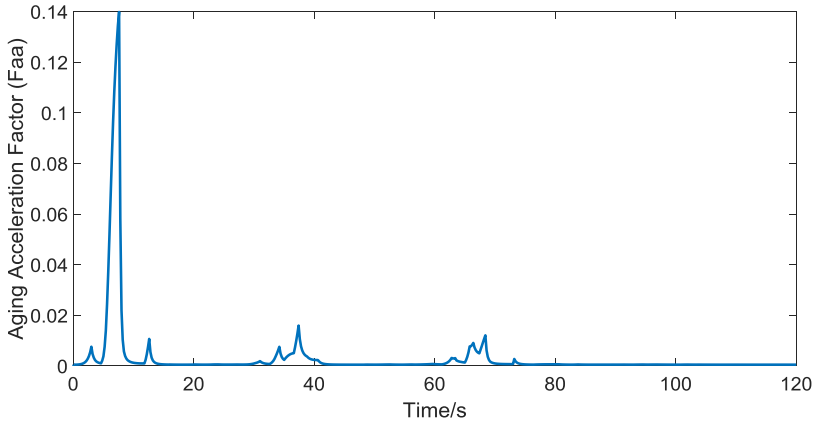

Figure 5. 14 No. 7 TPSS Ageing Acceleration Factor vs time

In this case, the total loss of life over a single run of 120 s (2 min) is 3.5×10^{-6} years, which is equivalent to 0.03066 h (1.839 min). Compared to scenario 1, in which the loads are slightly over the rated power, the total loss of life of the system in this simulation is very small. There will be a slight extension of lifespan compared to its normal life under rated power operation. It can be seen that operating below the rated load of the transformer has a negligible impact on its life and reliability; overloading has a great influence on the system, which will reduce the life of the transformer.

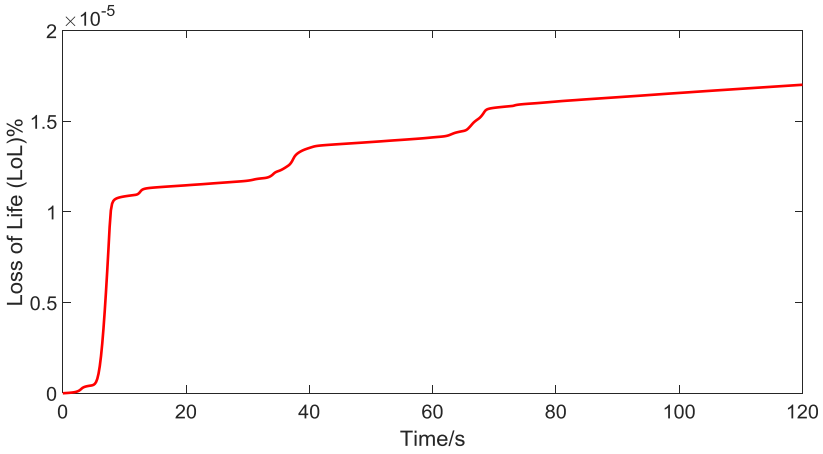

Figure 5. 15 No. 7 TPSS loss of life vs time

5.5.3 Scenario 3 – full year of operation

The daily average failure rate and reliability of each TPSS are predicted using the reliability evaluation indices listed in Chapter 4.1.1. The RUL of the substations is also calculated, as illustrated in Table 5.2. According to the simulation data listed, under the condition that the same timetable is operated on the whole line for 1 year, the third substation Tuas Crescent will bear the largest load, and the estimated remaining service life is 14.215 years, which is much shorter than for other substations. The simulation results can more accurately reflect the real-time operation conditions of TPSSs. When developing a maintenance or replacement plan, emphasis should be placed on this traction substation. It can be concluded that due to the influence of dynamic traction load, each substation on the same line has different life effects. Predictive maintenance could be carried out when necessary.

Table 5. 2 Substation data for East West Line

	Platform	Abbreviation	Location [m]	Rectifier rating	Maximum F_{aa}	Failure rate	Average reliability	Remaining useful life (years)
1	Tuas Link	TLK	0	2 MW ×2	65.91	4.15×10^{-3}	0.995	14.599
2	Tuas West Road	TWR	1330	2 MW ×2	3.75	5.39×10^{-4}	0.999	19.312
3	Tuas Crescent	TCR	2765	2 MW ×2	67.84	4.32×10^{-3}	0.995	14.215
4	Gul Circle	GCL	4440	2 MW ×2	55.58	9.89×10^{-4}	0.997	16.943
5	Joo Koon Station	JKN	6787	2 MW ×2	25.36	7.34×10^{-4}	0.997	17.874
6	Pioneer Station	PNR	9449	3 MW ×2	24.54	7.29×10^{-4}	0.998	17.925
7	Lakeside	LKS	12210	2 MW ×2	0.14	8.36×10^{-5}	0.999	21.754
8	Chinese Garden	CNG	13606	2 MW ×2	1.59	5.30×10^{-4}	0.999	19.578
9	Jurong East	JUR	15125	2 MW ×2	0.87	7.48×10^{-5}	0.999	20.146
10	Sungei Uiu Pandan Online	SUO	16869	2 MW ×2	20.42	4.46×10^{-4}	0.998	19.024
11	Commonwealth Online	CWO	19456	2 MW ×2	34.87	6.65×10^{-4}	0.998	18.344
12	Buona Vista	BNV	21678	2 MW ×2	55.36	8.87×10^{-4}	0.997	17.036
13	Queenstown	QUE	24011	2 MW ×2	49.87	8.25×10^{-4}	0.997	17.874
14	Delta Online	DLO	25992	2 MW ×2	44.69	8.17×10^{-4}	0.997	17.364
15	Outram Park	OTP	28133	2 MW ×2	50.74	8.32×10^{-4}	0.997	17.567
16	Raffles Place	RFP	30299	2 MW ×2	20.15	4.67×10^{-4}	0.998	19.176
17	City Hall	CTH	31325	2 MW ×2	10.81	6.47×10^{-4}	0.998	18.674
18	Lavender	LVR	33421	2 MW ×2	25.87	1.25×10^{-3}	0.997	16.368
19	Aljunied	ALJ	35947	2 MW ×2	14.35	7.02×10^{-4}	0.998	18.341
20	Paya Lebar	PYL	37099	2 MW ×2	10.69	5.27×10^{-4}	0.999	19.394
21	Eunos	EUN	38201	2 MW ×2	29.36	7.75×10^{-4}	0.998	17.964
22	Kembangan	KEM	39337	2 MW ×2	28.65	6.83×10^{-4}	0.998	18.156
23	Bedok	BDK	41301	2 MW ×2	44.58	8.06×10^{-4}	0.998	17.440
24	Sungei Bedok Online	SBO	43787	2 MW ×2	30.58	6.19×10^{-4}	0.998	18.343
25	Simei	SIM	45641	2 MW ×2	1.87	3.65×10^{-4}	0.999	19.890
26	Tampines	TAM	47087	2 MW ×2	0.56	8.04×10^{-5}	0.999	20.694
27	Pasir Ris	PSR	49458	2 MW ×2	0.19	8.96×10^{-5}	0.999	21.866

In this way, running a 24-hour timetable and analysing the simulation results, we can find out which time slot for each TPSS is the most risky and which substation is most

likely to fail. During this time period, it is important to monitor substations that have the highest risk of failure. If the utilization rate and reliability of the current power supply system can be improved, it can not only save the operation cost for railway utilities, but also optimize the allocation of power resources and make contributions to energy conservation. Theoretically, by optimising the timetable and train running diagram, the impact of traction load on the system can be reduced without compromising energy consumption and travel time. It can also provide guidance for future power supply system design and optimal operation of the system once it is built.

5.6 Summary

In this chapter, an innovative method is proposed to investigate the influence of traction load on TPSS reliability and life. A comprehensive evaluation and simulation model of a DC traction power system is proposed. The reliability of a typical 750 V DC TPSS is evaluated by using a fault tree model and a series of reliability indices. According to the fault mechanism of the electrical components, a thermal model of the transformer and simulation model of traction load are established. The model is used for evaluating the system and for optimal operational plan decision-making. The impact of traction load on system reliability is clearly shown. The weakest links and time slots of the system are found. Through case analysis of the Singapore metro line, it is found that although the same timetable is operated on the same line, the impact of dynamic load on substation life is different. Due to the large random fluctuations and non-linear

characteristics of traction load, a change of load will have a certain impact on the reliability of the system and equipment.

This experimental method can be used for simulation verification when designing a new power supply system. The developed simulator can be used to verify whether the location and sizing of the traction substations are reasonable. Similarly, this method can be used to upgrade the existing power supply systems and the capacity of substations to cope with overload. If the utilization rate and reliability of the current power supply system can be improved, it can not only save the operation cost for railway utilities, but also optimize the allocation of power resources.

Load growth is a very important factor that needs to be considered in traction substation sizing. In future research, this method can be used to predict the impact of load growth on system reliability, and reduce cost by optimizing substation sizing. A new train fleet and climate change will also have a certain impact on a system. This study provides a way to pre-diagnose a system and make predictions. It can help determine when to maintain or replace certain components based on present load, future growth and ambient operation conditions.

6 Optimal operation plan

6.1 Introduction

As mentioned above, system simulation based on the train running diagram and timetable has gradually become the mainstream of urban rail traction power supply simulation analysis: according to train running diagram data and traction calculation results, one can determine the number, position and power of trains in up and down directions at each operation time, establish the equivalent power supply network, and obtain the traction network voltage and substation load, etc. at each operation time through power flow calculation.

The research of Chapters 4 and 5 has shown that overload will have a great impact on the service life of a transformer and on system reliability. Urban rail transit is characterised by high-density operation. Sometimes the departure interval of some urban rail transit lines is less than 120 s, and the power system will be overloaded. In the process of daily operation, the traction load is affected by stations, route, passenger flow and other aspects. Due to the large random fluctuation and non-linear characteristics of traction load, a change of load will have a certain impact on the reliability of the system and equipment. However, the current research on railway traction load does not link optimisation of the timetable and train trajectory with the load. Little research has taken both the energy and system reliability into consideration.

The impact of traction load and the actual operation of trains on system reliability are not considered when designing a DC railway power supply system. If the utilisation rate and reliability of the current power supply system can be improved, it can not only save the operational cost of railway utilities but also optimise the allocation of power resources and make contributions to energy conservation.

In order to make a reasonable operation scheme for a power supply system, the reliability and economy of traction transformer operation should be considered comprehensively; that is to say, under the condition of meeting the minimum operational reliability of the system, the economic benefits can be obtained to the maximum extent. This chapter will focus on the effects of overload on the substations of railway traction power systems and find out the factors that can reduce the impact of overload. The dynamic process of train operation and changing the power supply system power flow over time is simulated by computer, so that the effect of traction load on substations in different passenger flow periods can be displayed intuitively. The purpose of this study is to take into account the substations of the entire line, and optimise the timetable and train running diagram to balance the traction load of the whole line, so that the average remaining useful life of all substations is maximised. This method is proposed for railway operators to maximise the optimal use of their existing infrastructure, to select the appropriate transformer size and to determine the operation strategy. It can help make decisions for an optimal operation plan and reduce the operation risk of the power system as well as saving energy.

6.2 Dynamic traction load simulation

A dynamic model of a single train simulation and power supply system has been established in Matlab. It is based on a discrete time operation at which the power and energy consumption are calculated over 0.1s time period. The train route is divided into segments with equal length to calculate the dynamic parameters at different locations. In the simulation we can get a series of outputs, including energy, power and system life, some reliability indicators, etc. The purpose is to explore the impact of the traction load on the system, and whether there is a way to maximise system reliability without affecting the normal operation of the power supply system. The proposed simulation framework in this chapter is shown in Figure 6.1. The dynamic inputs are train driving strategies and timetables, the outputs are reliability-related system reliability and remaining useful life.

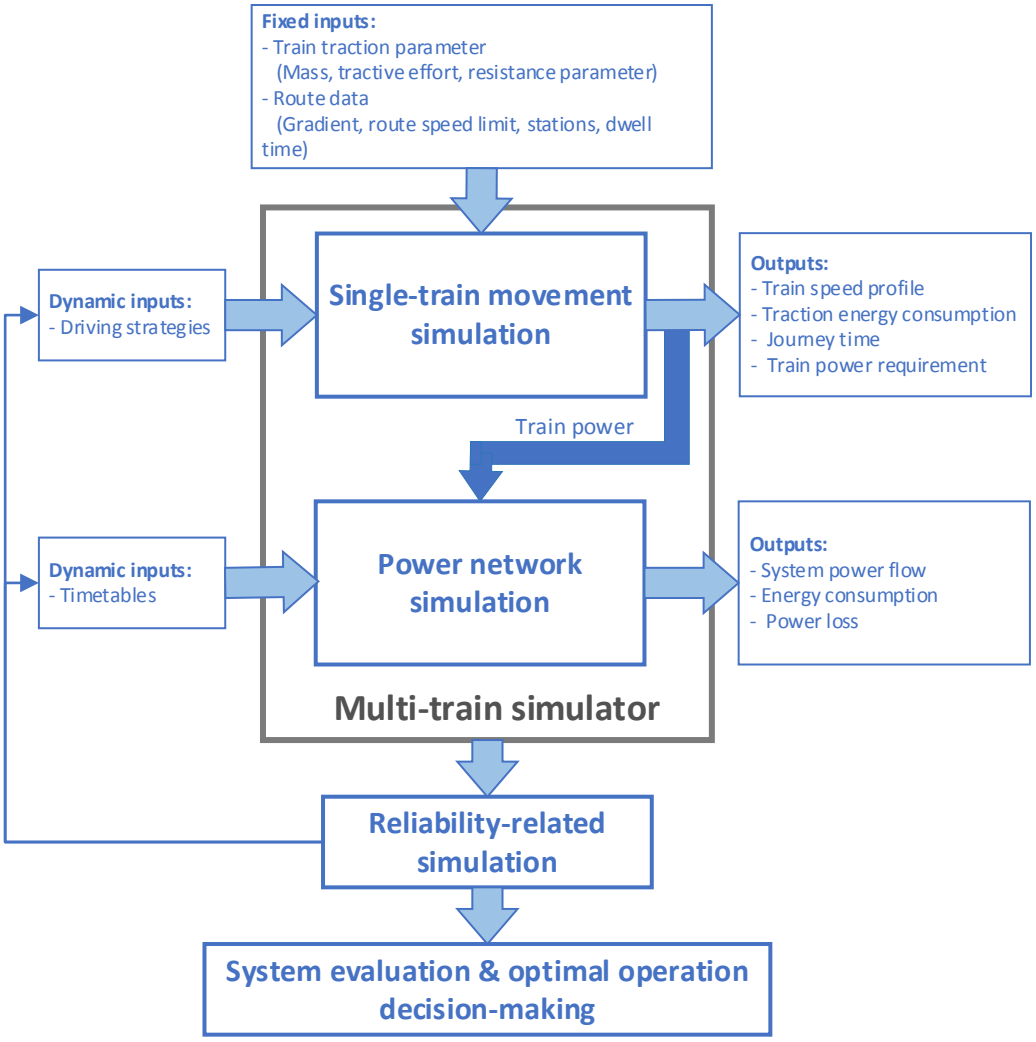

Figure 6. 1 Diagram of the overall simulation structure

In this research, a simple metro line is built up as a dynamic traction load simulation example. It is 9.45 km in length with six stations and four traction substations. The substation locations and rectifier ratings are listed in Table 6.1.

Table 6. 1 Substation data for Singapore line

Station	Location [km]	Substation	Rectifier rating
Station-1	0	Sub-1	2 MW × 2

Station-2	1.33		-
Station-3	2.76	Sub-2	2 MW × 2
Station-4	4.44		-
Station-5	6.79	Sub-3	2 MW × 2
Station-6	9.45	Sub-4	2 MW × 2

6.2.1 Inputs: different driving strategies

A single train simulator (STS) has been developed in MATLAB to simulate the train movement. Please refer to Chapter 3.4.1 for the specific modelling method of the STS. Given the vehicle type, driving strategy and route information, including the route gradient profile, position of stations, train maximum speed, maximum acceleration and dwell time, the STS can calculate the instantaneous traction power, journey time and energy consumption of a single train journey. It is based on a discrete time operation in which the power and energy consumption are calculated over a time period of 0.1 s. The train route is divided into segments of equal length to calculate the dynamic parameters at different locations.

The following parameters can be changed to formulate different driving strategies:

Coasting, maximum speed, acceleration and braking speed, dwell time, etc.

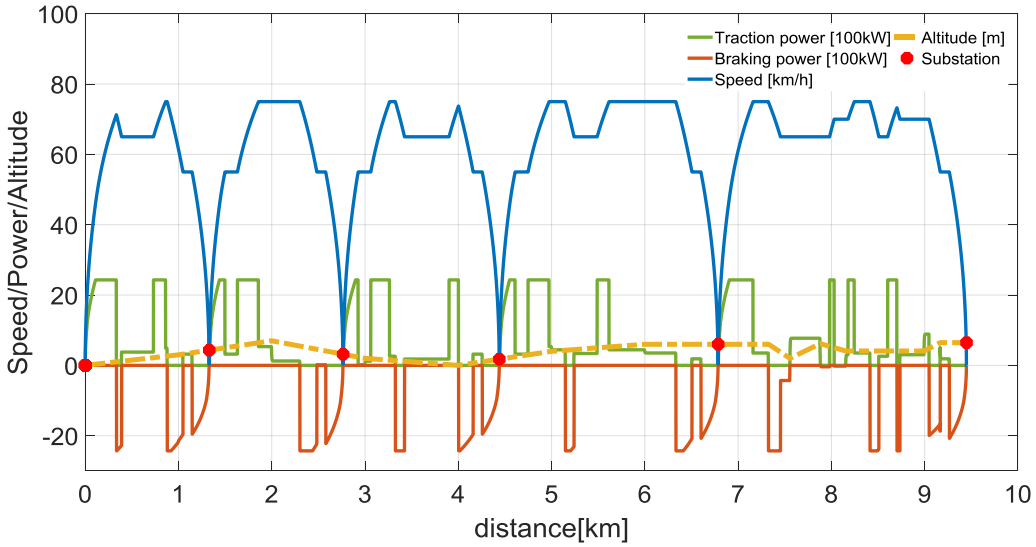

a. Driving strategy-1

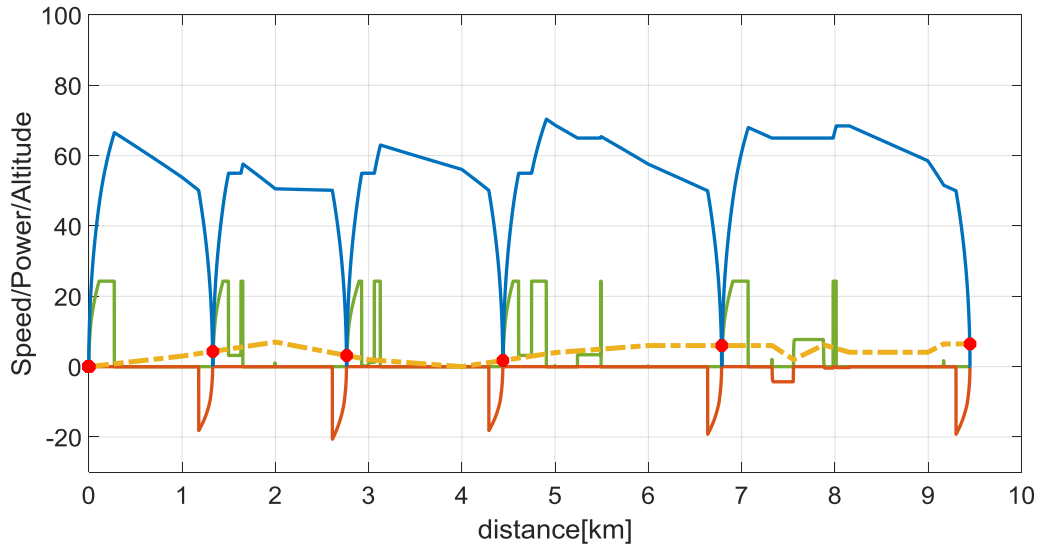

b. Driving strategy-2

Figure 6. 2 Speed and power profiles of a single train journey

The principle of changing inputs to form different driving strategies is described in detail in Chapter 3. Figure 6.2 shows the speed and power profiles of two different driving styles. In Figure 6.2 a, the train is moving at full speed, with a maximum speed

of 75 km/h, so the energy consumed and the required traction power are larger, while the driving strategy in Figure 6.2 b uses coasting to save energy, and the maximum train speed is about 70 km/h. It is obvious from the figure that the traction power required by the train in driving strategy-2 is much lower than that for driving strategy-1.

6.2.2 Inputs: different timetables

A multi-train power simulator (MTS) has been developed to calculate the substations' power and energy consumption with different timetables. A power flow iterative calculation method is used to calculate the substations' output power with running trains at different locations. MTS is covered in detail in Chapter 3.4.2.

The following parameters can be changed to make different timetables:

Headway, turn-around time, etc.

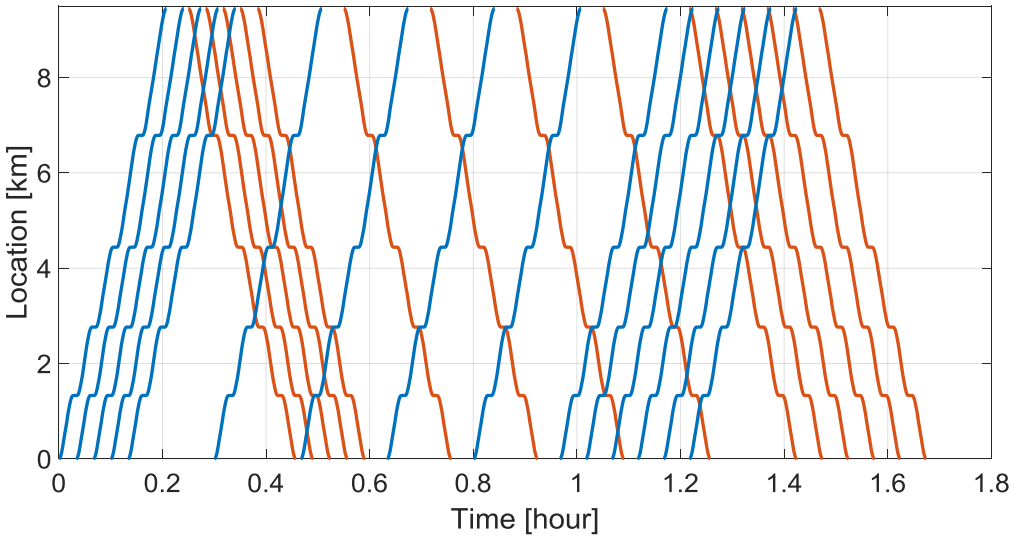

a. Timetable-1 (2 min, 10 min, 3 min)

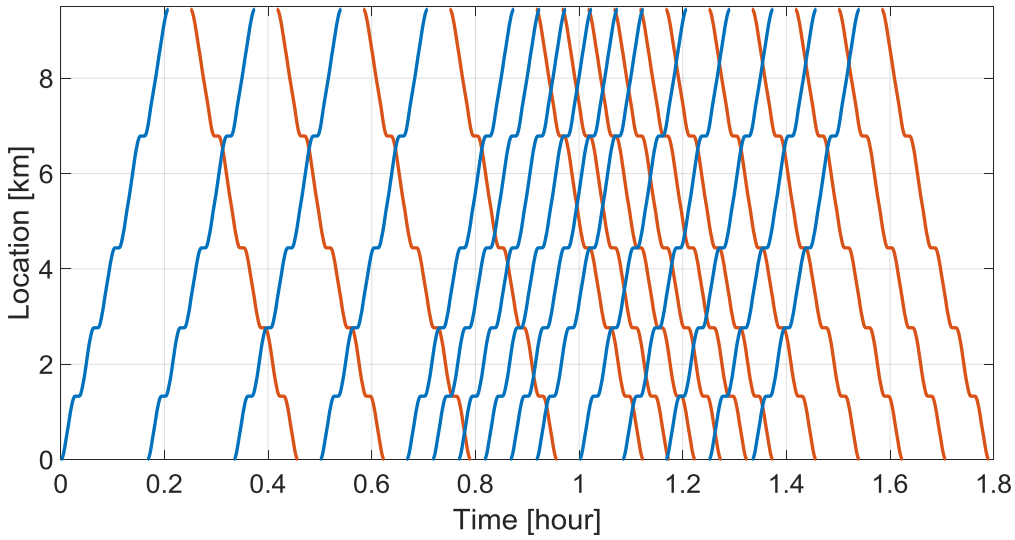

b. Timetable-2 (10 min, 3 min, 5 min)

Figure 6. 3 Timetables of multi-train operation

Figure 6.3 shows two different multi-train operation timetables. In both schedules, the total number of trains running is the same (30); the difference is their departure intervals (headways). In Figure 6.3 a, the headway of the 1st to 5th trains is 2 min, the headway of the 6th to 10th trains is 10 min, and the headway of the 10th to 15th trains is 3 min. Similarly, in Figure 6.3 b, the headway of the first five trains is 10 min, the headway of the 6th to 10th trains is 3 min, and the headway of the last five trains is 5 min.

6.2.3 Outputs

There are a few outputs that can be used for system evaluation and optimal operation plan decision-making:

Failure rate, reliability, remaining useful life, energy consumption, journey time, etc.

6.3 Impact on reliability and energy analysis

In this experiment, the two driving strategies and two train schedules are arranged and combined, as illustrated in Figure 6.4, and the results of four case studies can be obtained. From this, the Faa, loss of life percentage and remaining life of each substation are obtained. It is found that for different substation infrastructure, different operation strategies have a great difference on the life and energy consumption of each substation.

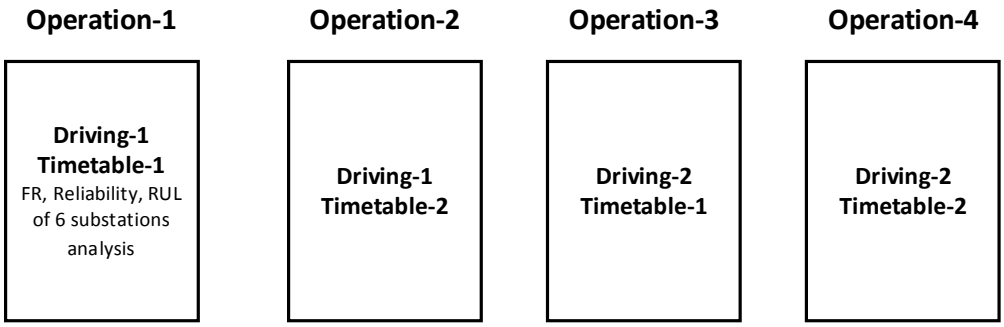

Figure 6. 4 Arrangement and combination of two driving strategies and two timetables

6.3.1 Six-substation case study

In this simple subway line, there are six stations in total, and there are six traction substations with a rated power of 4 MW beside all stations. Using different operation strategies, the reliability index, energy consumption and life loss index of each substation are obtained as shown in the tables below.

Table 6. 2 Substation reliability and energy evaluation results (6 substations, Operation-1)

Substation	Location [km]	Rectifier rating	Maximum Faa	Loss of life [%]	Remaining useful life [years]	Energy [MWh]	Life loss [min/day]
Sub-1	0	2 MW × 2	0.01574	3.169×10^{-7}	20.208	7.123	492.48
Sub-2	1.33	2 MW × 2	0.01333	2.355×10^{-7}	20.296	7.417	365.76
Sub-3	2.76	2 MW × 2	0.04606	2.453×10^{-7}	20.285	8.012	381.60
Sub-4	4.44	2 MW × 2	0.08717	4.988×10^{-7}	20.010	9.181	777.6
Sub-5	6.79	2 MW × 2	1.443	1.008×10^{-6}	19.461	10.49	1568.16
Sub-6	9.45	2 MW × 2	0.00284	1.694×10^{-7}	20.367	5.214	263.52
Total	-	-	-	-	-	47.437	3849.12

Table 6. 3 Substation reliability and energy evaluation results (6 substations, Operation-2)

Substation	Location [km]	Rectifier rating	Maximum Faa	Loss of life [%]	Remaining useful life [years]	Energy [MWh]	Life loss [min/day]
Sub-1	0	2 MW × 2	0.00325	1.447×10^{-7}	20.394	6.516	224.64
Sub-2	1.33	2 MW × 2	0.00325	1.443×10^{-7}	20.394	6.737	224.64
Sub-3	2.76	2 MW × 2	0.002154	1.515×10^{-7}	20.386	7.531	236.16
Sub-4	4.44	2 MW × 2	0.03298	2.458×10^{-7}	20.285	8.267	381.6
Sub-5	6.79	2 MW × 2	4.903	2.615×10^{-6}	17.726	9.390	4066.56
Sub-6	9.45	2 MW × 2	0.001176	1.256×10^{-7}	20.414	5.091	195.84
Total	-	-	-	-	-	43.532	5329.44

Table 6. 4 Substation reliability and energy evaluation results (6 substations, Operation-3)

Substation	Location [km]	Rectifier rating	Maximum Faa	Loss of life [%]	Remaining useful life [years]	Energy [MWh]	Life loss [min/day]
Sub-1	0	2 MW × 2	0.42	6.145×10^{-7}	19.886	4.806	956.16
Sub-2	1.33	2 MW × 2	0.0148	2.089×10^{-7}	20.324	4.064	325.44
Sub-3	2.76	2 MW × 2	0.04606	2.698×10^{-7}	20.259	4.717	419.04
Sub-4	4.44	2 MW × 2	0.04216	3.567×10^{-7}	20.165	5.583	554.40
Sub-5	6.79	2 MW × 2	0.6347	9.942×10^{-7}	19.476	6.651	1546.56
Sub-6	9.45	2 MW × 2	0.00457	1.838×10^{-7}	20.351	2.705	286.56
Total	-	-	-	-	-	28.526	4088.16

Table 6. 5 Substation reliability and energy evaluation results (6 substations, Operation-4)

Substation	Location [km]	Rectifier rating	Maximum Faa	Loss of life [%]	Remaining useful life [years]	Energy [MWh]	Life loss [min/day]
Sub-1	0	2 MW × 2	0.06273	2.959×10^{-7}	20.230	4.508	460.80
Sub-2	1.33	2 MW × 2	0.00483	1.529×10^{-7}	20.385	3.851	237.60
Sub-3	2.76	2 MW × 2	0.01898	1.835×10^{-7}	20.352	4.459	285.12
Sub-4	4.44	2 MW × 2	0.07933	4.941×10^{-7}	20.016	5.333	768.96
Sub-5	6.79	2 MW × 2	4.903	2.627×10^{-6}	17.713	6.244	4085.28
Sub-6	9.45	2 MW × 2	0.001179	1.313×10^{-7}	20.408	2.510	204.48
Total	-	-	-	-	-	26.905	6042.24

According to the results listed in Tables 6.2, 6.3, 6.4 and 6.5, there are great differences between the reliability index and energy consumption of each substation for the four operation schemes. The estimated remaining life of each substation varies greatly: that of Sub-5 is 17.713 years and that of Sub-6 is 20.408 years in Operation-4. And the substation energy consumption ranges from 2.510 to 1.049 MWh. High energy consumption for a substation does not mean that the remaining life of this substation

will be reduced: there is not a linear relationship between them. The substation life loss is mainly affected by the load peak. The reason why energy consumption is not correlated to life loss needs to be further investigated.

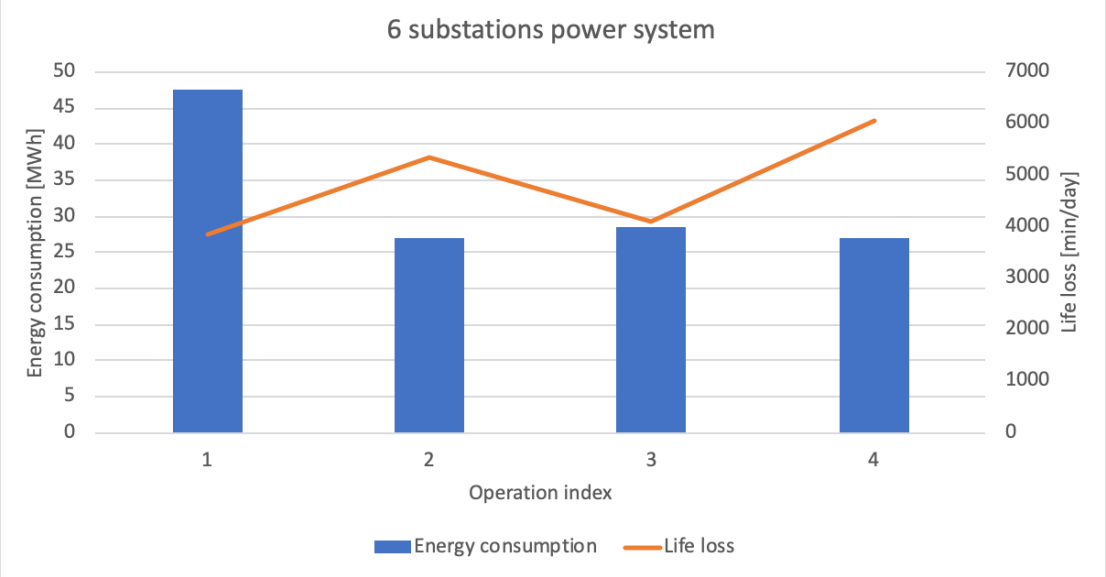

Figure 6. 5 Six-substation power system energy consumption and life loss under four operation strategies

Figure 6.5 shows the total energy consumption and life loss for a six-substation power supply system under the four different operation strategies. From the simulation results of the four operation strategies, it is difficult to directly judge which operation strategy is better based on the values of substation energy consumption and life loss. Many factors need to be considered to select the optimal operation strategy.

6.3.2 Four-substation case study

In this case, there are four traction substations with a rated power of 4 MW. Similarly, using different operation strategies, the life loss and energy consumption index of each substation are obtained through MTS simulation. The substation reliability and energy evaluation results using different operations are listed in Tables 6.6, 6.7, 6.8 and 6.9.

Table 6. 6 Substation reliability and energy evaluation results (four substations, Operation-1)

Substation	Location [km]	Rectifier rating	Maximum Faa	Loss of life [%]	Remaining useful life [years]	Energy [MWh]	Life loss [min/day]
Sub-1	0	2 MW × 2	1.347	4.513×10^{-6}	19.114	12.120	2067.84
Sub-2	2.76	2 MW × 2	3.854	6.528×10^{-6}	18.473	16.549	2990.88
Sub-3	6.79	2 MW × 2	3.53	6.901×10^{-6}	18.355	14.600	3160.80
Sub-4	9.45	2 MW × 2	0.00392	5.029×10^{-7}	20.390	5.993	230.40
Total	-	-	-	-	-	49.262	8449.92

Table 6. 7 Substation reliability and energy evaluation results (four substations, Operation-2)

Substation	Location [km]	Rectifier rating	Maximum Faa	Loss of life [%]	Remaining useful life [years]	Energy [MWh]	Life loss [min/day]
Sub-1	0	2 MW × 2	4.763	4.644×10^{-6}	20.208	11.105	492.48
Sub-2	2.76	2 MW × 2	12.895	1.420×10^{-5}	16.033	15.270	6504.48
Sub-3	6.79	2 MW × 2	2.867	4.694×10^{-6}	19.057	13.041	2149.92
Sub-4	9.45	2 MW × 2	0.0048	5.319×10^{-7}	20.381	5.753	243.36
Total	-	-	-	-	-	45.169	9390.24

Table 6. 8 Substation reliability and energy evaluation results (four substations, Operation-3)

Substation	Location [km]	Rectifier rating	Maximum Faa	Loss of life [%]	Remaining useful life [years]	Energy [MWh]	Life loss [min/day]
Sub-1	0	2 MW × 2	0.4484	1.273×10^{-6}	20.145	7.580	583.20
Sub-2	2.76	2 MW × 2	0.1324	5.568×10^{-7}	20.372	9.486	256.32
Sub-3	6.79	2 MW × 2	15.693	1.799×10^{-5}	14.828	9.202	8239.68
Sub-4	9.45	2 MW × 2	0.0023	3.597×10^{-7}	20.435	3.180	165.60
Total	-	-	-	-	-	29.448	9244.8

Table 6. 9 Substation reliability and energy evaluation results (four substations, Operation-4)

Substation	Location [km]	Rectifier rating	Maximum Faa	Loss of life [%]	Remaining useful life [years]	Energy [MWh]	Life loss [min/day]
Sub-1	0	2 MW × 2	0.4484	9.696×10^{-7}	20.241	7.132	444.96
Sub-2	2.76	2 MW × 2	3.7856	4.628×10^{-6}	19.078	9.079	2119.68
Sub-3	6.79	2 MW × 2	9.4596	1.193×10^{-5}	16.755	8.684	5464.80
Sub-4	9.45	2 MW × 2	0.00459	3.555×10^{-7}	20.437	2.981	162.72
Total	-	-	-	-	-	27.876	8192.16

Similarly, in the case of these four substations, the energy consumption and remaining life of each substation vary widely. Compared with the case study of six substations, the average energy consumption of each substation will be increased and the average life expectancy will be reduced due to the reduction of the number of substations. This is because the load allocated to each substation has increased.

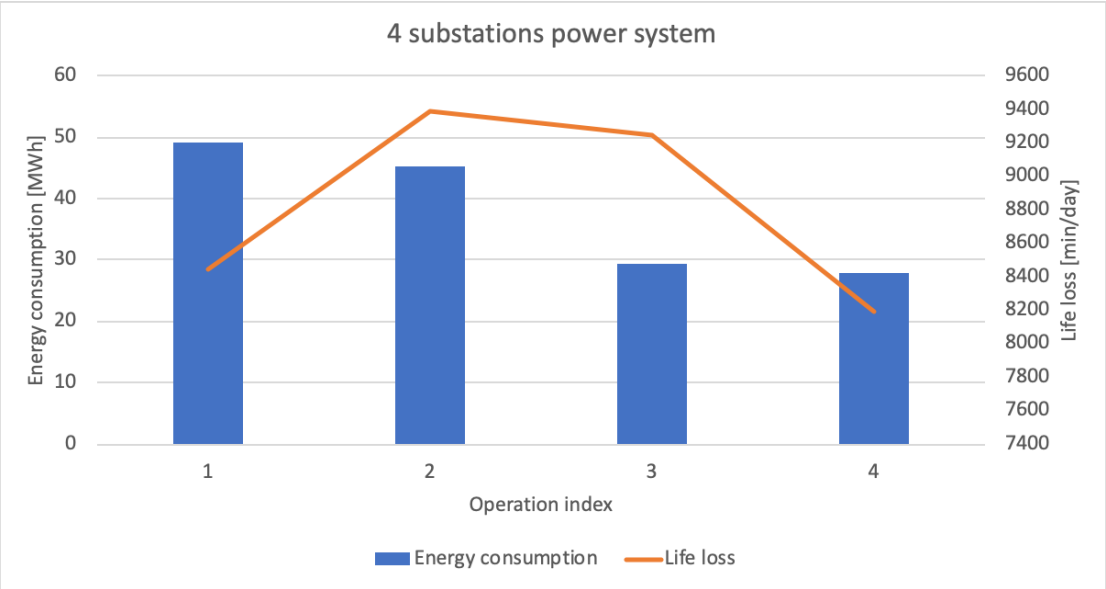

Figure 6. 6 Four-substation power system energy consumption and life loss under four operation strategies

The MTS simulation results for six substations and four substations show that different operation strategies have a great influence on the energy consumption and life of each substation in a traction power supply system. The results vary greatly. How to use a series of indicators for evaluating reliability and energy consumption to select a suitable operation strategy is very worthy of in-depth study. The next part of this chapter will elaborate how to use a genetic algorithm to optimise driving strategy and timetable, to get the optimal operation strategy.

6.4 Optimisation methodology

The purpose of this study is to improve the equipment utilisation and reliability of the power supply system, reduce energy consumption and system losses, and achieve good economic benefits through reasonable train operation planning. The absolute optimal solution can be obtained by a brute force method, but the simulation takes a long time. It will take a few days to do all the simulations (it takes about 20 s to run a simulation for each parameter change).

Therefore, heuristic algorithms can be considered to find the relative optimal solution and to improve the optimisation efficiency. The most typical and simple convergence algorithms used in engineering design are ant colony optimisation (ACO), genetic algorithm (GA), particle swarm optimisation (PSO) and k-means algorithm in machine learning. The more advanced neural networks algorithm and batch gradient descent algorithm in deep learning can be used. Compared with a traditional convergence algorithm such as GA, a deep learning algorithm can find a better local optimal solution, but its computation is relatively larger and more complex.

For the three-variable optimisation problem in this study, a traditional convergence algorithm is enough to find the local optimal solution. GA was chosen to solve this inter-dependent optimisation problem because of its ability to solve complex problems through natural evolution.

6.4.1 Algorithm selection

The GA was first introduced by Prof. John Holland of Michigan University in his book *Adaptation in Natural and Artificial Systems* (1975). The GA is now widely used as a search method for solving optimisation problems based on a natural selection process. It repeatedly modifies a population of individuals, representing different solutions to different problems. A GA was chosen to find an optimal operation strategy in this study because it is simple and flexible to implement, and it provides good, reasonably fast solutions for this non-linear and inter-dependent optimisation problem. The algorithm has powerful ability for global searching and an expandable structure which can be implemented easily with high efficiency.

The implemented GA can be divided into six modules: (1) coding method, (2) initial population, (3) fitness function, (4) selection, (5) crossover and (6) mutation. A conventional GA has three elementary genetic operators: selection, crossover and mutation.

6.4.2 Variables

At peak time, overload is a bigger problem with more life loss. Off-peak hours have little impact on the life of a TPSS, so it is only necessary to optimise the train schedule during peak hours. The headway could be increased or decreased by 1~60 s (timetable), and the train maximum speed, coasting speed and dwell time could be changed (driving

strategy) to flatten the load curve. Variables to be optimised in this study are: train maximum speed V_{train_max}, coasting velocity $V_{coasting}$, station dwell time T_{dwell} and headway $T_{headway}$.

6.4.2.1 Encoding and decoding method

Binary, permutation and tree coding methods are most commonly adopted in developing a GA. The study of train performance and timetable optimisation requires a large search space and high precision for the variables, so the Gray binary coding method is used in my GA. Each chromosome/individual of a population is coded as a fixed-length binary string. For example, if the encoding of a 10-bit chromosome is <1010101010> and the domain of the individual is [20,80], the decoding from a binary string $< b_9 b_8 b_7 b_6 b_5 b_4 b_3 b_2 b_1 b_0 >$ into a decimal number D should be $D = \sum_{i=0}^{9} b_I \, 2^i = 2^9 + 2^7 + 2^5 + 2^3 + 2^1 = 682$. So, the real number (train maximum speed) is interpreted as $X = Min + D \frac{Max - Min}{2^{bits} - 1} = 20 + 682 \times \frac{80-20}{2^{10}-1} = 60$.

6.4.2.2 Initial population

A population of individuals is formed by randomly creating strings of binary numbers with a fixed length. Each individual represents a driving strategy (including train maximum speed, coasting speed and station dwell time) that will be given to the STS to get different train performance.

6.4.3 Genetic operators of selection, crossover and mutation

6.4.3.1 Selection

The selection operator is also called the duplication process. A proportion of the current population is selected to form a new generation according to its level of fitness. Individuals with higher fitness values are more likely to be chosen. The roulette wheel selection method, also known as fitness proportionate selection, is used as the selection operator in my GA. The probability of each chromosome being selected is associated with its fitness level. The probability is $P_i = \frac{f_i}{\sum_{j=1}^{n} f_j}$, where f_i is the fitness of individual i and n is the number of individuals in the current population (note that $\sum_{i=1}^{n} P_i = 1$). Chromosomes with better fitness are more likely to be selected.

6.4.3.2 Crossover

A one-point crossover is adopted as the crossover operator in my algorithm. A random crossover point is selected in the two parent chromosomes, then these two chromosomes will exchange their parts from the crossover point and form new offspring, as illustrated in Figure 6.7. These offspring retain some basic characteristics of their parent chromosomes as well as producing some new characteristics of their own. So, the crossover operator makes the GA more effective at performing a global search and helps the algorithm converge quite quickly.

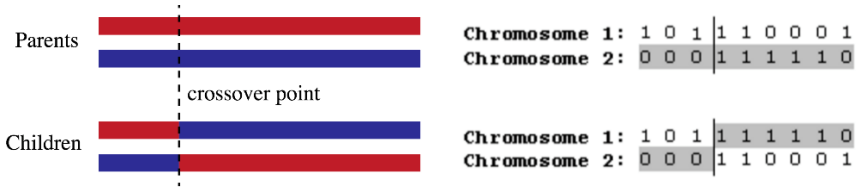

Figure 6. 7 One-point crossover process

6.4.3.3 Mutation

The purpose of mutation in a GA is to maintain genetic diversity from one generation to the next. It allows the algorithm to improve its local search ability by preventing the individuals from being too similar to each other. For a chromosome of a 10-bit binary string, a mutation point is randomly formed and the gene value at this point is altered from its initial state. This is called a single-point mutation. Figure 6.8 shows the process of one-point mutation. Two or more gene values can be changed to the opposite binary state in the mutation process by forming different mutation points.

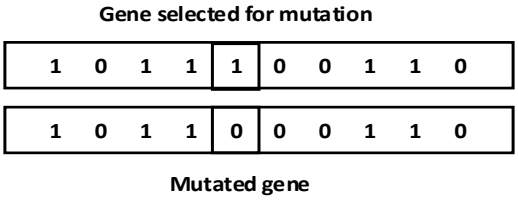

Figure 6. 8 One-point mutation process

6.4.4 Constraints

There are several constraints in the simulation:

1. No reduction in the total number of trains per day.

2. The time of a single train journey is within the maximum allowed time. In this optimisation, T_{max} is defined as +5% of one single journey time in normal operation. The constraint of single train journey time is shown in equation (6.1) where $T_{journey}$ is the single train journey time in simulation and $T_{journey\_o}$ is the original journey time.

$$T_{journey} \leq T_{max} = (1 + 5\%) \times T_{journey\_o} \quad (6.1)$$

3. The energy consumption of the system is within the maximum allowable value. In this optimisation, E_{max} is defined as +5% of the energy consumed in normal operation. The constraint of system energy consumption is shown in equation (6.2) where E is the system energy consumption in simulation and E_o is the original energy consumption.

$$E \leq E_{max} = (1 + 5\%) \times E_o \quad (6.2)$$

4. In this simulation, the headway of each train is taken as plus or minus 60 s based on the original departure interval. For example, if the headway between the second train and the first train in the original timetable is 120 s, the search range of this headway is set as 60~180 s. The constraint of headway is shown in equation (6.3)

where $T_{headway}$ is the train headway in simulation and $T_{headway\_o}$ is the original train headway.

$$T_{headway\_o} - 60 \leq T_{headway} \leq T_{headway\_o} + 60 \quad (6.3)$$

6.4.5 Cost function

In this study, the index in economics and the total Revenue Requirement (RR) is used as the cost function of this optimisation problem. The total RR is the total cost incurred by the utility in providing the service. A simplified RR is used to represent the cost function, and a cost–benefit analysis will be performed. The operation strategy problem of this study is then transformed into the objective function optimisation problem. The cost function is defined as shown in equation (6.4).

$$\begin{aligned} Cost\ function &= Initial\ cost + Operation\ cost + Maintenance\ cost \\ &= P_{sub} \times \frac{£1{,}000}{kW} + E_{sub} \times \frac{£0.1}{kWh} + \frac{P_{sub} \times \frac{£1{,}000}{kW}}{RUL_{sub}} \end{aligned} \quad (6.4)$$

where P_{sub} is the substation's rated power, E_{sub} is the substation's energy consumption and RUL_{sub} is the substation's remaining useful life.

6.4.5.1 Initial cost

Generally speaking, the initial cost (also called capital cost) related to railway transportation services is the cost of purchasing or building railway infrastructure, rolling stock, equipment, etc [126]. In order to simplify the model, this study defines

the initial cost as the investment cost of traction substations. The initial cost per substation rating can be assumed:

$$Initial\ cost = P_{sub} \times \frac{£1{,}000}{kW} \tag{6.5}$$

6.4.5.2 Operation cost

Operating cost is cost associated with operating railway services, and are usually directly related to the actual energy consumption [126, 127]. Here, the electricity cost is regarded as the system operation cost, and other factors are not considered. A unit cost of electricity in UK is around 0.1 £/kWh. The operation cost can be calculated as:

$$Operation\ cost = E_{sub} \times \frac{£0.1}{kWh} \tag{6.6}$$

6.4.5.3 Maintenance cost

Substation maintenance can generally be divided into three types: periodic maintenance (scheduled maintenance), preventive maintenance and failure maintenance. Periodic maintenance is the regular maintenance mode, which means that the equipment is inspected regularly (such as once a year or twice a year); preventive maintenance refers to the maintenance of equipment before its function significantly deteriorates; fault maintenance refers to the maintenance after a failure occurs. At present, most conventional substations adopt a periodic maintenance system.

In this study, the preventive maintenance method is used to simplify the cost model for calculating the average annual maintenance cost. For the case where the life loss of the traction transformer is less than 24 h (1440 min) per day, it is only necessary to consider paying the operating cost, that is, the basic electricity cost. For life loss of the traction transformer exceeding 24 h per day, not only the operating cost but also the preventive maintenance cost should be considered. The cost of replacing the transformer and the construction cost should be averaged to calculate the maintenance cost every year. The substation maintenance cost is defined as shown in equation (6.7).

$$Maintenance\ cost/year = \frac{replacement\ cost}{substation\ remaining\ life} = \frac{P_{sub} \times \frac{£1{,}000}{kW}}{RUL_{sub}} \qquad (6.7)$$

6.4.6 Sensitivity analysis

Sensitivity analysis is a financial model that determines how target variables are affected based on changes in other variables known as input variables. This model is also referred to as what-if or simulation analysis. It is a way of predicting the outcome of a decision given a certain range of variables. By creating a given set of variables, an analyst can determine how changes in one variable affect the outcome. The method and formula of sensitivity analysis, not detailed here, can be found in the papers by Opalski [128, 129].

Table 6. 10 Sensitivity analysis of cost function parameters

	−6%	−5%	Normal	+5%	+6%
Energy (MWh)	48000	48500	51100	53700	54200
RUL (years)	8.46	8.55	9	9.45	9.54
Initial cost	40000	40000	40000	40000	40000
Operation cost	4800000	4850000	5110000	5370000	5420000
Maintenance cost	4728.13	4678.36	4444.44	4232.80	4192.87
Cost-1	4804444	4854444	5114444	5374444	5424444
Energy sensitivity	1.0102				
Cost-2	5118728	5118678	5118444	5118232	5118192
RUL sensitivity	−0.000819				
Cost-3	5114444	5114444	5114444	5114444	5114444
Initial cost sensitivity	0				

Through sensitivity analysis, it is found that for this cost function, the impact of operation cost on the result is much higher than that of maintenance cost. The energy cost sensitivity is 1.0102, while the initial cost and maintenance cost sensitivity are almost 0. The higher the sensitivity, the greater the influence of changing this parameter on the results. In order to reflect the importance of maintenance, the weightings on the three costs have been adjusted to make the sensitivity of the three variables consistent. The weighting on maintenance cost is determined by sensitivity analysis of the input variables, and is unique for this optimisation problem. After adjusting the sensitivity weightings, the cost function is as follows:

$$Cost\ function = Initial\ cost^{a} + Operation\ cost^{b} + Maintenance\ cost^{c}$$
$$= P_{sub} \times \frac{£1{,}000}{kW} + E_{sub} \times \frac{£0.1}{kWh} + (\frac{P_{sub} \times \frac{£1{,}000}{kW}}{RUL_{sub}})\text{^}1.9 \quad (6.8)$$

6.4.7 Fitness function

The fitness function is the key point of a GA process because it measures the quality of the output. Choosing an appropriate fitness function will improve the convergence speed of the algorithm and help find the best solution to a specific problem. In this study, the aim of optimisation is to search for the optimal driving strategy and timetable to minimise the total RR, which also means minimising substation energy consumption and increasing system reliability. The fitness function in equation (6.9) is transformed from the cost function after the weight of sensitivity analysis is determined.

$$\begin{aligned} Fitness\ function &= min\left\{\sum_{n=1}^{N} CF\_n\right\} \\ &= min\left\{\sum_{n=1}^{N}\left(P_{sub} \times \frac{£1{,}000}{kW} + E_{sub} \times \frac{£0.1}{kWh} + (\frac{P_{sub} \times \frac{£1{,}000}{kW}}{RUL_{sub}})\text{^}1.9\right)\right\} \end{aligned} \tag{6.9}$$

6.5 Case study

Taking the Singapore East–West metro line as an example, the GA has been applied to simulate the above optimisation model and to search for the optimal operation plan. The search for the optimal operation strategy can be divided into two parts: train running diagram optimisation and timetable optimisation.

6.5.1 Train running diagram optimisation

Under the above constraints, the train running diagram is optimised to obtain the optimal driving strategy. The aim is to reduce energy consumption and flatten the load curve within the single train running time constraints. This optimisation is usually applied to the Driver Advisory System (DAS), one of the latest methods of railway intelligent operation.

The station locations are shown in Table 6.11. There are 33 passenger stations, of which 23 are connected to a traction substation and 10 are tie stations. The simulation parameters of the GA are shown in Table 6.12.

Table 6. 11 SMRT East–West line station location (eastbound)

No.	Station	Abbreviation	Location [m]	Station type	Substation rating
1	Tuas Link	TLK	0	TPSS	2 MW × 2
2	Tuas West Road	TWR	1330	TPSS	2 MW × 2
3	Tuas Crescent	TCR	2765	TPSS	2 MW × 2
4	Gul Circle	GCL	4440	TPSS	2 MW × 2
5	Joo Koon	JKN	6787	TPSS	2 MW × 2
6	Pioneer	PNR	9449	TPSS	3 MW × 2
7	Boon Lay	BNL	10441	Tie	-
8	Lakeside	LKS	12210	TPSS	2 MW × 2
9	Chinese Garden	CNG	13606	TPSS	2 MW × 2
10	Jurong East	JUR	15125	TPSS	2 MW × 2
11	Clementi	CLE	18613	Tie	-
12	Dover	DOV	20299	Tie	-
13	Buona Vista	BNV	21678	TPSS	2 MW × 2
14	Commonwealth	COM	22782	Tie	-
15	Queenstown	QUE	24011	TPSS	2 MW × 2
16	Redhill	RDH	25384	Tie	-
17	Tiong Bahru	TBR	26601	Tie	-

18	Qutram Park	OTP	28133	TPSS	2 MW × 2
19	Tanjong Pagar	TPG	29119	Tie	-
20	Raffles Place	RFP	30299	TPSS	2 MW × 2
21	City Hall	CTH	31325	TPSS	2 MW × 2
22	Bugis	BGS	32309	Tie	-
23	Lavender	LVR	33421	TPSS	2 MW × 2
24	Kallang	KAL	34515	Tie	-
25	Aljunied	ALI	35947	TPSS	2 MW × 2
26	Paya Lebar	PYL	37099	TPSS	2 MW × 2
27	Eunos	EUN	38201	TPSS	2 MW × 2
28	Kembangan	KEM	39337	TPSS	2 MW × 2
29	Bedok	BDK	41301	TPSS	2 MW × 2
30	Tanah Merah	TNM	43165	Tie	-
31	Simei	SIM	45641	TPSS	2 MW × 2
32	Tampines	TAM	47087	TPSS	2 MW × 2
33	Pasir Ris	PSR	49458	TPSS	2 MW × 2

Table 6. 12 GA parameters

Population size	100
Crossover	0.9
Mutation	0.03
Maximum iteration	200

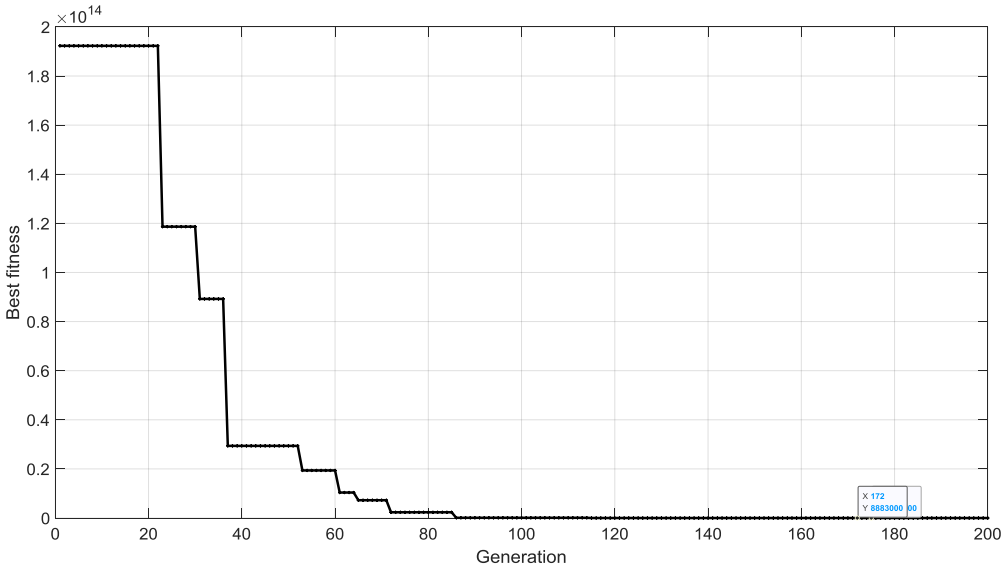

Figure 6. 9 GA convergence of optimised operation

Figure 6.9 shows the best solution for each generation and the convergence of the GA. It can be seen that after around 90 generations, the best fitness remains the same. It is assumed that at generation 100, the best solution for train operation is obtained. The single train operation simulation results are detailed in Table 6.13. The single journey time has been increased by 12 s after optimising the driving strategy. The time of a single train journey is within the maximum allowed time.

Table 6. 13 STS simulation results

	Distance (km)	**Journey time (s)**	**Energy consumption (kWh)**	**Maximum speed (km/h)**	**Coasting speed (km/h)**	**Station dwell time (s)**
Original plan	49.45	4449	576	78	60	30
Optimised plan	49.45	4461	523	80	55	28

This traction optimisation method is applied to every interstation journey, that is, the same driving strategy is used for the travel between each station. The first interstation travel between TLK and TWR is taken as an example to illustrate how the optimised driving strategy should be implemented. The driving mode instructions are illustrated in Figure 6.10. The instruction usually consists of four phases: acceleration, cruising, coasting and braking information. Figure 6.10 a shows that the current driving mode is acceleration, the next stage instruction is cruising, and the maximum target speed is 78 km/h. According to Figure 6.10 c, the train will be switched to braking mode when coasting to the target speed of 55 km/h. The train driver controls the train according to DAS instructions.

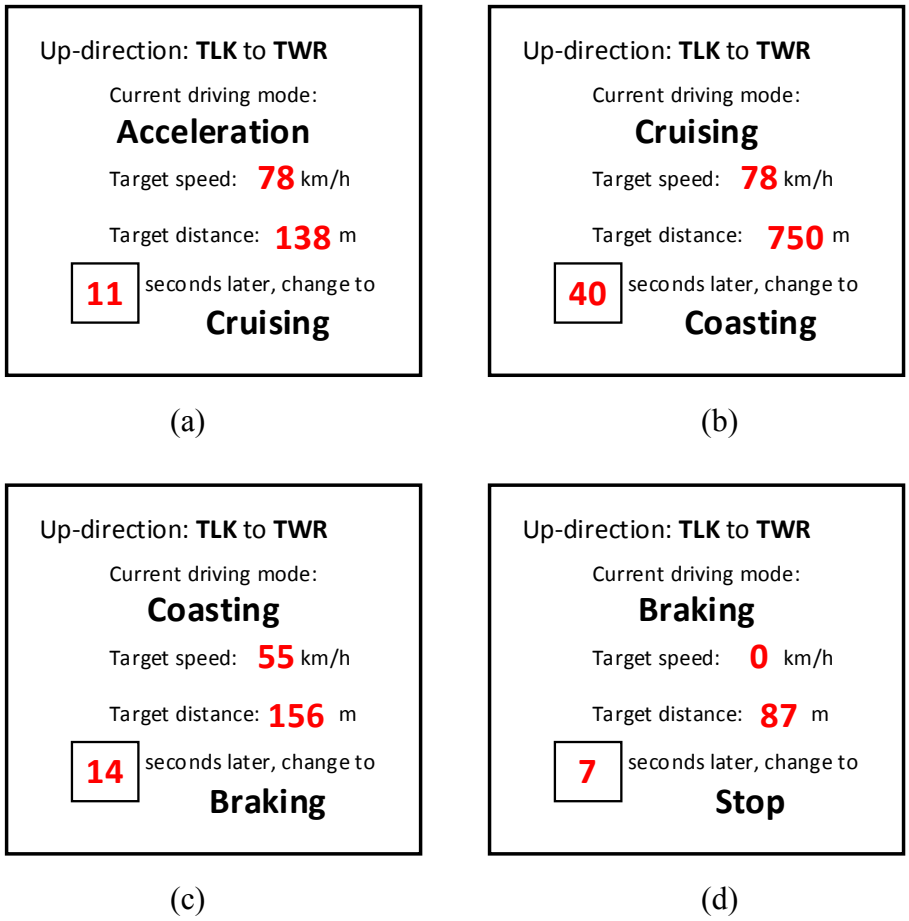

Figure 6. 10 Driving mode instructions for interstation journey between TLK and TWR

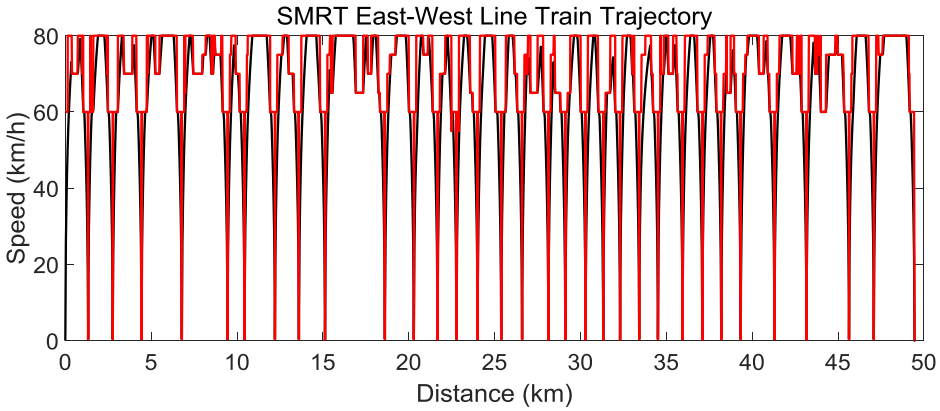

a. Original train operation

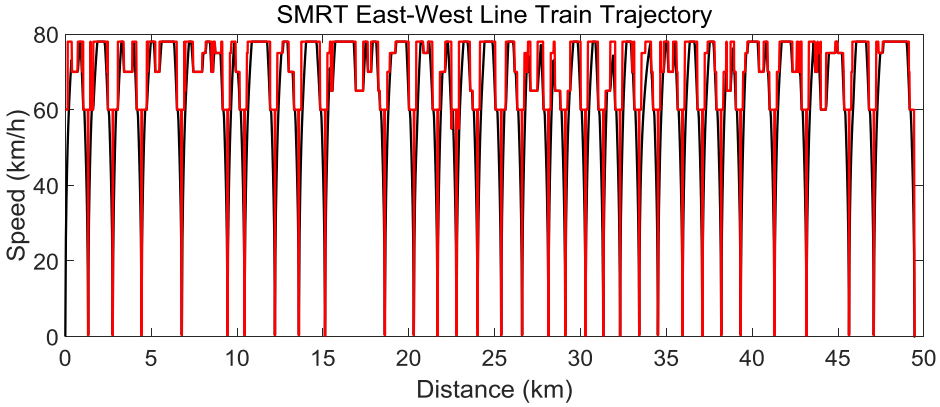

b. Optimised train operation

Figure 6. 11 SMRT line eastbound train operation speed profile

Figure 6.11 shows the speed profiles for original and optimised train operation. The journey time, station dwell time and energy consumption for each interstation journey are detailed in Table 6.14. Comparing the original results with the optimised results, it can be seen that the total one-way running time is increased by 12 s, and the energy consumption is reduced by 53 kWh, that is, the energy consumption of a single journey is reduced by 9.2%.

Table 6. 14 Optimal train driving profiles for SMRT up-direction

No.	Station	Original journey time (s)	Original dwell time (s)	Optimised journey time (s)	Optimised dwell time (s)	Original energy consumption (kWh)	Optimised energy consumption (kWh)
1	TLK	-	-	-	-		-
2	TWR	68.36	30	72.44	28	18.69	16.95
3	TCR	107.52	30	112.17	28	16.48	14.36
4	GCL	117.64	30	120.69	28	16.26	14.45
5	JKN	151.48	30	155.21	28	24.47	22.51
6	PNR	164.57	30	167.31	28	25.36	23.49
7	BNL	82.16	30	84.63	28	12.31	10.64
8	LKS	122.61	30	127.75	28	17.29	15.19
9	CNG	99.71	30	101.05	28	20.86	19.33
10	JUR	105.61	30	108.23	28	22.15	20.34
11	CLE	211.19	30	212.89	28	23.57	22.22
12	DOV	112.61	30	114.81	28	22.56	20.71
13	BNV	105.43	30	105.59	28	15.54	14.50
14	COM	88.81	30	91.38	28	14.41	11.60
15	QUE	94.46	30	94.60	28	14.37	13.33
16	RDH	103.16	30	106.61	28	14.14	12.25
17	TBR	93.83	30	97.52	28	9.94	8.51
18	OTP	109.94	30	110.84	28	16.09	14.56
19	TPG	79.78	30	79.88	28	11.94	10.92
20	RFP	91.03	30	93.50	28	15.00	13.17
21	CTH	82.99	30	85.23	28	14.67	12.89
22	BGS	79.07	30	79.17	28	16.42	15.46
23	LVR	84.80	30	84.93	28	15.48	14.48
24	KAL	85.39	30	85.50	28	29.44	28.41
25	ALI	103.43	30	105.72	28	17.48	15.65
26	PYL	89.73	30	91.67	28	15.52	13.84
27	EUN	86.97	30	89.28	28	16.60	14.79
28	KEM	88.54	30	89.52	28	14.71	13.15
29	BDK	127.32	30	129.06	28	23.36	21.61
30	TNM	130.12	30	135.30	28	16.37	14.46
31	SIM	160.69	30	161.51	28	28.94	27.44
32	TAM	107.70	30	111.55	28	16.01	14.28
33	PSR	152.74	30	158.76	28	19.81	17.73
	Total	3489.40	960	3564.30 (+12 s)	896	576.24	523.19 (−9.2%)

6.5.2 Timetable optimisation

It is assumed that the whole day operation time of the subway is from 5:00 to 23:00. The morning peak is from 6:30 to 9:30, and the evening peak is from 16:00 to 19:00. The departure interval is every 4 min in off-peak hours and every 2 min in peak hours. Figure 6.12 shows the output power of the substation when running a full-day timetable. The part circled in red circle in Figure 6.12 shows that the output power of the substation is higher than its rated power, which is regarded as overload operation. This study mainly focuses on optimisation of the peak load to flatten the load curve, to reduce the adverse effects of overload.

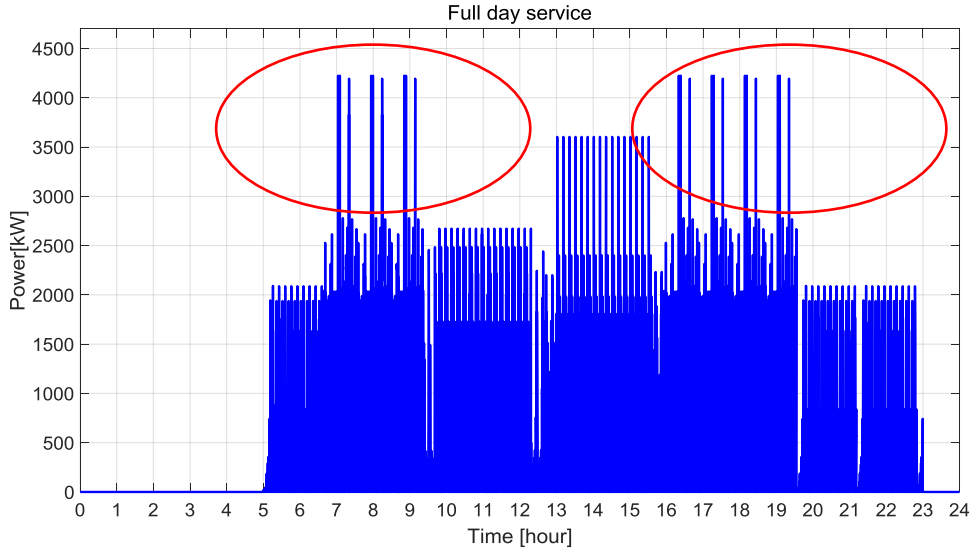

Figure 6. 12 Output power of substation when running a full-day timetable

Table 6.15 shows the schedule of a full day's operation of the Singapore Metro. In the process of operation optimisation, it is necessary to ensure that the total number of trains

in operation remains unchanged, that is, the total number of trains departing in the whole day is 720.

Table 6. 15 Operation timetable and train headway

Time	Headway (s)	Total trains
5:00–6:30	240	22 ×2
6:30–9:30 (peak)	120	90 ×2
9:30–16:00	240	98 ×2
16:00–19:00 (peak)	120	90 ×2
19:00–23:00	240	60 ×2
Total	-	360 ×2

It is set that the driving strategy in STS is applied to each train. The results of the GA-optimised timetable are shown in Table 6.16. The departure intervals between each vehicle are listed separately.

Table 6. 16 Timetable headway optimisation results

	Original headway (s)	Optimised headway (s)		Original headway (s)	Optimised headway (s)		Original headway (s)	Optimised headway (s)
1	120	119	**31**	120	125	**61**	120	121
2	120	118	**32**	120	126	**62**	120	122
3	120	118	**33**	120	120	**63**	120	122
4	120	116	**34**	120	120	**64**	120	125
5	120	117	**35**	120	119	**65**	120	127
6	120	120	**36**	120	120	**66**	120	126
7	120	121	**37**	120	118	**67**	120	124
8	120	120	**38**	120	121	**68**	120	122
9	120	120	**39**	120	122	**69**	120	121
10	120	119	**40**	120	121	**70**	120	123
11	120	122	**41**	120	120	**71**	120	121
12	120	123	**42**	120	115	**72**	120	120
13	120	125	**43**	120	116	**73**	120	117
14	120	120	**44**	120	116	**74**	120	124

15	120	122	**45**	120	125	**75**	120	122
16	120	121	**46**	120	126	**76**	120	121
17	120	110	**47**	120	127	**77**	120	123
18	120	117	**48**	120	125	**78**	120	122
19	120	120	**49**	120	121	**79**	120	121
20	120	119	**50**	120	122	**80**	120	122
21	120	120	**51**	120	122	**81**	120	120
22	120	121	**52**	120	123	**82**	120	118
23	120	124	**53**	120	120	**83**	120	119
24	120	125	**54**	120	116	**84**	120	121
25	120	128	**55**	120	117	**85**	120	118
26	120	124	**56**	120	118	**86**	120	120
27	120	123	**57**	120	119	**87**	120	122
28	120	120	**58**	120	115	**88**	120	121
29	120	119	**59**	120	117	**89**	120	120
30	120	122	**60**	120	119	**90**	120	121
Total time (s)			Original			Optimised		
			10800			10870		
						+70		

During the 3-hour peak period, the total journey time is increased by 87 s, which meets the time constraints in the simulation. Under the constraint conditions, the total number of trains remains unchanged at 90×2.

6.5.3 Economic evaluation of power system

The above STS and MTS results are input into the software to evaluate the power system's reliability and energy consumption. The detailed simulation and economic evaluation results of the two types of operation are shown in Table 6.17. The energy consumption and remaining useful life of each substation are obtained and intuitively shown. During the 3-hour peak time operation, the total remaining life of all substations

in the power supply system has increased by 3.14%. The power system energy consumption (operation cost) is reduced by 20.7%.

Table 6. 17 MTS results of each TPSS during 3-hour peak time operation

		Energy consumption (MWh)		Remaining useful life (years)		Operation cost (£)		Maintenance cost (£)	
		Original	Optimised	Original	Optimised	Original	Optimised	Original	Optimised
1	TLK	1.28	3.05	19.599	17.899	128.15	305.44	204.09	223.48
2	TWR	1.73	4.47	19.312	19.312	172.98	446.71	207.13	207.13
3	TCR	3.48	4.98	16.215	18.215	347.99	497.98	246.69	219.60
4	GCL	9.59	9.59	15.943	16.943	959.02	959.02	250.89	236.09
5	JKN	6.63	6.63	17.874	17.864	663.38	663.38	223.79	223.91
6	PNR	14.76	12.06	16.925	17.436	1476.38	1205.87	236.34	229.41
7	LKS	10.47	6.22	17.754	21.754	1046.69	621.85	225.30	183.87
8	CNG	7.49	3.84	19.578	20.374	749.22	384.29	204.31	196.33
9	JUR	6.50	6.25	19.146	20.766	650.05	625.00	208.92	192.62
10	SUO	8.68	8.68	19.024	19.024	867.56	867.56	210.26	210.26
11	CWO	7.75	7.79	18.344	18.348	774.66	778.55	218.05	218.01
12	BNV	11.55	7.74	17.036	18.624	1154.70	774.16	234.80	214.78
13	QUE	12.20	8.84	16.874	18.274	1219.85	884.22	237.05	218.89
14	DLO	10.97	10.92	17.364	17.368	1097.49	1092.43	230.36	230.31
15	OTP	8.76	4.13	17.567	17.987	876.22	412.67	227.70	222.38
16	RFP	7.88	4.14	19.176	18.796	788.07	414.08	208.59	212.81
17	CTH	6.04	4.59	18.674	18.986	604.16	459.49	214.20	210.68
18	LVR	4.94	6.38	16.368	16.618	493.79	638.14	244.38	240.70
19	ALJ	3.22	3.21	18.341	18.341	322.00	321.00	218.09	218.09
20	PYL	3.22	3.78	19.394	19.389	322.00	378.00	206.25	206.30
21	EUN	6.88	1.90	17.964	20.786	688.41	190.33	222.67	192.44
22	KEM	6.81	2.65	18.156	19.357	680.65	264.74	220.31	206.64
23	BDK	7.35	5.26	17.440	18.124	734.99	526.22	229.36	220.70
24	SBO	7.24	2.99	18.343	18.453	723.78	298.89	218.07	216.77
25	SIM	5.51	1.14	19.890	19.789	551.27	114.33	201.11	202.13
26	TAM	2.81	2.81	20.694	20.694	281.10	281.10	193.29	193.29
27	PSR	1.12	3.47	21.866	20.866	112.03	347.29	182.93	191.70
	Total	184.87	147.53	494.86	510.39	18486.57	14752.74	5924.93	5739.33
	%	−20.70		+3.14		−20.70		−3.13	

The energy consumption and remaining useful life of each substation for original operation and optimised operation are compared in Figures 6.13 and 6.14. From Figure 6.13, it can be seen that substation No. 6 (PNR) consumes the most energy in the original operation. The peak has been flattened using the proposed operation. After optimisation, the energy consumption of most substations tends to decrease. It can be seen from Figure 6.14 that the remaining life of substations No. 3 (TCR), No. 7 (LKS), No. 9 (JUR) and No. 21 (EUN) has been significantly improved after operation optimisation.

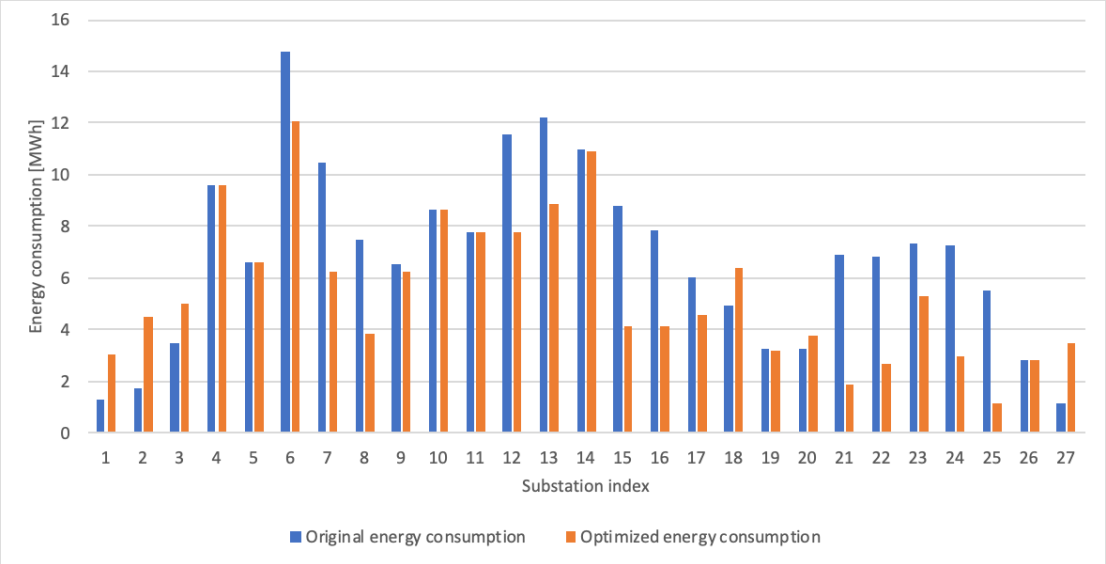

Figure 6. 13 Comparison of substation energy consumption for original operation and optimised operation

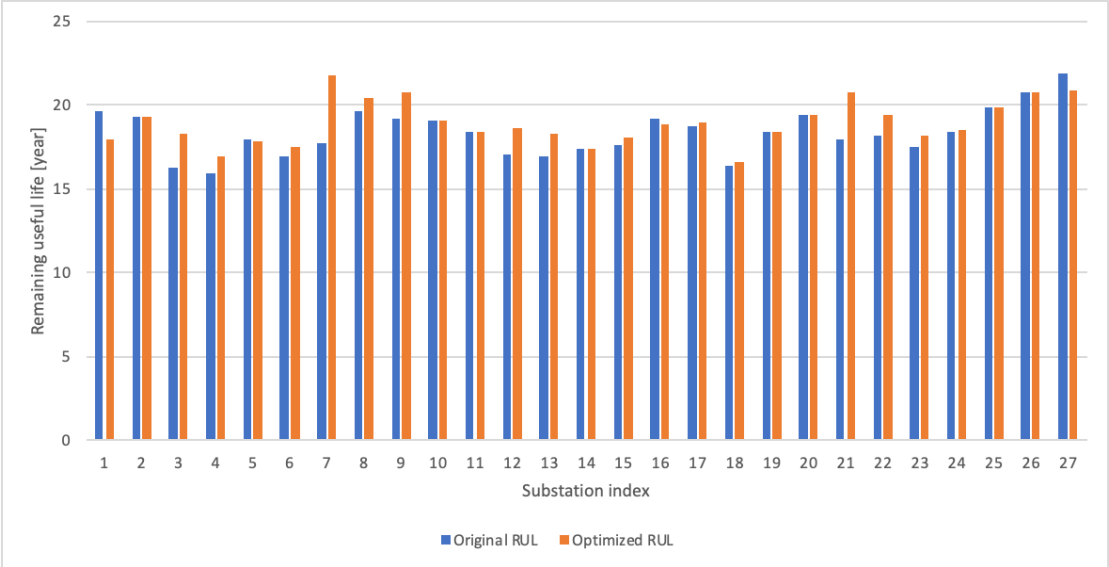

Figure 6. 14 Comparison of substation remaining useful life for original operation and optimised operation

Through in-depth study of the control mode, operation simulation and operation optimisation of urban rail transit system, the influencing factors of the train operation process can be found, which can help to improve the level of train control, ensure service quality and system reliability, and reduce the operational energy consumption. This proposed research method can be used for engineering design of railway power supply systems, including comparison and selection of multiple schemes, optimisation of the design scheme, improvement of design efficiency, project investment savings, reduction of operational costs and operational guidance for existing systems.

The time of the whole optimization simulation depends on the processing speed of CPU. The simulation time for a 3-hour timetable optimisation on an 8 GB memory, 2.3 GHz Dual-Core Intel Core i5 computer is approximately 2 hours.

6.6 Summary

Under the condition that the power supply system has been built and the infrastructure is not changed, this chapter proposes a new method to optimise the train schedule and driving strategy to reduce the impact of load on the reliability and life of the system, without reducing the number of trains running throughout the day. By selecting the optimal driving strategy and timetable, the impact of the traction load on the power supply system can be minimised, and an optimal operation plan can be obtained. In this way, it is not necessary to upgrade the existing power supply equipment, nor does it affect the normal operation of the train, and in the meantime it can ensure the highest reliability of the system and minimise operational risk. This can provide guidance for existing train operators to choose the best operating strategy with minimum operating and maintenance costs.

This experimental method can also be used for simulation verification when designing a new power supply system. Simulation can be used to verify whether the location and sizing of the traction substations are reasonable. Similarly, this method can be used to upgrade existing power supply systems and the capacity of substations to cope with overload. Load growth is a very important factor that needs to be considered in traction substation sizing. In future research, this method could be used to predict the impact of load growth on system reliability and reduce cost by optimising substation sizing.

Due to the complexity of the train operation environment, the constraints of each operation subsystem and the complexity of the route, there are different degrees of simplification in the process of research on train operation and system optimisation. This research only focuses on off-line optimisation of multiple trains.

From the literature review looking at the research of other scholars, there are few applications involving real-time optimisation of the system. There are three reasons: firstly, real-time optimisation is more complex, and requires more accurate train models, route models, etc.; secondly, a real-time optimisation algorithm requires a higher calculation speed and robustness of the calculation method itself; thirdly, for real-time train timetable optimisation, it is necessary to obtain information of the front train position and signal related to its operation and to make real-time responses to various situations. As for real-time system optimisation, further research needs to be carried out.

7 Conclusions and future work

7.1 Conclusions

Ensuring the high reliability of the traction power supply system is of great significance to the operation of the railway. Simulation of the train operation process and calculation of the traction power supply can simulate the actual operation process of urban rail transit. In the electrification design stage, the power capacity of the system can be determined according to the situation of power supply facilities, or the traction power supply system can be optimised according to the simulation results. Starting from train operation and power supply simulation, this thesis studies the influence of traction load on system life and considers the evaluation and optimisation of a traction power supply system based on the train operation diagram and timetable.

The key achievements of this thesis and recommendations for future work are as follows:

7.2 Key achievements

The key achievements of this research are listed below.

(1) The structure of an urban rail transit power supply system is elaborated and summarised in detail. This includes the components of a metro traction power

supply system. Then the traction load of an urban rail train is modelled and simulated. The process and characteristics of train motion are analysed in detail, and the STS program is compiled. Through the calculation of train traction, the change curve of the train running position and power requirement with time is obtained, which provides basic data for the MTS program.

(2) The power flow calculation method of a DC traction network is studied and the corresponding subprogram is developed. The power correction model of a regenerative braking locomotive is studied to ensure convergence of the iterative algorithm of power flow calculation.

(3) In order to increase the universality and practicability of MTS, an advanced GUI is designed, so that users do not need to deal with program code directly. The user only needs to type in the basic data in the input box of the interface and click the corresponding button to run the calculation program or draw the output results.

(4) An innovative method is proposed to evaluate the reliability of a DC power supply system under different traction loads. When studying the influence of traction load, the pulse and time-varying characteristics of load have been taken into account.

(5) Considering the train running diagram and timetable, the system is dynamically optimised. Through the optimisation algorithm and designed objective function, the optimal operation scheme of the railway traction system is determined.

(6) The Singapore East-West metro line 3-hour peak time operation has been optimised using the GA. Compared to the normal operation, simulation results show that adopting the optimised driving strategy and timetable, the total remaining life of all the substations has increased by 3.14%, and the system energy consumption is reduced by 20.7%.

7.3 Recommendations for future work

The research still has some deficiency and needs to be further strengthened. In the future, it is recommended to do more in-depth research on the following topics:

(1) In order to make the evaluation result more accurate, more field measurement data should be collected for evaluation, so that the calculation results are more in line with the actual situation of the industry. The simulation results should be compared with the field test results, and the simulation results and methods should be corrected according to the measured data.

(2) The purpose of system evaluation is to reduce or eliminate risk. Therefore, in the follow-up study, targeted operation and maintenance measures should be formulated to achieve the purpose of reasonable risk avoidance.

(3) When a train is running on the route, it will also be affected by different signal blocks and other train operations. The actual operation of the train is the result of

many factors in a complex and changeable environment. The development and research of a train group control system need to be further deepened.

(4) In order to improve the calculation speed, other efficient intelligent optimisation algorithms can be introduced to optimise the operation of a multi-train system in the future. The research can be promoted to the level of real-time optimisation.

(5) The uncertainties of the train mass and energy consumption caused by different passenger flow need to be further studied.

(6) Research and application of energy storage devices are more and more extensive. Generally, a traction substation is equipped with ground energy storage devices, such as ground resistance, super capacitor, flywheel energy storage, etc., to absorb regenerative braking energy, to reduce the consumption of regenerative energy on vehicle braking resistance, inhibit tunnel temperature rise and reduce vehicle weight. It is one of the development directions of the MTS in the future to consider the traction network power flow calculation of different ground energy storage devices.

Appendix A Publications

Papers published during PhD study are listed as follows.

[1] Y. Chen, Z. Tian, S. Hillmansen, C. Roberts, and N. Zhao, "DC Traction Power Supply System Reliability Evaluation and Robust Design," in 2019 IEEE 3rd International Electrical and Energy Conference (CIEEC), 2019, pp. 1153-1158.

[2] Y. Chen, Z. Tian, C. Roberts, S. Hillmansen, and M. Chen, "Reliability and life evaluation of a DC traction power supply system considering load characteristics," IEEE Transactions on Transportation Electrification, pp. 1-1, 2020.

Appendix B References

[1] X. Bao, "Urban Rail Transit Present Situation and Future Development Trends in China: Overall Analysis Based on National Policies and Strategic Plans in 2016–2020," *Urban Rail Transit,* vol. 4, no. 1, pp. 1-12, 2018.

[2] G. Christophe. (2020) U-Bahn, S-Bahn & Tram in Paris - Urban Rail in the French Capital. *Robert Schwandl Verlag*. 8.

[3] S. Robert. (2014) U-Bahn, S-Bahn & Tram in Berlin - Urban Rail in Germany's Capital City. *Robert Schwandl Verlag*. 8.

[4] (5 November 2020). *Rail Infrastructure and Assets 2019-20 Annual Statistical Release*. Available: https://dataportal.orr.gov.uk/media/1842/rail-infrastructure-assets-2019-20.pdf

[5] N. Rail, "Technical Plan, Chapter 11 "Network Capability", page 7 "Electrification"," 2003.

[6] P. Fouracre, C. Dunkerley, and G. Gardner, "Mass rapid transit systems for cities in the developing world," *Transport Reviews,* vol. 23, no. 3, pp. 299-310, 2003.

[7] R. D. White, "AC/DC Railway Electrification and Protection," in *IET 13th Professional Development Course on Electric Traction Systems*, 2014, pp. 1-42.

[8] R. R. Pecharroman, A. Lopez-Lopez, A. P. Cucala, and A. Fernandez-Cardador, "Riding the Rails to DC Power Efficiency: Energy efficiency in dc-electrified metropolitan railways," *IEEE Electrification Magazine,* vol. 2, no. 3, pp. 32-38, 2014.

[9] K. Ghoseiri, F. Szidarovszky, and M. J. Asgharpour, "A multi-objective train scheduling model and solution," *Transportation Research Part B: Methodological,* vol. 38, pp. 927-952, 2004.

[10] P. G. Howlett, "Optimal strategies for the control of a train," *Automatic,* vol. 32, no. 4, pp. 519-532, 1996.

[11] P. G. Howlett, J. Cheng, and P. Pudney, "Optimal strategies for energy-efficient train control," *Control Problems in Industry,* 1995.

[12] P. G. Howlett, P. Pudney, and V. Xuan, "Local energy minimization in optimal train control," *Automtica,* vol. 2009, no. 45, pp. 2692-2698, 2009.

[13] A. Adinolfi, R. Larnedica, C. Modesto, and e. al., "Experimental assessment of energy saving due to trains regenerative braking in an electrified subway line," *IEEE Transactions on Power Delivery,* vol. 13, no. 4, pp. 1536-1542, 1998.

[14] E. Khmelnitsky, "On an optimal control problem of train operation," *IEEE Transactions on Automatic Control,* vol. 45, no. 7, pp. 1257-1266, 2000.

[15] C. S. Chang and S. S. Sim, "Optimising train movements through coast control using generatic algorithms," *IEEE Transactions on Power Application,* vol. 144, no. 1, pp. 65-73, 1997.

[16] K. K. Wong and T. K. Ho, "Coast control for mass rapid transit railways with searching methods," *IEEE Transactions on Power Application,* vol. 151, no. 3, pp. 365-376, 2004.

[17] B. R. Ke, M. C. Chen, and C. L. Lin, "Block-layout design using max-min ant system for saving energy on mass rapid transit systems," *IEEE Transactions on Intelligent Transportation Systems,* vol. 10, no. 2, pp. 226-235, 2009.

[18] N. Zhao, C. Roberts, S. Hillmansen, Z. Tian, P. Weston, and L. Chen, "An integrated metro operation optimization to minimize energy consumption," *Transportation Research Part C: Emerging Technologies,* vol. 75, pp. 168-182, 2017.

[19] Z. Tian, P. Weston, S. Hillmansen, C. Roberts, and N. Zhao, "System energy optimisation of metro-transit system using Monte Carlo Algorithm," in *2016 IEEE International Conference on Intelligent Rail Transportation (ICIRT)*, 2016, pp. 453-459.

[20] *BS EN 50126:1999+1:2017 Railway Applications - the Specification and Demonstration of Reliability, Availability, Maintainability and Safety (RAMS). Generic RAMS Process*, 2017.

[21] *IEC 62278:2002 Railway applications - Specification and demonstration of reliability, availability, maintainability and safety (RAMS)*, 2002.

[22] S. Sagareli, "Traction power systems reliability concepts," in *Proceedings of the 2004 ASME/IEEE Joint Rail Conference*, 2004, pp. 35-39.

[23] Z. Wang, D. Feng, S. Lin, and Z. He, "Research on reliability evaluation method of catenary of high speed railway considering weather condition," in *2016 International Conference on Probabilistic Methods Applied to Power Systems (PMAPS)*, 2016, pp. 1-6.

[24] D. Feng, S. Lin, Q. Yang, X. Lin, Z. He, and W. Li, "Reliability Evaluation for Traction Power Supply System of High-Speed Railway Considering Relay Protection," *IEEE Transactions on Transportation Electrification,* vol. 5, no. 1, pp. 285-298, 2019.

[25] S. K. Chen, T. K. Ho, and B. H. Mao, "Reliability evaluations of railway power supplies by fault-tree analysis," *IET Electric Power Applications,* vol. 1, no. 2, pp. 161-172, 2007.

[26] B.-H. Ku and J.-M. Cha, "Reliability Assessment of Electric Railway Substation by using Minimal Cut Sets Algorithm," *Journal of International Council on Electrical Engineering,* vol. 1, no. 2, pp. 135-139, 2011.

[27] S. K. E. Awadallah, J. V. Milanović, and P. N. Jarman, "Reliability Based Framework for Cost-Effective Replacement of Power Transmission Equipment," *IEEE Transactions on Power Systems,* vol. 29, no. 5, pp. 2549-2557, 2014.

[28] D. Feng, Z. He, and Q. Wang, "A reliability assessment method for traction transformer of high-speed railway considering the load characteristics," in *2015 IEEE Conference on Prognostics and Health Management (PHM)*, 2015, pp. 1-7.

[29] G. Shirkoohi and A. Jenkins, "Computation of rectifier transformers employed in railway networks," in *2017 IEEE International Conference on Industrial Technology (ICIT)*, 2017, pp. 521-526.

[30] H. Berg and E. Wolfgang, "Advanced IGBT modules for railway traction applications: Reliability testing," *Microelectronics Reliability,* vol. 38, no. 6, pp. 1319-1323, 1998.

[31] C. R. Avery, "Power electronics reliability in rail traction," in *IEE Colloquium on Power Electronics Reliability - Promise and Practice. Does it Deliver?* , 1998, pp. 61-67.

[32] H. Hayashiya, M. Masuda, Y. Noda, K. Suzuki, and T. Suzuki, "Reliability analysis of DC traction power supply system for electric railway," in *2017 19th European Conference on Power Electronics and Applications (EPE'17 ECCE Europe)*, 2017, pp. 1-6.

[33] K. Li, Q. Yang, Z. Cui, Y. Zhao, and S. Lin, "Reliability Evaluation of a Metro Traction Substation Based on the Monte Carlo Method," *IEEE Access,* vol. 7, pp. 172974-172980, 2019.

[34] M. R. Vuluvala and L. M. Saini, "Load balancing of electrical power distribution system: An overview," in *2018 International Conference on Power, Instrumentation, Control and Computing (PICC)*, 2018, pp. 1-5.

[35] H. Xiao-qing, W. Gai-ping, W. Zhong, and W. Jie-xin, "Influence of large-scale impulsive load on adjacent power plant generating units," in *2009 International Conference on Sustainable Power Generation and Supply*, 2009, pp. 1-5.

[36] R. D. White, "Interfacing electrification and system reliability," in *IET Conference on Railway Traction Systems (RTS 2010)*, 2010, pp. 1-6.

[37] R. D. White, "DC electrification supply system design," in *7th IET Professional Development Course on Railway Electrification Infrastructure and Systems (REIS 2015)*, 2015, pp. 1-29.

[38] C. S. Chang, J. S. Low, and D. Srinivasan, "Application of tabu search in optimal system design and operation of MRT power supply systems," *Electric Power Applications,* vol. 146, pp. 75-80, 1999.

[39] J. R. Jimenez-Octavio and E. Pilo, "Optimal design of power supply systems using genetic algorithms," *WIT Transactions on the Built Environment,* vol. 103, pp. 391-400, 2008.

[40] H. Chen and Q. Jiang, "Optimization design of electrified railway traction substation and installation of capacity," *Proceedings of the CSU-EPSA,* vol. 28, no. 11, pp. 104-110, 2016.

[41] B. R. Benjamin, A. M. Long, and I. P. Milroy, "Control of railway vehicles for energy conservation and improved time keeping," *In Proc. IEA Conf. Railway Eng, Perth Western Australia,* pp. 41-47, 1987.

[42] B. R. Benjamin and I. P. Milroy, "Energy-efficient operation of long-haul trains," *Proceeding of the Fourth International Heavy Haul Railway Conference, Institution of Engineers Australia,* pp. 369-372, 1989.

[43] J. Cheng and P. G. Howlett, "Application of critical velocities to the minimisation of fuel consumption in the control of tains," *Automatic,* vol. 28, no. 1, pp. 165-169, 1992.

[44] J. Cheng and P. G. Howlett, "A note on the calculation of optimal strategies for the minimization of fuel consumption in the control of trains," *IEEE Transactions on Automatic Control,* vol. 38, no. 11, pp. 1730-1734, 1993.

[45] I. P. Milroy, "Aspects of Automatic train control," *Australia, Loughborough University,* 1980.

[46] Y. H. Chang, C. H. Yeh, and C. C. Shen, "A multiobjective model for passenger train services planning: application to Taiwan's high-speed rail line," *Transportation Research Part B: Methodological,* vol. 34, no. 2, pp. 91-106, 2000.

[47] H. J. Chuang, C. S. Chen, L. J. Fan, and C. Y. Ho, "Enhancement of power system operation for Taipei MRT network," presented at the International Conference on Power System Technology, 2006.

[48] S. Schwarze and A. Schobel, "A game-theoretic approach to line planning," *ATMOS 2006 - 6th Workshop on Algorithm Methods and Models for Optimization of Railways, Dagstuhl, Germany,* 2006.

[49] S. Schwarze, "Path player games: analysis and applications," *Berlin: Springer,* 2008.

[50] T. K. Ho, Y. L. Chi, L. Ferreira, and e. al., "Evaluation of maintenance schedules on railway traction power systems," *Proceedings of the Institution of Mechanical Engineers, Part F: Journal of Rail and Rapid Transit,* vol. 220, no. 2, pp. 91-102, 2006.

[51] A. Higgins, "Scheduling of railway track maintenance activities and crews," *Journal of the Operational Research Society,* vol. 49, no. 10, pp. 1026-1033, 1998.

[52] S. Chen, X. Wang, Y. Bai, and e. al, "Lowest costs-based optimum maintenance scheduling model for catenaries of railways," *Journal of the China Railway Society,* vol. 35, no. 12, pp. 37-42, 2013.

[53] I. El-Amin, S. Duffuaa, and M. Abbas, "A tabu search algorithm for maintenance scheduling of generating units," *Electric Power Systems Research,* vol. 54, no. 2, pp. 91-99, 2000.

[54] M. Gopalakrishnan, S. Mohan, and Z. He, "A tabu search heuristic for preventive maintenance scheduling," *Computers and Industrial Engineering,* vol. 40, no. 1-2, pp. 149-160, 2001.

[55] W. E. Moudani and F. Mora-Camino, "A dynamic approach for aircraft assignment and maintenance scheduling by airlines," *Journal of Air Transport Management,* vol. 6, no. 4, pp. 233-237, 2000.

[56] C. Sriram and A. Haghani, "An optimization model for aircraft maintenance scheduling and re-assignment," *Transportation Research Part A,* vol. 37, no. 1, pp. 29-48, 2003.

[57] C. M. F. Lapa, C. M. N. A. Pereira, and M. P. Barros, "A model for preventive maintenance planning by genetic algorithms based in cost and reliability," *Reliability Engineering and System Safety,* vol. 91, no. 2, pp. 233-240, 2006.

[58] C. Faith, "System maintenance scheduling with prognostics information using genetic algorithm," *IEEE Transactions on Reliability,* vol. 58, no. 3, pp. 539-552, 2009.

[59] R. Fortouhi, S. Farshad, and S. Fazel, "A new novel dc booster circuit to reduce stray current and rail potential in ds railways," presented at the Compatibility and Power Electronics, 2009.

[60] L. Yu-quan, W. Guo-pei, H. Huang-sheng, and W. Li, "Research for the effects of high-speed electrified railway traction load on power quality," in *2011 4th International Conference on Electric Utility Deregulation and Restructuring and Power Technologies (DRPT)*, 2011, pp. 569-573.

[61] M. Savaghebi, A. Gholami, and A. Jalilian, "Transformer dynamic loading capability assessment under nonlinear load currents," in *2008 43rd International Universities Power Engineering Conference*, 2008, pp. 1-5.

[62] F. Weihui, J. D. McCalley, and V. Vittal, "Risk assessment for transformer loading," *IEEE Transactions on Power Systems,* vol. 16, no. 3, pp. 346-353, 2001.

[63] H. J. Chuang, C. S. Chen, C. H. Lin, C. H. Hsieh, and C. Y. Ho, "Design of optimal coasting speed for mrt systems using ann models," *IEEE Transactions on Industry Applications,* vol. 45, p. 2090, 2009.

[64] S. Lu, S. Hillmansen, T. K. Ho, and C. Roberts, "Single-Train Trajectory Optimization," *IEEE Transactions on Intelligent Transportation Systems,* vol. 14, no. 2, pp. 743-750, 2013.

[65] N. Zhao, C. Roberts, S. Hillmansen, and G. Nicholson, "A Multiple Train Trajectory Optimization to Minimize Energy Consumption and Delay," *IEEE Transactions on Intelligent Transportation Systems,* vol. 16, no. 5, pp. 2363-2372, 2015.

[66] S. Acikbas and M. T. Soylemez, "Coasting point optimisation for mass rail transit lines using artificial neural networks and genetic algorithms," *IET Electric Power Applications,* vol. 2, no. 3, pp. 172-2008, 2008.

[67] X. Yang, X. Li, Z. Gao, H. Wang, and T. Tang, "A Cooperative Scheduling Model for Timetable Optimization in Subway Systems," *IEEE Transactions on Intelligent Transportation Systems,* vol. 14, no. 1, pp. 438-447, 2013.

[68] A. Ramos, M. T. Pena, A. Fernandez, and P. Cucala, "Mathematical programming approach to underground timetabling problem for maximizing time synchronization," *Journal of Management, Organization and Business Administration,* vol. 35, pp. 88-95, 2008.

[69] A. Caprara, M. Fischetti, and P. Toth, "Modeling and Solving the Train Timetabling Problem," *Operations Research,* vol. 50, pp. 851-861, 2002.

[70] L. Kroon *et al.*, "The new dutch timetable: The OR revolution," *Interfaces,* vol. 39, no. 1, pp. 6-17, 2009.

[71] R. M. Goverde and I. Hansen, "Performance indicators for railway timetables," presented at the IEEE International Conference of the Intelligent Rail Transportation (ICIRT), 2013.

[72] R. Borndorfer and M. E. Pfetsch, "Routing in line planning for public transportation," in *Operations research proceedings Berlin: Springer*, 2006.

[73] R. Borndorfer, M. Grotschel, and M. E. Pfetsch, "A column-generation approach to line planning in public transport," *Transportation Science,* vol. 41, no. 1, pp. 123-132, 2007.

[74] A. Nasri, M. F. Moghadam, and H. Mokhtari, "Timetable optimization for maximum usage of regenerative energy of braking in electrical railway systems," in *SPEEDAM 2010*, 2010, pp. 1218-1221.

[75] X. Sun, S. Zhang, H. Dong, and H. Zhu, "Optimal train schedule with headway and passenger flow dynamic models," in *2013 IEEE International Conference on Intelligent Rail Transportation Proceedings*, 2013, pp. 307-312.

[76] C. Zhang, Y. Gao, W. Li, L. Yang, and Z. Gao, "Robust Train Scheduling Problem with Optimized Maintenance Planning on High-Speed Railway Corridors: The China Case," *Journal of Advanced Transportation,* vol. 2018, p. 16, 2018, Art. no. 6157192.

[77] N. Zhao, C. Roberts, and S. Hillmansen, "The application of an enhanced Brute Force algorithm to minimise energy costs and train delays for differing railway train control systems," *Proceedings of the Institution of Mechanical Engineers, Part F: Journal of Rail and Rapid Transit,* vol. 228, no. 2, pp. 158-168, 2012.

[78] W. ShangGuan, X. Yan, B. Cai, and J. Wang, "Multiobjective Optimization for Train Speed Trajectory in CTCS High-Speed Railway With Hybrid Evolutionary Algorithm," *IEEE Transactions on Intelligent Transportation Systems,* vol. 16, no. 4, pp. 2215-2225, 2015.

[79] P. Wang, R. M. P. Goverde, and L. Ma, "A Multiple-Phase Train Trajectory Optimization Method under Real-Time Rail Traffic Management," in *2015 IEEE 18th International Conference on Intelligent Transportation Systems*, 2015, pp. 771-776.

[80] X. Yan, B. Cai, B. Ning, and W. ShangGuan, "Moving Horizon Optimization of Dynamic Trajectory Planning for High-Speed Train Operation," *IEEE Transactions on Intelligent Transportation Systems,* vol. 17, no. 5, pp. 1258-1270, 2016.

[81] F. Liu, J. Xun, and N. Bin, "An optimization method for train driving trajectory in urban rail systems," in *2016 31st Youth Academic Annual Conference of Chinese Association of Automation (YAC)*, 2016, pp. 413-418.

[82] Y. S. Tzeng, R. N. Wu, and N. Chen, "Unified AC/DC power flow for system simulation in DC electrified transit railways," *IEE Proceedings - Electric Power Applications,* vol. 142, no. 6, pp. 345-354, 1995.

[83] Y. Cai, M. R. Irving, and S. H. Case, "Modelling and numerical solution of multibranched DC rail traction power systems," *IEE Proceedings - Electric Power Applications,* vol. 142, no. 5, pp. 323-328, 1995.

[84] K. J. Kutsmeda, K. G. Fehrle, and P. J. Trick, "Computer modeling, simulation, and validation by field testing of a traction power system for electric trolley buses," *Proceedings of the 1995 IEEE/ASME Joint Railroad Conference,* pp. 87-91, 1995.

[85] Elbas, "Elbas tools [EB/OL]," *http://www.elbas.ch*.

[86] K. Harris, "Jane's World Railways," *UK: Jane's Information Group Limited,* 2001.

[87] *BS EN 50163:2004+A1:2007 Railway applications - Supply voltages of traction systems*, 2013.

[88] R. D. White, "DC electrification supply system design," in *6th IET Professional Development Course on Railway Electrification Infrastructure and Systems (REIS 2013)*, 2013, pp. 57-85.

[89] Z. Tian *et al.*, "Energy evaluation of the power network of a DC railway system with regenerating trains," *IET Electrical Systems in Transportation,* vol. 6, no. 2, pp. 41-49, 2016.

[90] B. Rochard and F. Schmid, "A review of methods to measure and calculate train resistances," *Proceedings of The Institution of Mechanical Engineers Part F-journal of Rail and Rapid Transit - PROC INST MECH ENG F-J RAIL R,* vol. 214, pp. 185-199, 2000.

[91] Y. Cai, M. R. Irving, and S. H. Case, "Iterative techniques for the solution of complex DC-rail-traction systems including regenerative braking," *IEE Proceedings - Generation, Transmission and Distribution,* vol. 142, no. 5, pp. 445-452, 1995.

[92] C. J. Goodman and L. K. Sin, "DC railway power network solutions by diakoptics," in *Proceedings of IEEE/ASME Joint Railroad Conference*, 1994, pp. 103-110.

[93] K. Bih-Yuan and L. Jen-Sen, "Solution of DC power flow for nongrounded traction systems using chain-rule reduction of ladder circuit Jacobian matrices," in *ASME/IEEE Joint Railroad Conference*, 2002, pp. 123-130.

[94] Z. Tian *et al.*, "Modeling and simulation of DC rail traction systems for energy saving," in *17th International IEEE Conference on Intelligent Transportation Systems (ITSC)*, 2014, pp. 2354-2359.

[95] C. Goodman, *Modelling and simulation*. 2011, pp. 22-31.

[96] Y. Cai, M. R. Irving, and S. H. Case, "Compound matrix partitioning and modification for the solution of branched autotransformer traction feeds," *IEE Proceedings - Electric Power Applications,* vol. 143, no. 3, pp. 251-257, 1996.

[97] R. Murata, M. Miyatake, T. Akiba, and M. Tajima, "Study on a feeding circuit model formulated to use multipurpose solvers for multi-train simulators," in *2016 International Conference on Electrical Systems for Aircraft, Railway, Ship Propulsion and Road Vehicles & International Transportation Electrification Conference (ESARS-ITEC)*, 2016, pp. 1-9.

[98] C. L. Pires, S. I. Nabeta, and J. R. Cardoso, "ICCG method applied to solve DC traction load flow including earthing models," *IET Electric Power Applications,* vol. 1, no. 2, pp. 193-198, 2007.

[99] M. Z. Chymera, A. C. Renfrew, M. Barnes, and J. Holden, "Modeling Electrified Transit Systems," *IEEE Transactions on Vehicular Technology,* vol. 59, no. 6, pp. 2748-2756, 2010.

[100] T. Ratniyomchai, S. Hillmansen, and P. Tricoli, "Energy loss minimisation by optimal design of stationary supercapacitors for light railways," in *2015 International Conference on Clean Electrical Power (ICCEP)*, 2015, pp. 511-517.

[101] T. Ratniyomchai, S. Hillmansen, and P. Tricoli, "Optimal capacity and positioning of stationary supercapacitors for light rail vehicle systems," in *2014 International Symposium on Power Electronics, Electrical Drives, Automation and Motion*, 2014, pp. 807-812.

[102] X. Li and H. K. Lo, "Energy minimization in dynamic train scheduling and control for metro rail operations," *Transportation Research Part B: Methodological,* vol. 70, pp. 269-284, 2014.

[103] X. Li and H. K. Lo, "An energy-efficient scheduling and speed control approach for metro rail operations," *Transportation Research Part B: Methodological,* vol. 64, pp. 73-89, 2014.

[104] D. He, Y. Yang, J. Zhou, and Y. Chen, "Optimal Control of Metro Energy Conservation Based on Regenerative Braking: A Complex Model Study of Trajectory and Overlap Time," *IEEE Access,* vol. 7, pp. 68342-68358, 2019.

[105] M. Dominguez, A. Fernández-Cardador, A. P. Cucala, and R. R. Pecharroman, "Energy Savings in Metropolitan Railway Substations Through Regenerative Energy Recovery and Optimal Design of ATO Speed Profiles," *IEEE Transactions on Automation Science and Engineering,* vol. 9, no. 3, pp. 496-504, 2012.

[106] J. Xun, T. Liu, B. Ning, and Y. Liu, "Using Approximate Dynamic Programming to Maximize Regenerative Energy Utilization for Metro," *IEEE Transactions on Intelligent Transportation Systems,* vol. 21, no. 9, pp. 3650-3662, 2020.

[107] BS-EN50163, "Railway applications - Supply voltages of traction systems," *BSI,* 2007.

[108] J. H. Saleh and K. Marais, "Highlights from the early (and pre-) history of reliability engineering," *Reliability Engineering & System Safety,* vol. 91, no. 2, pp. 249-256, 2006.

[109] W. Denson, "The history of reliability prediction," *IEEE Transactions on Reliability,* vol. 47, no. 3, pp. 321-328, 1998.

[110] A. Coppola, "Reliability engineering of electronic equipment a historical perspective," *IEEE Transactions on Reliability,* vol. R-33, no. 1, pp. 29-35, 1984.

[111] E. Zio, "Reliability engineering: Old problems and new challenges," *Reliability Engineering & System Safety,* vol. 94, no. 2, pp. 125-141, 2009.

[112] P. P. D. Meyer, *The Reliability of the Electric Transmission Infrastructure in the 21st Century*. IEEE, 2006, p. 1.

[113] K. Hou *et al.*, "A Reliability Assessment Approach for Integrated Transportation and Electrical Power Systems Incorporating Electric Vehicles," *IEEE Transactions on Smart Grid,* vol. 9, no. 1, pp. 88-100, 2018.

[114] F. Zheng, H. J. v. Zuylen, X. Liu, and S. L. Vine, "Reliability-Based Traffic Signal Control for Urban Arterial Roads," *IEEE Transactions on Intelligent Transportation Systems,* vol. 18, no. 3, pp. 643-655, 2017.

[115] W. S. Lee, D. L. Grosh, F. A. Tillman, and C. H. Lie, "Fault Tree Analysis, Methods, and Applications & A Review," *IEEE Transactions on Reliability,* vol. R-34, no. 3, pp. 194-203, 1985.

[116] E. Ruijters and M. Stoelinga, "Fault tree analysis: A survey of the state-of-the-art in modeling, analysis and tools," *Computer Science Review,* vol. 15-16, pp. 29-62, 2015.

[117] F. Abdul Rahman, A. Varuttamaseni, M. Kintner-Meyer, and J. C. Lee, "Application of fault tree analysis for customer reliability assessment of a distribution power system," *Reliability Engineering & System Safety,* vol. 111, pp. 76-85, 2013.

[118] Z. Li, J. Gu, T. Xu, L. Fu, J. An, and Q. Dong, "Reliability analysis of complex system based on dynamic fault tree and dynamic Bayesian network," in *2017 Second International Conference on Reliability Systems Engineering (ICRSE)*, 2017, pp. 1-6.

[119] S. Kabir, "An overview of fault tree analysis and its application in model based dependability analysis," *Expert Systems with Applications,* vol. 77, pp. 114-135, 2017.

[120] O. E. Gouda, G. M. Amer, and W. A. A. Salem, "Predicting transformer temperature rise and loss of life in the presence of harmonic load currents," *Ain Shams Engineering Journal,* vol. 3, no. 2, pp. 113-121, 2012.

[121] D. Susa, M. Lehtonen, and H. Nordman, "Dynamic thermal modelling of power transformers," *IEEE Transactions on Power Delivery,* vol. 20, no. 1, pp. 197-204, 2005.

[122] "IEEE Std 1653.2-2009-IEEE Standard for Uncontrolled Traction Power Rectifiers for Substation Applications Up to 1500 V DC Nominal Output," pp. 1-48, 2009.

[123] "IEEE Std C57.91-2011 (Revision of IEEE Std C57.91-1995) - IEEE Guide for Loading Mineral-Oil-Immersed Transformers and Step-Voltage Regulators," pp. 1-123, 2012.

[124] "IEEE Std C37.14-2015 (Revision of IEEE Std C37.14-2002)-IEEE Standard for DC (3200 V and below) Power Circuit Breakers Used in Enclosures," pp. 1-80, 2015.

[125] M. Hakirin Roslan, N. Azis, Z. Kadir, J. Jasni, Z. Ibrahim, and A. Ahmad, "A Simplified Top-Oil Temperature Model for Transformers Based on the Pathway of Energy Transfer Concept and the Thermal-Electrical Analogy," *Energies,* vol. 10, p. 1843, 2017.

[126] D. Gattuso and A. Restuccia, "A Tool for Railway Transport Cost Evaluation," *Procedia - Social and Behavioral Sciences,* vol. 111, pp. 549-558, 2014.

[127] P. Mancuso and P. Reverberi, "Operating costs and market organization in railway services. The case of Italy, 1980–1995," *Transportation Research Part B: Methodological,* vol. 37, no. 1, pp. 43-61, 2003.

[128] L. J. Opalski, "Efficient global sensitivity analysis method for models of systems with functional outputs," in *2015 European Conference on Circuit Theory and Design (ECCTD)*, 2015, pp. 1-4.

[129] F. Mach, "Reduction of Optimization Problem by Combination of Optimization Algorithm and Sensitivity Analysis," *IEEE Transactions on Magnetics,* vol. 52, no. 3, pp. 1-4, 2016.